Co-funded by the European Union's Horizon 2020 research and innovation programme under Grant Agreement no. 691797

STORE&GO

Innovative large-scale energy storage technologies and Power-to-Gas concepts after optimization

D7.7

Analysis on future technology options and on techno-economic optimization

Due Date	28 February 2019 (M36)
Deliverable Number	D7.7
WP Number	WP7: Reducing Barriers
Responsible	Robert Tichler, EIL
Author(s)	Andreas Zauner, Hans Böhm, Daniel C. Rosenfeld, Robert Tichler
Reviewer	Steffen Schirrmeister, TKIS
Status	Started / Draft / Consolidated / **Review** / Approved / Submitted / Accepted by the EC / Rework

Dissemination level

✘	**PU**	Public
	PP	Restricted to other programme participants (including the Commission Services)
	RE	Restricted to a group specified by the consortium (including the Commission Services)
	CO	Confidential, only for members of the consortium (including the Commission Services)

Document history

Version	Date	Author	Description
1.0	2018-12-20	Andreas Zauner	First draft
2.0	2019-04-01	Andreas Zauner	Final version
3.0	2019-07-04	Andreas Zauner	Implementation of comments done by various reviewers

Table of contents

Executive Summary

An ecologically sustainable energy supply that is economically viable and socially acceptable is a high priority in European policy. The European energy supply must be transformed due to energy-related, social, economic, and environmental/climatic factors. The use of green gases on the basis of renewable electrical energy (as hydrogen, synthetic methane, or alternative hydrocarbons from hydrogen) has numerous advantages, which can significantly assist Europe in transitioning its energy system. These gases can also address major issues facing the development of renewable energy sources, including the long-term storage of fluctuating renewable electricity sources, alternative energy transport via the existing gas infrastructure, the reduction of greenhouse gas emissions, the need to find new renewable energy sources for mobility and industrial processes, and the increase in local production and use. Sector coupling via power-to-gas (PtG) is fundamental to the transformation of the European energy system and a significant economic parameter. Further, the decarbonization of the European energy system must be seen as an opportunity to decisively boost European leadership in innovative energy technology, energy-related transport technology and services, and the application and implementation of mature, green gas-related technologies.

Since the market launch and development of PtG technology depend on, among other things, the profitability (and thus mainly on the investment costs) of the plant, the potential cost reduction are examined in this Deliverable D7.7. In addition to the key technological characteristics (e.g., state of the art and future projects), new developments, technologies and materials, and potential future fields of application are analyzed. Finally, the SNG production costs are calculated for different applications in order to demonstrate PtG's potential.

Both main components of the PtG-technology, electrolyzer and methanation systems, show promising cost reduction behavior related to scaling effects and technological learning throughout the investigating period, see Figure 1-1 and Figure 1-2.

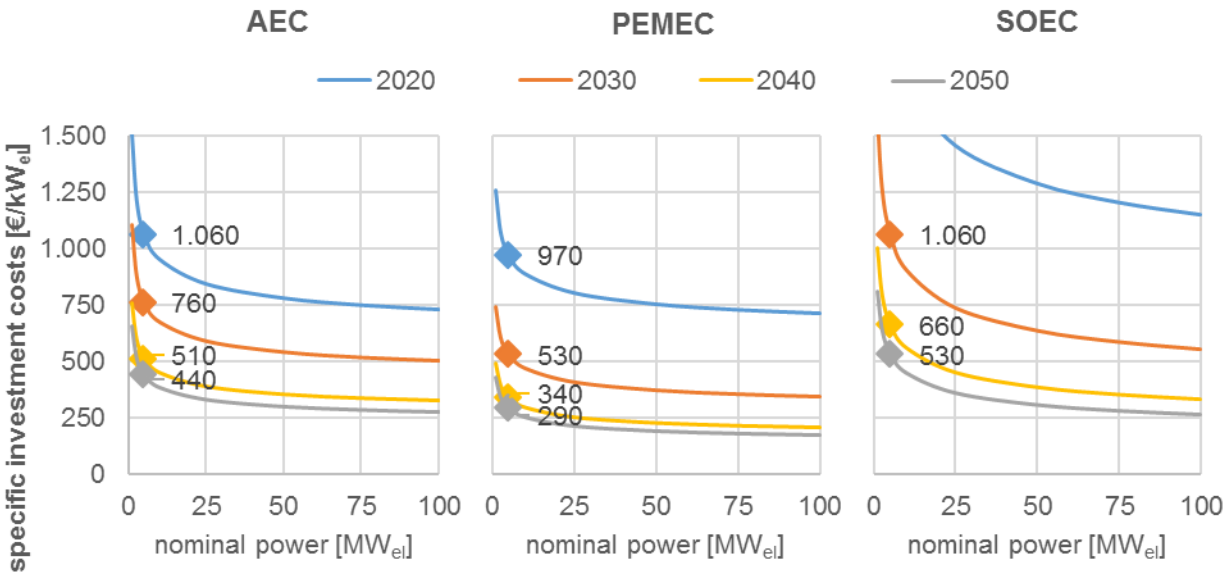

Figure 1-1: Cost development of electrolysis systems related to scaling effects and technological learning

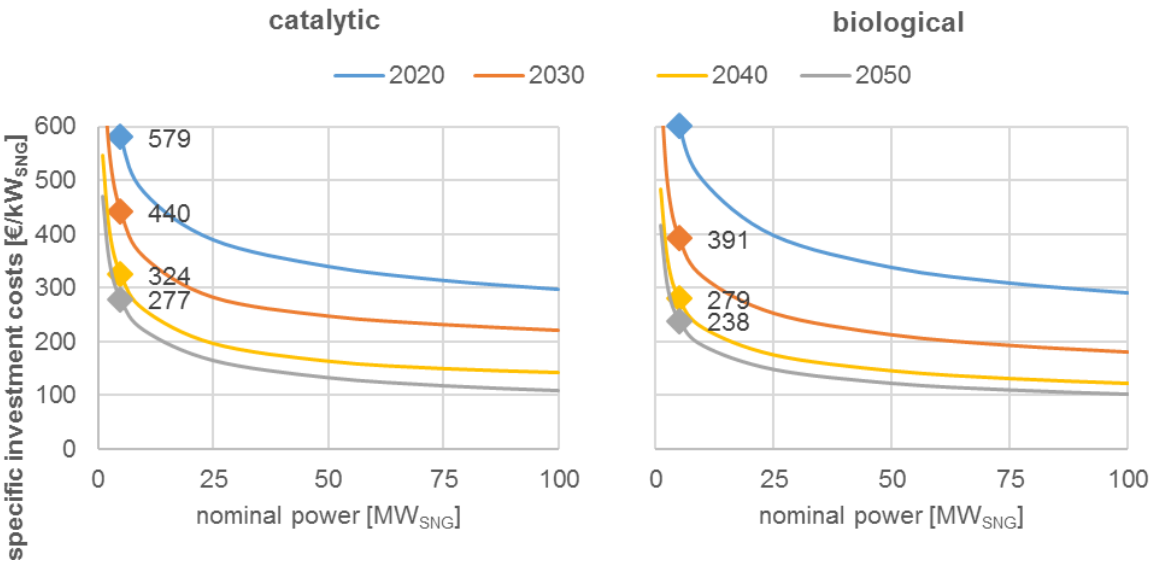

Figure 1-2: Cost development of methanation systems related to scaling effects and technological learning

The economic evaluation is based on the calculation of the specific production costs for SNG in 2020, 2030, and 2050 for a 100 MW_{el} PtG plant for three different fields of application (PtG plant powered by a photovoltaic power plant (PtG-PV); a PtG plant powered by a wind farm (PtG-Wind); and a PtG plant powered by the public grid (PtG-Grid)). Additionally, the SNG production costs are calculated for different PtG technologies, which are combinations of a AEC, PEMEC, and SOEC, with a catalytic or biological methanation unit.

Figure 1-3 summarizes the results of all the calculations performed, providing a range of costs for each scenario. The variety among the costs is due to the different technologies used for SNG production. In early applications (i.e., 2020 and 2030), the sole use of surpluses, electricity from PV or wind does not provide acceptable SNG production costs, due to the still relatively high investment costs and the low achievable full load hours of the plant. In the PtG-Grid operating mode, the PtG plant is connected to the public electricity grid and operates at times with the cheapest electricity prices on the spot market. In early applications, PtG plants will need to run at high full-load hours (> 4,000 h/a) to achieve low SNG production costs. In future, the lowest costs will be achieved with a lower number of full-load hours (3,000 h/a) when the plant is operated only during periods with the lowest electricity prices. However, several factors, such as the need to produce green gas, may argue for higher full-load hours, albeit with higher SNG costs.

In general, there is little difference in SNG production costs according to the technology used, whereby in future PtG plants with an alkaline electrolyzer will have slightly higher SNG production costs than those with a PEM electrolyzer, and a PtG plant built with an SOEC and catalytic methanation will tend to have slightly lower SNG production costs. Concerning the methanation technology used there is hardly no difference in the SNG production costs. The lower SNG production costs of the PtG plant with an SOEC and catalytic methanation unit can be attributed to higher system efficiency. However, to achieve these very high efficiencies, the SOEC requires an additional waste heat source, which is not available at every location. By contrast, it is assumed that waste heat can be sold in the variants where an AEC or PEMEC is connected to a catalytic or biological methanation unit. If waste heat cannot be sold, then the SNG costs would rise in these variants. Thus, the SOEC variant would have the lowest SNG costs by far.

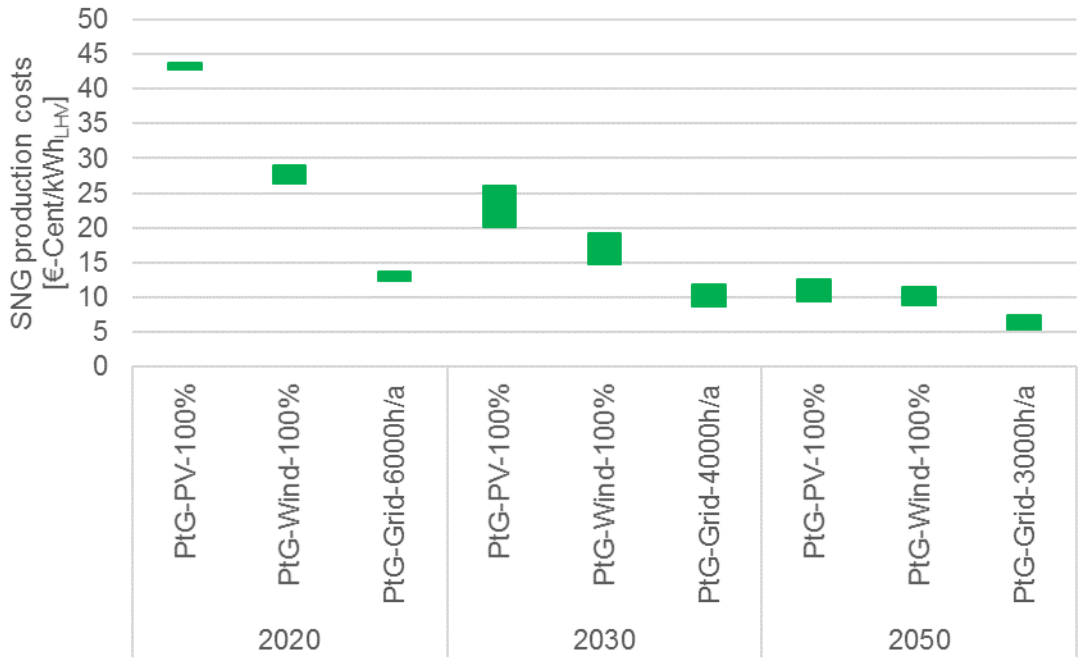

Figure 1-3: Range of SNG production costs of a 100 MW plant in 2020, 2030 and 2050 for different scenarios

A PtG plant can be used in a variety of ways in the energy system. In most of the cases, the fundamental goal is the production of renewable gas. It may be reasonable (while taking the market situation for renewable gases into account) to not operate the plant with about 3,000 full-load hours in or-der to achieve the lowest SNG production costs but, rather, to increase the output of the PtG plant by increasing the full-load hours, although this would lead to higher SNG production costs. However, as mentioned, excessively high full-load hours (> 5,000 h/a) leads to significantly higher SNG costs. Incidentally, in a renewable energy-based energy system with a large share of fluctuating energy sources, the PtG plant should be operated in such a way as to ensure that the power grid is not additionally charged but is best supported. This can be done, for example, by converting the surpluses from wind and PV produced in the summer into SNG and transferring them into the winter months (i.e., long-term storage, sector coupling). Since power generation bottlenecks are likely in the winter months (less electricity production form PV), leading to higher electricity prices, the PtG plant should not be operated at these times. Thus, a continuous operation (full-load hours > 6000 h/a) of the PtG plant is not desirable. The full-load hours for reasonable PtG plant operation (gas production, SNG production costs, and grid suitability) are regarded to be in the range of 3,000 to 5,000, incurring costs of about 5.5 to 7.5 Cent/kWh in 2050.

The sensitivity analysis indicates that reducing SNG costs requires purchasing low-cost electricity, maximizing plant efficiency, reducing investment costs, and in cases where the plant is connected to a PV or wind park, building the PV or wind park in good locations with high full-load hours.

The deliverable shows that barriers and prejudices can be reduced to enable the successful implementation of PtG plants. However, the development of PtG technology is subject to fundamental energy and climate policy decisions; thus, assumptions made about the future can change significantly. This has a major impact on the future SNG production costs calculated in this report.

1 Introduction

An ecologically sustainable energy supply that is economically viable and socially acceptable is a high priority in European policy. The European energy supply must be transformed due to energy-related, social, economic, and environmental/climatic factors. The use of green gases on the basis of renewable electrical energy (as hydrogen, synthetic methane, or alternative hydrocarbons from hydrogen) has numerous advantages, which can significantly assist Europe in transitioning its energy system. These gases can also address major issues facing the development of renewable energy sources, including the long-term storage of fluctuating renewable electricity sources, alternative energy transport via the existing gas infrastructure, the reduction of greenhouse gas emissions, the need to find new renewable energy sources for mobility and industrial processes, and the increase in local production and use. Sector coupling via power-to-gas (PtG) is fundamental to the transformation of the European energy system and a significant economic parameter.

Central contributions of PtG to the energy system

- Storage and transport solution: Seasonal fluctuations of renewable electricity generators can be balanced through the injection and storage of energy carriers produced from renewable electricity like hydrogen and/or synthetic methane produced from hydrogen into the existing natural gas infrastructure.[1] New power lines or a grid expansion can be substituted by shifting the transportation of energy from the electric power grid to the natural gas grid. The advantage of energy transport via the existing natural gas infrastructure is the high energy density of the natural gas grid. An expansion of the natural gas network would lead to a much smaller topographical intervention than an expansion of the electricity network, which would increase public acceptance and reduce real estate costs.[2]

- Infrastructure solution: In addition to power plants, central Europe's gas infrastructure includes a high-quality transmission and distribution grid as well as enormous capacities for gas storage in caverns and porous reservoirs. Thus, the integration of renewable gases such as hydrogen or SNG into the natural gas infrastructure would avoid the need for enormous stranded investments in the existing energy infrastructure. Sectoral coupling of the electrical and gas grids via hydrogen production (with optional methanation) would also allow the integration of biogas and thus an increased greening of the gas sector. In other words, the long-term use of the existing gas infrastructure will depend on the degree of integration of renewable gases. Climate and energy policies can thus be advanced by the existing gas infrastructure, which can also be used to secure the long-term use of this infrastructure.

- Supply of all segments by renewable energy sources: Green hydrogen and therefrom produced renewable hydrocarbons such as methane can be used in all energy segments (e.g., process heat, mobility, space heating, and electrical energy), and thus foster the greening of the European energy system. In addition to battery-based electric mobility, the use of green hydrogen or methane from PtG plants will significantly accelerate the transition to a sustainable transport system with low or no emissions. Hydrogen and hydrogen-based synthetic methane can be used in combustion engines and fuel cells, and they have a strong potential to reduce primary energy input, emissions of air pollutants (e.g., particulates and NO_X), and greenhouse gas emissions. Besides its utilization for energy production, hydrogen as a renewable resource is also important for manufacturing

[1] Therefore, refer to R. Tichler, J. Lindorfer, C. Friedl, G. Reiter, H. Steinmüller (2014) FTI-Roadmap Power-to-Gas für Österreich, Energieinstitut an der JKU Linz. Herausgeber: bmvit, Schriftenreihe 50/2014.

[2] Therefore, refer to G. Reiter J. Lindorfer (2013) Möglichkeiten der Integration von Power-to-Gas in das bestehende Energiesystem. In: Steinmüller, Hauer, Schneider (Hrsg.) Jahrbuch Energiewirtschaft 2013. NWV Verlag.

industries in terms of material utilization. In the steel industry, for instance, hydrogen can be used as a reducing agent in pig iron production (hydrogen reduces iron ores by removing the containing oxygen) to aid in low-carbon steel production. Instead of reformers using natural gas to produce hydrogen, it would be possible to shift to carbon-neutral hydrogen produced in electrolysis plants under certain conditions (if there are no natural gas pipelines or only low amounts of hydrogen available at a certain location).

Therefore, endeavors toward the decarbonization of the European energy system must be considered an opportunity to boost European leadership in innovative energy technology, energy-related transport technology and services, and in the application and implementation of mature, green gas-related technologies. European policies often intend the direct usage of electricity. However, this faces restrictions and limits, which can be effectively negated by transitioning to gaseous green sources like PtG products, green hydrogen, and green synthetic natural gas (SNG). Although its technological efficiency is relatively low, the production of SNG allows for the unrestricted use of the existing natural gas infrastructure and offers a completely mature technology and market availability for all system-relevant components, from storage to the final consumer.

The main objective of work package WP7 of the STORE&GO project is dealing with the technological, economic, regulatory, environmental, and social barriers that must be reduced for PtG to be successfully implemented. Task 7.2 addresses the techno-economic optimization of the PtG system, focusing on reducing investment costs through experience curves, learning effects, and economies of scale. This Deliverable D7.7, “Analysis on future technology options and on techno-economic optimization,” examines the investment cost reductions enabled by PtG applications through economies of scale (in this Deliverable, the term “economies of scale” refers to the effect of cost reduction through upscaling). This Deliverable is based on Deliverable D7.5, “Report on experience curves and economies of scale,” in which the term “economies of scale” refers solely to the effect of real cost reductions through increases in production volume, rather to increases in size via upscaling (e.g., of nominal power). Since the market launch and development of PtG technology depend on, among other things, the profitability (and thus mainly on the investment costs) of the plant, the potential cost reduction should be examined. In addition to the key technological characteristics (e.g., state of the art and future projects), new developments, technologies and materials, and potential future fields of application are also analyzed. Finally, the SNG production costs are calculated for different applications in order to demonstrate PtG’s potential. The Deliverable shows that barriers and prejudices can be reduced to enable the successful implementation of PtG plants.

This Deliverable provides a brief introduction, followed by a short summary of the previous Deliverable D7.5 “Report on experience curves and economies of scale,” which serves as a basis for the calculations of investment cost reductions due to up-scaling (economies of scale). The next chapter discusses the relevant technological characteristics (state of the art and future perspectives), providing a theoretical basis for the calculations performed in the economic evaluation. Chapters five and six analyze new developments, technologies, and materials as well as potential future fields of application through comprehensive literature reviews. Finally, an economic evaluation is performed by calculating the specific SNG production costs for different applications and operating modes. Sensitivity analyses are also performed by varying several key parameters in order to determine the main drivers of SNG production cost reduction.

2 Investigations on technological learning – Recapitulation of D7.5 results

This Deliverable D7.7 is based on the investigations of technological learning executed in Deliverable D7.5. Hence, this introductory chapter recapitulates that analysis and its results.

In general, the formal concept of experience curves describe the decline of real costs by a constant percentage (learning rate) for every cumulative doubling of its produced volume and therefore represents a relationship between the costs of a product and the experience, expressed in cumulative production of that product.

Note: In that context, economies of scale have also been investigated, in terms of the effect of real cost reductions through an increase in production volume but not that of cost reductions through size increases via upscaling (e.g., increases in nominal power), which are investigated separately in this Deliverable D7.7.

Cost reductions based on experience curves and economies of scale are due to the following factors, among others:

- fixed cost degression (increased utilization of different sectors in the company, such as administration, R&D, production, logistics, and distribution),
- reduction of production time (increased manpower efficiency due to learning effects),
- increased specialization (standardization, focus on core competence and product family),
- variation in resources (e.g., alternative and less expensive (raw-)materials, optimized employment of staff according to qualifications),
- improved production technologies,
- optimization of product design to simplify the production process.

The produced volume of PtG plants, and therefore the gained experience and economies of scale depend on the development of the future **global demand for PtG** products, which is subject to climate and policy measures (e.g., carbon taxes, the scope of government R&D, subsidies, and market introduction programs) and economic factors (e.g., economic growth).

While the literature's data on learning rates, investment costs, and future global demand for PtG products would principally allow a preliminary estimation of future investment costs for PtG applications, the available data do not meet our requirements, as they do not differentiate between different electrolysis or methanation technologies, between systems, or between stack (electrolysis) or reactor (methanation) costs. To obtain a detailed view of technological learning, a component-based approach was developed with the **CoLLeCT (Component Level Learning Curve Tool) model**. This model **allows for comparisons of learning effects between different technologies, the investigation of cost structure developments, and a consideration of spillover effects from concurrent technology sectors.** The potential for cost reductions through technological learning has been investigated for electrolysis and methanation systems.

Implementing the theory of learning curves requires estimating global PtG demand. Depending on the scenario, there would be a need to **install about 6,500 to 14,200 GW electrolysis power capacities and about 3,400 to 7,100 GW SNG-output power capacities to meet the demand in 2050.** These values seem to be very high. However, it is important to remember that, in a decarbonized energy system in 2050, not only natural gas but also other fossil energy sources such as oil and coal must be replaced by renewable energy carriers. Since not all areas of the energy system can be electrified, green molecules (renewable SNG and hydrogen produced by PtG) are also expected to play an important role in the future energy system. **To cover this relatively high demand and**

produce the required quantities (about 285,000 electrolyzer systems with an installed power of 50 MW would be required), **mass production would be necessary.** However, this implies products with a standardized and mass production-ready design (e.g., no individual installation planning or piping). The PtG systems must be planned on the basis of greenfield construction (with an interface power supply, gas connection for feed-in, and, possibly, a CO_2 supply) to meet the requirements of mass production.

The costs are stated as **real costs** (reference year 2017, $€_{2017}$). This means that the inflationary effects that are anticipated and will lead to rising nominal costs have not been considered. Additionally, **no significant changes in technology**, such as the implementation of additional functions, control elements and safety devices, or efficiency improvements, have been taken into account in the calculation of future investment costs. Solely this approach, of assessing the product according to the current functional scope and characteristics, allows for the investigation of future costs based on the theoretical concepts of experience curves and economies of scale.

The results indicate that alkaline electrolyzer (AEC) systems show lower potential for cost reductions than the proton exchange membrane electrolyzer (PEMEC) and solid oxide electrolyzer (SOEC). The AEC's estimated investment costs **of about 440 $€_{2017}/kW_{el}$ in 2050** are expected to be significantly higher than those for **PEMEC systems, expected to be about 290 $€_{2017}/kW_{el}$**. Besides the AEC's lower overall learning rate, this result may be due to the substantially higher starting value of cumulative productions, which means that significant learning effects have already occurred. Additionally, the PEMEC's learning rate decreases quickly along with increasing production volumes in the beginning, whereas this effect decreases at higher cumulative volumes. Conversely, the experience rate of the AEC is more harmonized over the entire period. **The SOEC shows the highest cost-reduction potential of all three investigated electrolysis technologies, with investment costs estimated to reach about 530 $€_{2017}/kW_{el}$ in 2050.**[3] This follows from a rather high learning rate that was defined on the SOEC itself, based on the relevant literature. Even though, calculations for the SOEC have been specified in more detail in the meantime, especially for this technology, further investigations into cost structures and experience rates are still necessary to allow reasonable estimations of future investment costs.

The experience curves for catalytic and biological methanation systems show similar cost-reduction trends. The investment costs for biological methanation are lower in the long term. This is mainly driven by the fact that the increase in the cumulative produced volume has to be substantially higher than that for the catalytic application to reach the presumed technology production share levels. Additionally, biological methanation lacks the catalyst component that catalytic methanation includes; the latter is expected to obtain learning effects that are low compared to those of other components in the reactor module. However, the **investment costs for both technologies remain on a similar level throughout the investigated period and are expected to reach values of 280 $€_{2017}/kW_{SNG}$ (catalytic) and 220 $€_{2017}/kW_{SNG}$ (biological), respectively, in 2050 under the presumed conditions.**

However, it has to be pointed out that the development of PtG technology is subject to fundamental energy and climate policy decisions.

[3] The calculations of technological learning for the SOEC have been improved, resulting in lower costs compared to the values stated in deliverable D7.5. Hence, the base values for the calculations in this deliverable represent up-to-date results for that technology.

3 Economies of scale

Unless otherwise mentioned, cost predictions for the PtG technology in this Deliverable are stated as **real costs** (reference year 2017, €$_{2017}$). This means that the inflationary effects that are anticipated and will lead to rising nominal costs have not been considered. Additionally, **no significant changes in technology**, such as an implementation of additional functions, control elements and safety devices or efficiency improvements, have been taken into account for calculating the future investment costs.

The term “economies of scale” is used in the literature to describe two different forms of cost reduction for a product. An EoS that directly affects the production process of a certain technology by going from unit, to batch, and then to series production, leading to reduced unit cost, is considered part of technological learning and is therefore included in the STORE&GO Deliverable D7.5 “Report on experience curves and economies of scale.” This Deliverable analyzes reductions in specific investment costs for individual PtG plants through the upscaling of nominal power, according to the reference value. The term “EoS” in this Deliverable refers solely to the effect of cost reduction attained through an increase in size/scale/power via upscaling (e.g., of nominal power).

Using a logarithmic relationship is a common method of estimating costs by scaling. This is known as the “six-tenth-factor rule” [1], or the “scale factor” or “cost-to-capacity” method:

$$C_b = C_a * \left(\frac{S_b}{S_a}\right)^f \qquad \text{Eq. 1}$$

where C_b stands for the questioned equipment costs at the appropriate scale S_b (size, capacity, nominal power) of the component, and $C_a$and S_a represent the costs and scale of the known reference component, respectively. f is the scale factor applied to the technology in question. If no other information is available, $f = 0.6$ can be used as a scale factor in an initial approximate cost estimation (this is where the term “six-tenth-factor” comes from) [1].

However, the value of the scale factor f is specific to the component because the influence of equipment scaling on cost is related to the design and structure of the individual component. PtG systems consist of a variety of individual components, resulting in a wide range of scaling effects and influences on the overall system costs. To enable an accurate estimation of the influence of scaling for PtG systems, these EoS are investigated in detail below. Based on the work on technological learning in the STORE&GO Deliverable D7.5 [2], a modular approach is taken by splitting up the investigated systems into separate modules and components. Furthermore, electrolysis and methanation systems are again investigated separately. Splitting the plant into individual modules and using several scale factors reduce the risk of using a single inappropriate scale factor for the entire plant.

3.1 Electrolysis

The electrolysis systems analyzed herein – based on AEC, PEMEC and SOEC technology – can or must be different in design depending on the requirements / framework conditions / operation purpose (e.g. required gas quality and conditions, heat management, and gas drying). This results in a large number of variants of individual electrolysis concepts, which also differ in investment costs.

Since not all possible variants can be analyzed in this study, the investment costs calculated thus serve as a guideline for cost estimations of future projects. The actual investment costs for a specific

project, where the respective requirements or framework conditions in the plant design are considered, have to be analyzed in detail by the manufacturers and may differ from those estimated herein.

3.1.1 Literature review on EoS of electrolysis systems

Using investment cost data taken from the literature review in Deliverable D7.5 and other sources, the scale factors for AEC and PEMEC are calculated using equation Eq. 1 and are presented in Table 3-1. The mean scale factor for both technologies is about 0.75; however, the range is wide, from about 0.51 to 0.96 for AEC and 0.53 to 0.97 for PEMEC. This wide range can be attributed to, among other things, the wide range (from 0.1 to 100 MW) of the analyzed system scales, because the scale factor for small-scale electrolyzers (< 5 MW) is lower than that for large-scale ones (> 5 MW). The mean scale factor for AEC is about 0.69 (< 5 MW) and 0.90 (> 5 MW) on average, and that for PEMEC is about 0.72 and 0.82, respectively. This means that the positive effect due to upscaling (EoS) declines for large-scale electrolyzers.

Table 3-1: Calculated scale factors for electrolysis systems based on cost data from literature

Nominal power /MW	Spec. investment costs /€/kW	Investment costs /Mio. €	Scale factor – rel. to the previous scale -	Mean scale factor -	Cost data based on source -
AEC					
0.5	1,800	0.9	-		[3]
2.5	1,200	3.0	0.75		
0.5	2,000	1.0	-		[4]
1.0	1,500	1.5	0.58		
10.0	1,000	10.0	0.82		
0.4	2,370	0.8	-		[5]
3.4	875	2.9	0.56		
0.5	1,893	0.9	-		[6]
1.0	1,795	1.8	0.92	0,75	
2.0	1,746	3.5	0.96		
0.7	2,521	1.9	-		[6]
1.5	1,845	2.7	0.54		
2.3	1,473	3.4	0.51		
1.0	1,150	1.2	-		[7]
5.0	710	3.6	0.70		
10.0	682	6.8	0.94		
50.0	620	31.0	0.94		
PEMEC					
0.1	3,500	0.4	-		[3]
1.0	1,750	1.8	0.70		
0.6	2,915	1.7	-		[5]
3.0	1,370	4.1	0.53		
5.0	1,130	5.7	-		[8]
30.0	940	28.2	0.90		
0.6	2,250	1.2	-		[6]
1.1	1,715	1.9	0.61		
2.2	1,390	3.1	0.70	0,75	
1.0	1,943	1.9	-		[6]
2.0	1,598	3.2	0.72		
0.5	1,450	0.7	-		[9]
1.0	1,300	1.3	0.84		
2.5	1,050	2.6	0.77		
5.0	1,000	5.0	0.93		
10.0	750	7.5	0.58		
100.0	700	70.0	0.97		

A similar scale factor of 0.7 (based on previous studies) is also presumed for use in calculating the influence of economies of scale, as in [10].

For SOEC systems, the available data (especially on systems with capacities above 500 kW) are insufficient to allow analysis comparable to what is shown in Table 3-1 for AEC and PEMEC. Though the components are comparable (at least in terms of production and scaling) and the EoS effects are thus expected to be in a similar range, the cost structures of SOEC systems are very different. Therefore, a reliable estimation cannot use data from the literature but requires a more detailed investigation. Such an analysis is performed below for all three technologies.

3.1.2 Calculation of specific investment costs of electrolyzer systems due to EoS

At a minimum, the following data are needed to estimate the development of the specific investment costs of electrolysis systems for different nominal power ranges resulting from EoS in a modular approach:

- total investment costs of the plant at a reference scale,
- appropriate cost shares of the individual modules, and
- their corresponding scale factors.

Table 3-2 presents the specific investment costs for 5 MW_{el} electrolyzer systems (AEC, PEMEC, and SOEC) in 2020, 2030, 2040, and 2050. The determination of these costs has already been extensively discussed in STORE&GO Deliverable D7.5[4] [2]. The cost reduction is based solely on experience/learning curve effects due to an increase in the cumulative production volume. The costs shown in Table 3-2 serve as a reference value (5 MW_{el} nominal power) for the calculation of investment costs for electrolyzers with a nominal power in the range of 1–100 MW_{el} through EoS.

Table 3-2: Calculated specific investment costs for a 5 MW electrolysis systems due to learning curves [2]

Year of installation	Specific investment costs [€/kW_{el}]		
	AEC	PEMEC	SOEC
2020	1,060	970	1,990
2030	760	530	1,060
2040	510	340	660
2050	440	290	530

The development of the cost structure of the 5 MW_{el} electrolyzer reference systems until 2050 (see Figure 3-1) was also calculated according to STORE&GO Deliverable D7.5. Since not all components or modules are affected by technological learning to the same extent, the cost structures of the systems change as cumulative production grows [2].

[4] The learning curves, and therefore the resulting costs of the SOEC systems, have changed slightly from the results shown in deliverable D7.5 because the underlying component structure specification has been refined and become more detailed based on more recently available literature data.

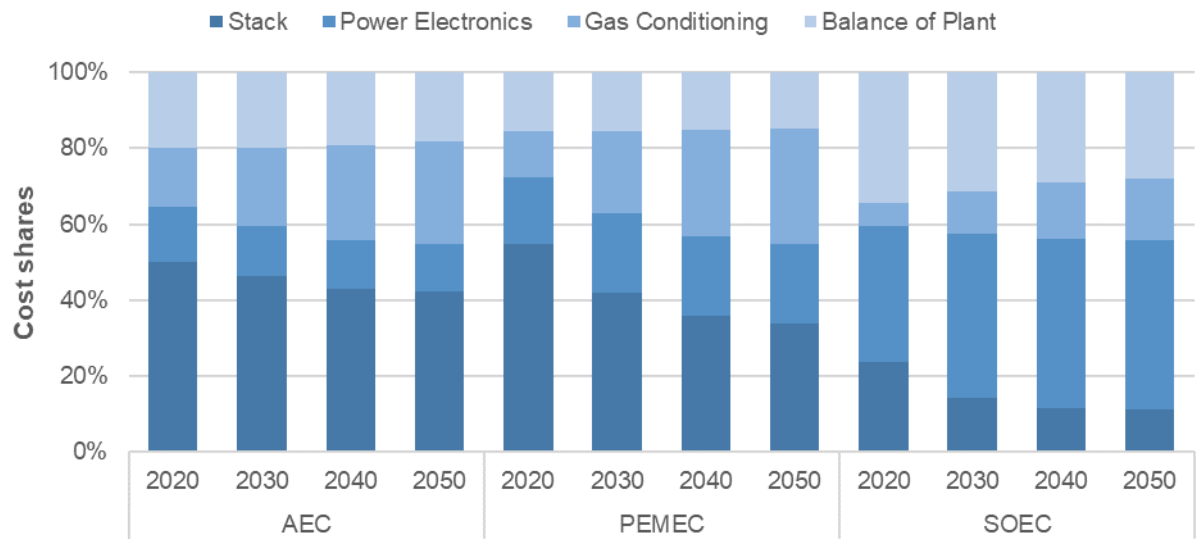

Figure 3-1: Development of the cost structure of a 5 MW electrolysis system due to learning curves [2]

A scale factor (see Table 3-3) is defined for each module of the electrolysis system, consisting of cell stack, power electronics, gas conditioning, and balance of plant (BoP).

Table 3-3: Scale factors of the main parts of an electrolysis system

Component	Scale factor		
	AEC	PEMEC	SOEC
Stack (initial)	0.88	0.89	0.87
Power electronics		0.75	
Gas conditioning		0.60	
BoP	0.68	0.73	0.73

The scale factor for the stack module is investigated in terms of the underlying components and is calculated as the product of the varying cost structure (according to the learning curves) and individual scaling effects (a detailed compilation is provided in the appendix). Thus, the scale factor varies with the changing cost structures due to the learning effects (cf. Deliverable 7.5 [2]). The stack does not show potential for large cost reduction via EoS because of its modular design (cf. [11]). An increase in stack power due to an upscaling of the electrolyzer cell is unlikely for many reasons (e.g., problems with leakage); therefore, the cell is limited in size. This maximum cell stack size is expected to increase as TRL and technological advances increase. To take those effects into account, a dynamic scale factor is implemented for the electrolysis cell stack based on an exponential function:

$$f = 1 - (1 - f_0) \cdot e^{-\frac{S}{S_0}} \qquad \text{Eq. 2}$$

where f_0 represents the basic scale factor as shown in Table 3-3, S is the questioned scale, and S_0 is the average maximum stack size for the period under study. This provides a scale factor that is dependent on the system scale itself and minimizes scaling effects for large-scale applications.

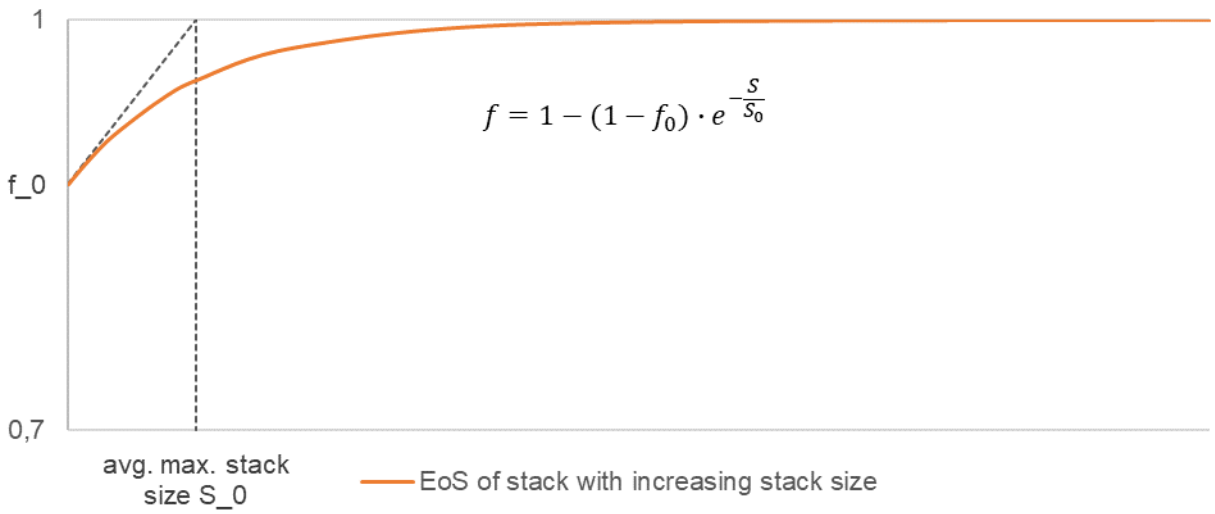

Figure 3-2: Dynamic scale factor for electrolysis cell stack

The following table shows the presumed average maximum stack size for the electrolysis technologies and installation years.

Table 3-4: Average maximum stack sizes used for electrolysis cell stacks per year of installation, based on [12]

Year of installation	avg. max. stack size S_0 [MW_{el}]		
	AEC	PEMEC	SOEC
2020	3.0	1.2	0.5
2030	4.0	2.0	1.0
2040	5.0	3.5	2.0
2050	5.0	5.0	3.0

Following [11], a scale factor of 0.75 is used for the power electronics (transformer and rectifier). The gas conditioning module consists mainly of components for gas drying and cooling (with an average scale factor of 0.52 [11,13]) and H_2 purification (with a factor of 0.81 [11]). Thus, an average scaling of 0.60 is used. Following data in the literature (cf. [1,11,13,14]) an average scale factor of 0.68 to 0.73, depending on the underlying system and its components, is defined for the overall module, which is a mixture of many different components, including piping (1.33), heat exchangers (0.59), valves and fittings (0.60), pumps (0.59) and further equipment. For BoP components, where no scale factor is available in the literature, an average factor for BoP of 0.6, according to the six-tenths rule, is assumed. These assumptions are largely supported by the data provided by [1]. A detailed compilation of the incorporated components and the presumed scale factors is presented in the appendix.

Based on the data described above (i.e., specific investment costs of the reference system, cost structure, and scale factors), the specific investment costs are calculated according to Eq. 1 for each individual module and subsequently summed up for the entire electrolysis system. The results for the development of the specific investment costs for electrolysis systems due to EoS for a nominal power of 1–100 MW in 2020, 2030, 2040, and 2050 are shown in Figure 3-3 for AEC, Figure 3-4 for PEMEC, and Figure 3-5 for SOEC.

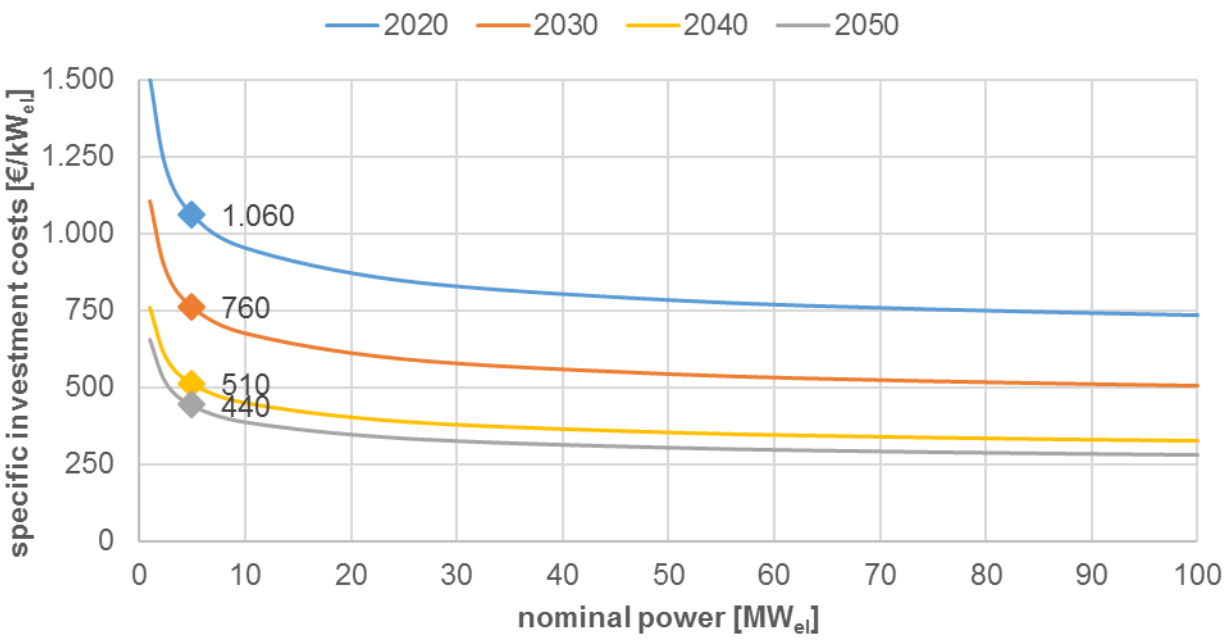

Figure 3-3: Specific investment costs of AEC due to economies of scale for a nominal power of 1-100 MW in 2020, 2030, 2040, and 2050

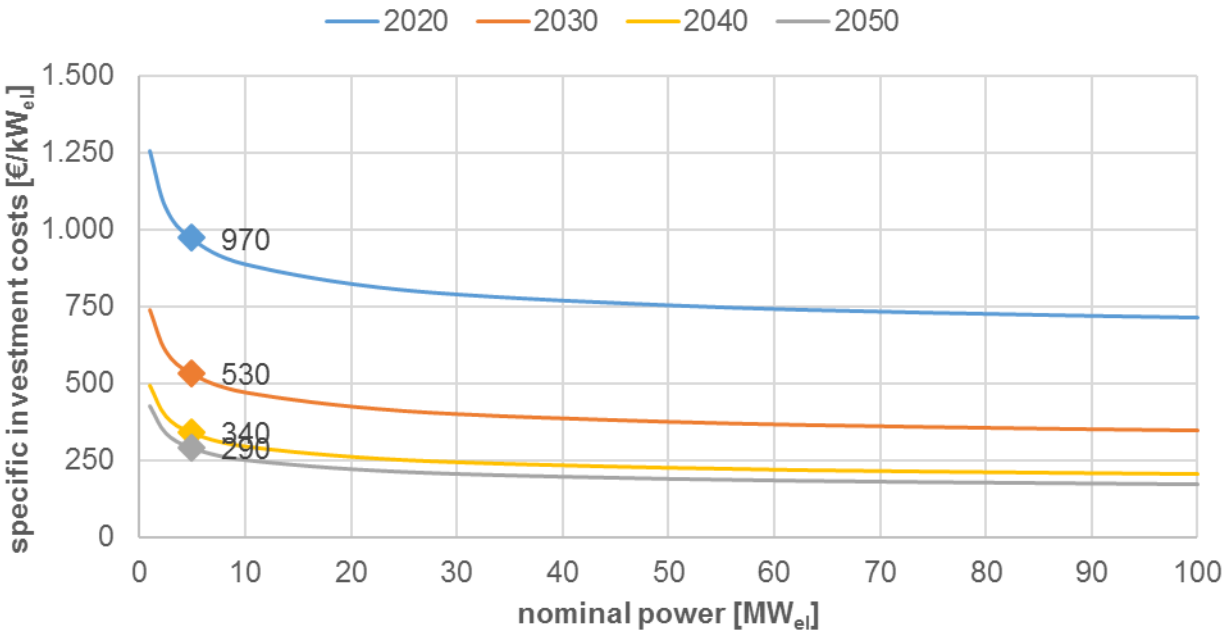

Figure 3-4: Specific investment costs of PEMEC systems due to economies of scale for a nominal power of 1-100 MW in 2020, 2030, 2040, and 2050

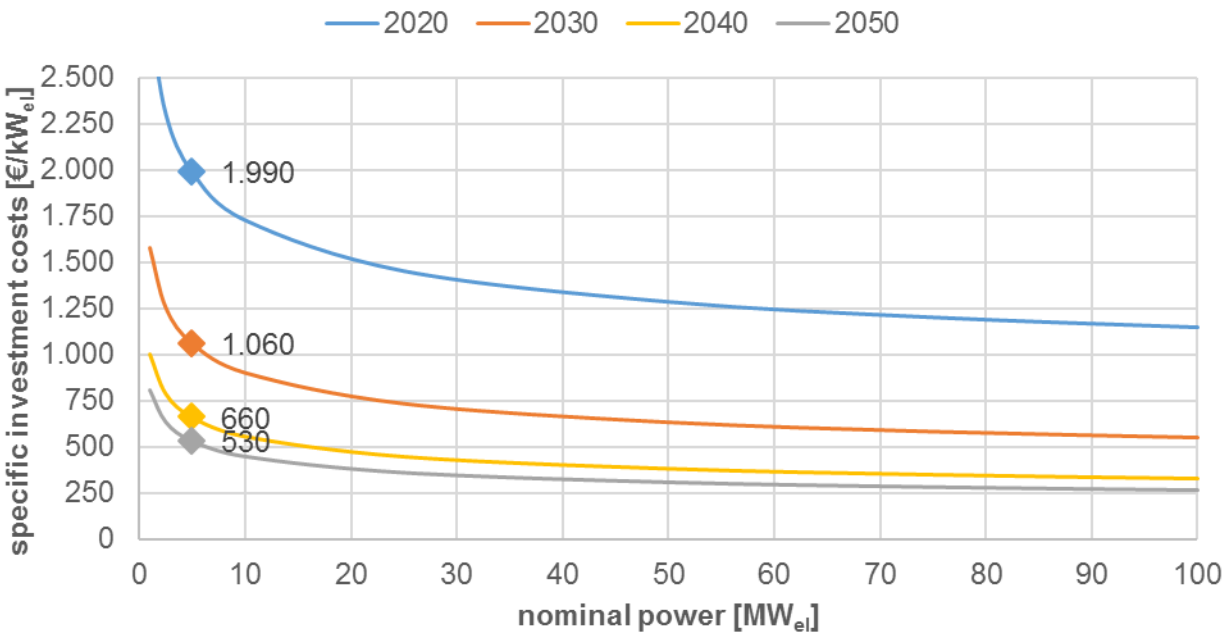

Figure 3-5: Specific investment costs of SOEC systems due to economies of scale for a nominal power of 1-100 MW in 2020, 2030, 2040, and 2050

The average scale factor for the entire electrolysis system can be determined based on the overall investment costs for the electrolysis system calculated from the individual modules. Figure 3-7 shows the development of the range and average scale factor for electrolysis systems with a nominal power of 1–100 MW in 2020, 2030, 2040, and 2050.

The resulting scale factor is affected by two parameters: (1) the system scale itself, due to the modular approach, which is intensified by the dynamic scaling of the stack; and (2) the year of installation, due to shifting cost shares as a result of technological learning. These effects can clearly be seen in Figure 3-6 for the AEC electrolysis systems.

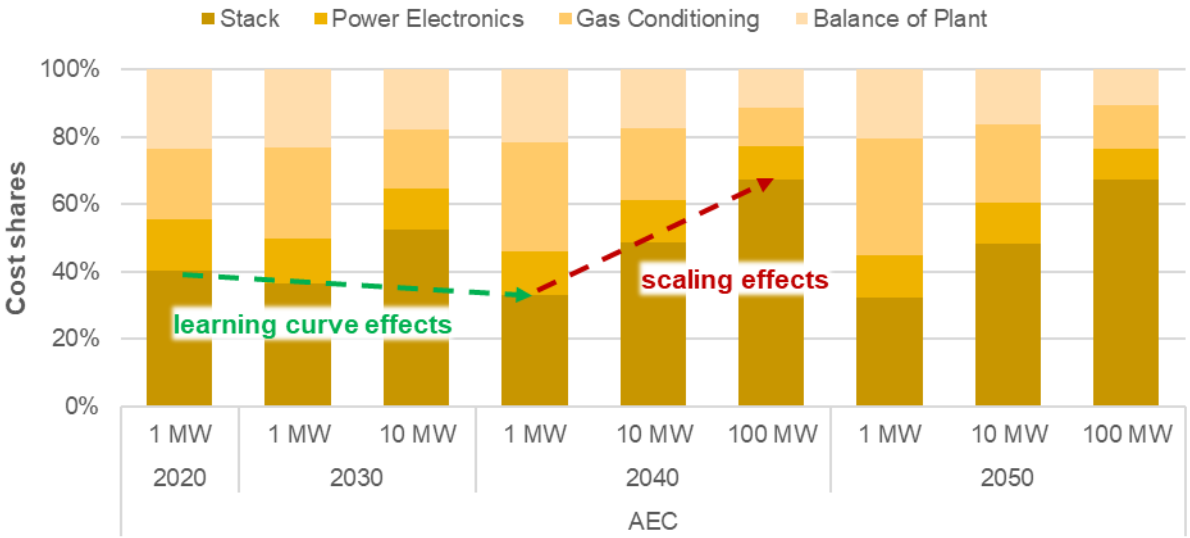

Figure 3-6: Development of module cost shares for AEC electrolysis systems in dependency of the system scale and the year of installation

The effect of EoS is more pronounced at lower nominal power levels than at higher levels. For example, the scale factor for AEC is about 0.78 for 1 MW and 0.88 for 100 MW in 2020 (see Figure 3-7). This peculiarity is due to the changes in the electrolysis system's cost structure caused by the

different scale factors of the individual modules. Due to the rather high scale factor (up to 1 in large systems), the costs of the stack do not decrease as much as do, for example, the costs of the gas conditioning (scale factor = 0.60). Relative to the reference system, this leads to an increased share of stack costs in the overall system for larger electrolysis systems, which reduces the overall effect of EoS.

Further, the effect of EoS is stronger in the future than in the present. For example, the scaling factor for the PEMEC reference system (5 MW) is calculated at 0.87 on average in 2020 but 0.78 in 2050. This difference is due to the development of the cost structure through the effects of technological learning (see Figure 3-1). As cumulative production increases, the module costs for the stack decrease due to learning effects more steeply than do, for instance, the costs of the gas conditioning module. For this reason, the scale factor of the entire electrolysis system declines in the future, since the modules with low learning-curve effects (gas conditioning, power electronics, and BoP) are more appropriate for scaling and represent higher shares of the overall system costs. Therefore, they dominate in the cost structure, which leads to a stronger overall effect of EoS.

The calculated scale factors for AEC and PEMEC are in a similar range, of about 0.75 to 0.90, though the average values are a little higher in the PEMEC case, particularly in early periods. The ranges for the SOEC system are mostly smaller, at about 0.74-0.82, due to the significantly differing cost structure and the fact to profit more from scaling due to the lower overall scale factors.

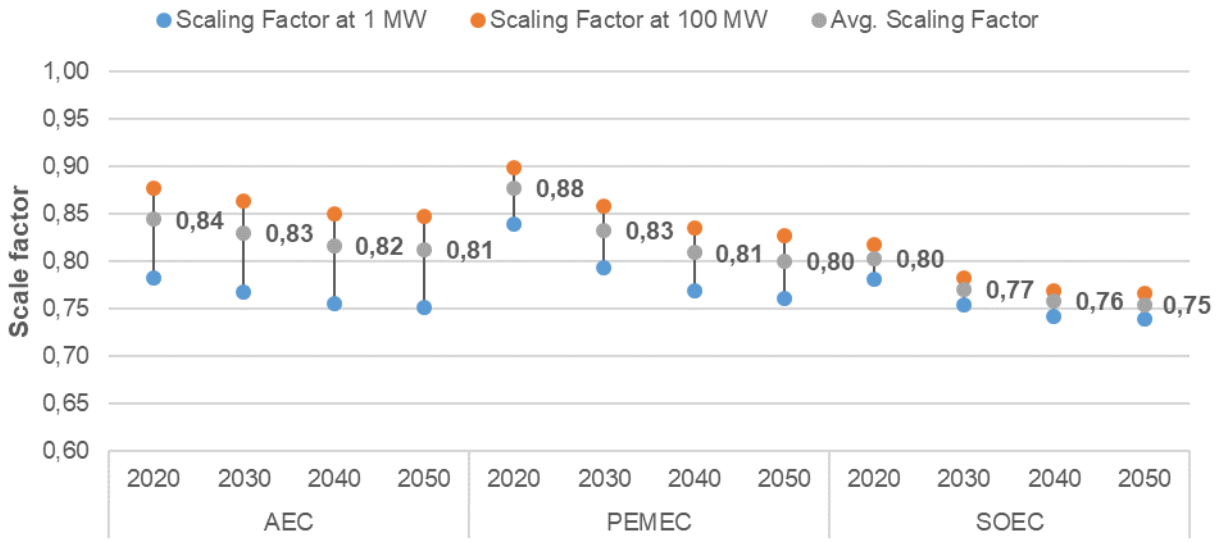

Figure 3-7: Future development of the range and average scale factor for electrolysis systems with a nominal power of 1–100 MW in 2020, 2030, 2040, and 2050

Comparing the calculated scale factors for AEC and PEMEC systems using the modular approach, with the values calculated from the analyzed literature cost data, shows that the limits of the former are closer, especially on the lower side. This occurs, first, because small applications below 1 MW_{el} that show low scale factors are not considered in our analysis. Second, some of the values calculated based on the literature cost data seem to be rather are low compared to scale factors of individual components found in the literature and used in the modular approach. This may indicate that the cost reductions in the analyzed literature data incorporate effects other than EoS (according to the definition used in this study), such as learning curve effects. Moreover, the values are not comparable, as the values in the literature use varying reference values due to data limitations, while our calculations use a fixed reference of 5 MW_{el}.

3.2 Methanation

The methanation systems analyzed herein – catalytic and biological – can be further subdivided into various processes and reactor technologies (e.g. for catalytic methanation reactor: fixed bed, fluidized bed, coated honeycomb, bubble column). The individual concepts can or must be different in design depending on framework conditions / requirements / operation purpose (e.g. gas qualities and conditions, reactor concept and stages, heat management, and gas drying). This results in a large number of variants, which also differ in the investment costs.

Since not all possible variants can be analyzed in this study, the investment costs calculated thus serve as a guideline for cost estimation of future projects. The actual investment costs for a specific project, where the adaptations of the methanation plant to the respective framework conditions are considered, have to be analyzed in detail by the manufacturers and may differ from those estimated herein.

3.2.1 Literature review on EoS for methanation systems

The scale factors for biological and catalytic methanation systems are calculated using equation Eq. 1 based on the investment cost data taken from the literature review in Deliverable D7.5 (see Table 3-5). The mean scale factor for biological methanation systems is about 0.52 (range 0.39–0.73), and that for catalytic systems is about 0.64 (range 0.58–0.71). As mentioned, these values are based solely on cost data taken from the literature, where the investment costs are estimated for further analyses, since no commercial plants are offered by the manufacturers. Therefore, these values can be used only as a rough guideline.

Table 3-5: Calculated scale factors for methanation systems based on cost date from literature

Nominal power [MW]	Spec. investment costs [€/kW]	Investment costs [Mio. €]	Scale factor – related to the previous scale -	Mean scale factor -	Cost data based on source -
Biological					
0.2	320	0.06	-	0,52	[15]
1	120	0.12	0.39		
2	90	0.18	0.58		
1	1,439	1.44	-		[16]
10	371	3.71	0.41		
20	243	4.86	0.39		
50	168	8.38	0.60		
1	1,200	1.20	-		[17]
110	340	37.40	0.73		
Catalytic					
1	1,500	1.50	-	0,64	[15]
3	1,000	3.00	0.63		
6	750	4.50	0.58		
5	300	1.50	-		[18]
30	160	4.80	0.65		
110	110	12.10	0.71		
5	400	2.00	-		[19]
110	130	14.30	0.64		

Ref. [20] analyzed the cost improvement in chemical process technologies and identified a scaling factor of 0.56, based on 20 processes. While some are comparable to methanation, like Lurgi gasification or ammonia and ethylene production, others are substantially different, like the direct reduction of iron ore or oil sands extraction.

Ref. [21] reports that recent biorefinery installations exhibited a scaling factor on capital costs in the range of 0.63 to 0.72.

3.2.2 Calculation of specific investment costs of methanation systems due to EoS

This section calculates the specific investment costs for methanation systems with a nominal SNG output power in the range of 1–100 MW for 2020, 2030, 2040, and 2050 using the scale factor method (see Eq. 1) on a modular basis. The analysis does not use a single scale factor but divides the entire methanation system into individual modules, each with a separate assigned factor. Using this measure increases the accuracy of the cost estimation because the individual components react separately to the EoS effect.

The specific investment costs shown in Table 3-6 are used as initial values for the cost estimation by scaling for 5 MW_{SNG} methanation systems in 2020, 2030, 2040, and 2050. These investment costs are calculated in STORE&GO Deliverable D7.5 [2] and are solely based on the experience/learning curve effects of a 5 MW_{SNG} methanation system due to an increase in cumulative production volumes.

Table 3-6: Calculated specific investment costs for 5 MW_{SNG} methanation systems due to learning curves in 2020, 2030, 2040, and 2050 [2]

Year of installation	Specific investment costs [€/kW_{SNG}]	
	Catalytic	Biological*
2020	580	600
2030	440	390
2040	320	280
2050	280	240

*Based on expert interviews and current data, the specific investment costs have changed slightly from those calculated in Deliverable D7.5.

To increase the accuracy of the cost estimation, the methanation system is split into sub-modules (see Figure 3-8). This breakdown and the development of the appropriate cost shares are shown in the analysis of learning curve effects in STORE&GO Deliverable D7.5 and are here used to analyze the effect of EoS. The cost structure change is a result of the modularized determination of learning curve effects, whereby the individual modules are affected to different degrees.

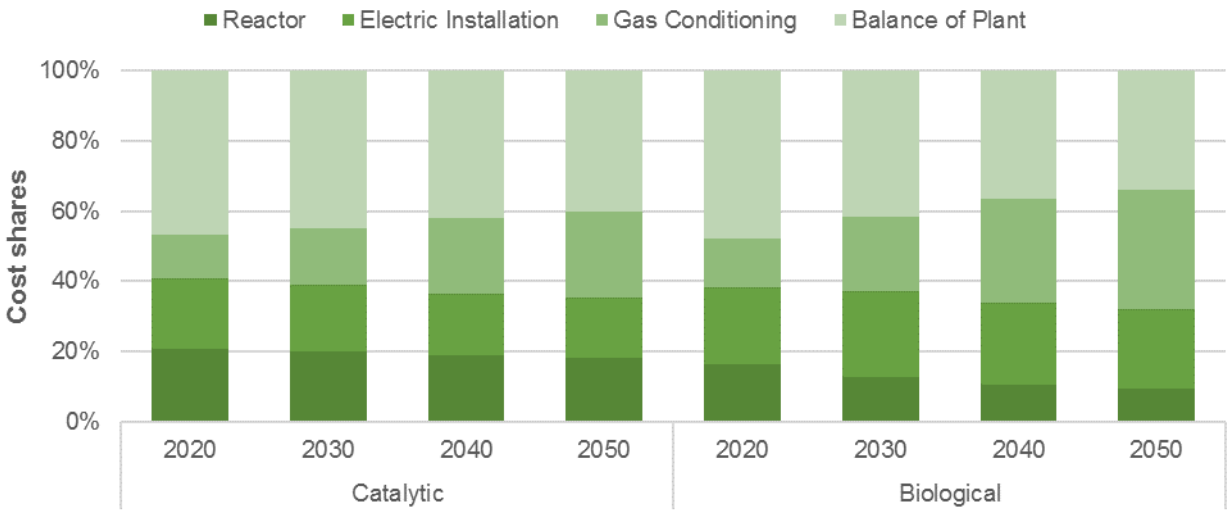

Figure 3-8: Development of the cost structure of 5 MW_{SNG} methanation systems due to learning curves in 2020, 2030, 2040, and 2050 [2]

For each module defined in Figure 3-8, an appropriate scale factor is assigned, as shown in Table 3-7. As the reactor module represents the primary difference between the two investigated methanation technologies, it is again treated in a more detailed way.

Table 3-7: Scale factors of the modules of methanation systems

Component	Scale factor	
	Catalytic	**Biological**
Reactor (initial)	0.67	0.51
Reactor	*0.56*	*0.50*
Catalyst	*1.00*	-
Heat Management	*0.56*	
Electric installation	0.75	
Gas conditioning	0.60	
BoP	0.67	

As was done for the stack modules of electrolysis systems, the scale factor for the methanation reactor module is calculated, based on the underlying components, as the product of cost shares and individual scaling exponents. Since the cost structure varies due to learning effects according to the installation time (cf. Deliverable 7.5 [2]), the resulting overall module scale factor is expected to be nonconstant as well.

The reactor is different for both technologies: for the catalytic reactor, a scale factor of 0.56 is used according to [1]; the biological case presumes an agitated reactor with an appropriate scale factor of 0.50 (cf. [13]). The catalyst, which represents the catalyst material itself in the catalytic methanation reactor, is not subject to EoS, as catalyst usage is presumed to be directly proportional to the nominal power and thus has a scale factor of 1. For heat management, mainly heat exchangers, a scale factor of 0.56 is assumed (cf. average values for heat exchangers in [1,13]). Additionally, especially the reactor for biological methanation does not show potential for large cost reduction via EoS because it is limited in design size for reasons like plant construction and transportation due to the height and diameter of the reactor. To increase the power of the SNG plant a numbering-up of reactors is necessary. To consider those effects, a dynamic scale factor is implemented for the reactor (cf. Eq.2), to provide a scale factor that is dependent on the system scale itself and minimizes scaling effects for large-scale applications.

The following table shows the presumed average maximum reactor size for biological methanation plants and installation years.

Table 3-8: Average maximum reactor sizes used for biological methanation plants per year of installation

Year of installation	avg. max. reactor size S_0 [MW_{SNG}]
	biological
2020	2
2030	5
2040	5
2050	5

Based on the power electronics of the electrolyzer, a scale factor of 0.75 is chosen for the electrical installation module of the methanation system. Based on data in the literature on gas conditioning components, mainly consisting of equipment for drying and cooling (scale factor: 0.52) and SNG purification (0.81), an average scale factor of 0.60 is set for that module. The BoP module includes many different components, like pumps, valves, tanks, fitting, piping, sensors, frame, and housing. According to the six-tenths rule, a scale factor of 0.60 is set for components for which data are missing (this assumption is supported by data in [1] and represents an average value). In combination with the scale factors found for the other components of the module (cf. [1,13]), an average medium scale factor for BoP of 0.67 is assumed. A more detailed compilation of the values and components used is provided in the appendix.

The investment cost of methanation plants in a power range of 1–100 MW are calculated for 2020, 2030, 2040, and 2050 by applying equation Eq. 1 to estimate the investment costs by scaling using the above data (specific investment costs for the 5 MW reference system, cost structure, and scale factors for the modules). The results are shown in Figure 3-9 and Figure 3-10 for catalytic and biological methanation systems, respectively.

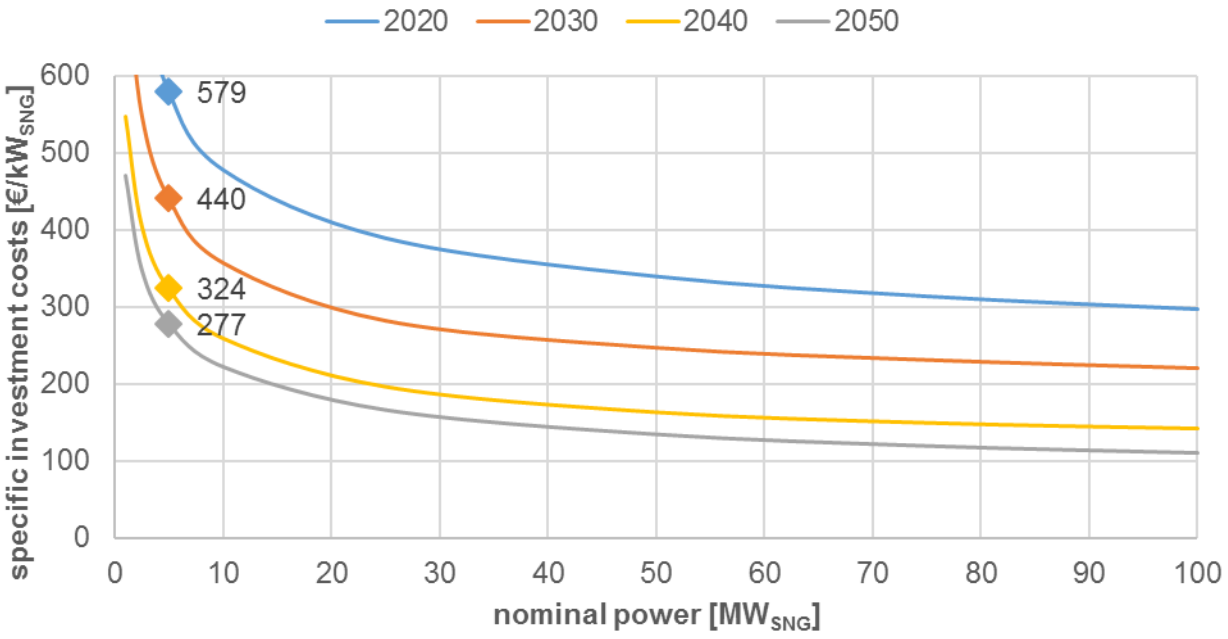

Figure 3-9: Specific investment costs of catalytic methanation systems due to economies of scale for a nominal power of 1–100 MW_{SNG} in 2020, 2030, 2040, and 2050

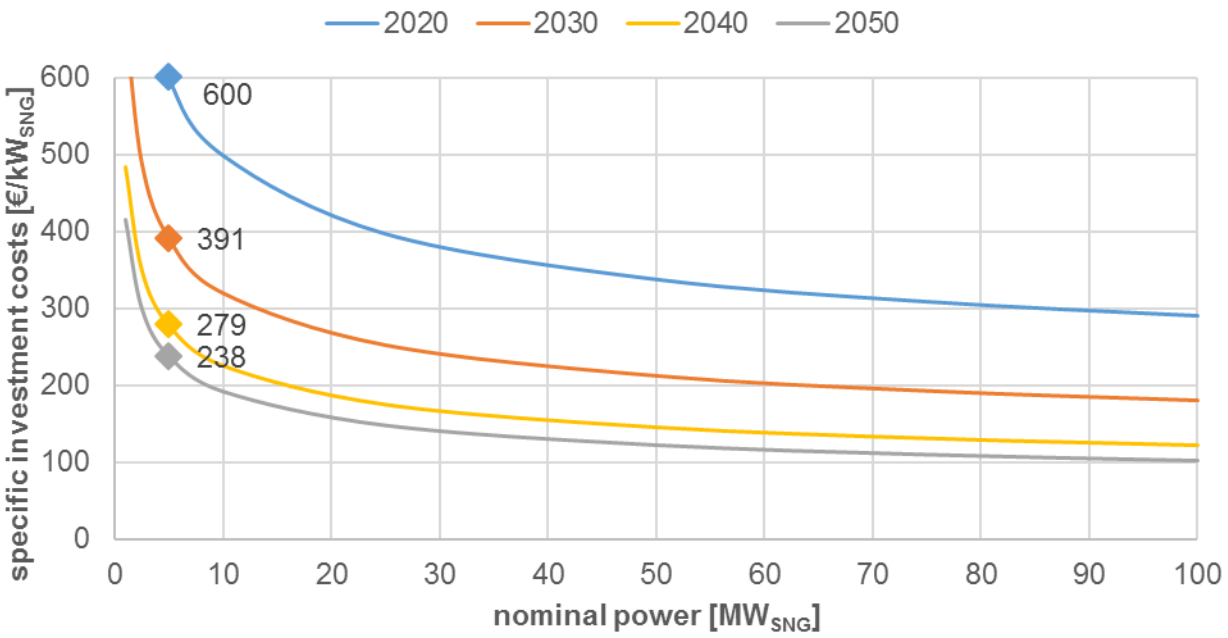

Figure 3-10: Specific investment costs of biological methanation systems due to economies of scale for a nominal power of 1–100 MW in 2020, 2030, 2040, and 2050

A single scale factor for the entire methanation system can be derived from the investment costs calculated using the modular approach, as shown in Figure 3-11. The calculated average scale factors for both methanation technologies are in the same range, of about 0.68 to 0.73 depending to installation time, since the cost structures do not significantly change. The difference in scale factor between smaller (1 MW) and larger (100 MW) systems range from 0.02 to 0.09. Larger systems have a higher scale factor due to the necessity of numbering up the reactors, since a larger reactor is not possible for manufacturing reasons (for biological methanation an average maximum reactor size of 5 MW is assumed).

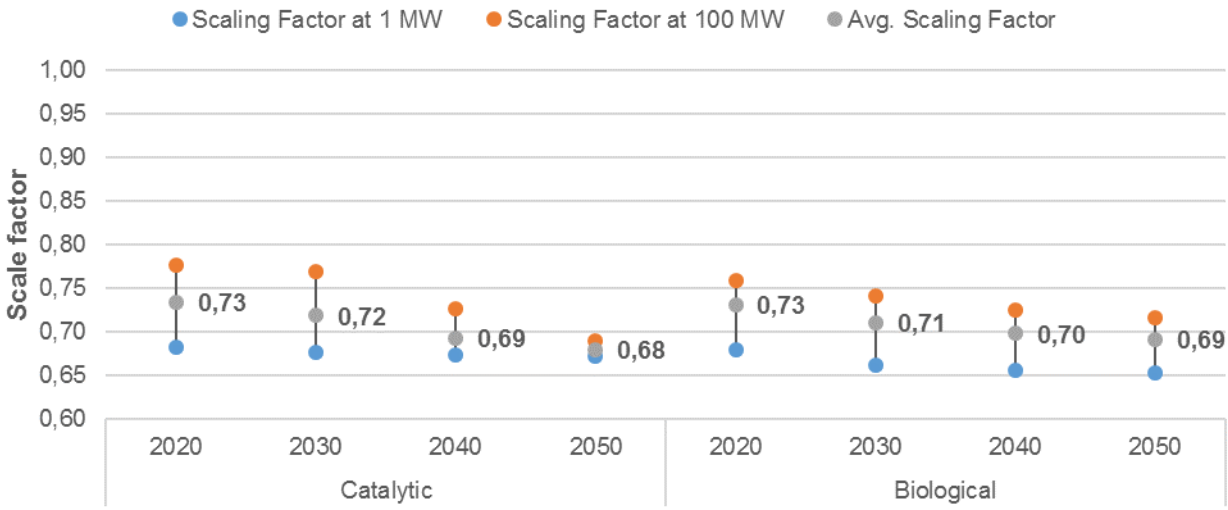

Figure 3-11: Future development of the range and average scale factors for methanation systems with a nominal SNG output of 1–100 MW

The results for the catalytic methanation system are close to the trends identified in the literature. The average values for the biological system calculated via the modular approach are a little higher than those in the literature. This is partly because this Deliverable's modular approach does not consider smaller-scale systems with capacities below 1 MW, given our focus on large-scale storage systems. Nevertheless, the investigations above suggest that scale factors < 0.60 seem to be rather

low. Therefore, it must be assumed that additional effects, like technological learning, are incorporated in the literature's data and that the values shown in Table 3-5 do not consider only EoS.

3.3 Alternative to scaling up: Modular design/Numbering up

Besides economies of scale, numbering up due to a modular plant design is another way to increase the nominal power of a PtG plant. A modular PtG plant structure can offer economic and technical advantages. The economic advantages include the following [22]:

- Costs: lower production costs due to series components;
- Delivery date: delivery time is shortened and on-time delivery increases massively
- Production time: low cycle time for modular systems (faster configuration and commissioning)
- Quality: larger quantities require and allow more time for development and design (higher cost pays off due to economies of scale)
- Flexibility: modules can be changed, replaced, modernized; thus, machines become more flexible and versatile, and their service life increases
- Service: better service options and faster reparation through standardized modules
- Operating factor: clear operating communication of modular machines leads to simple and intuitive operation

All the cost reductions due to series components, the reduced production time, and the increased quality lead to a reduction in investment costs. These were considered in the analyzes of learning curves in STORE&GO Deliverable D7.5 [2]. The modular design can also offer advantages in terms of technical parameters like plant efficiency, H_2 and SNG output, and lifetime, which in turn influence the economy of the plant. However, a modular design also has the disadvantage of losing the effect of EoS (especially in the case for methanation units).

In the modular design of a PtG plant, a distinction must be made between the two main components—the electrolyzer and the methanation—as these have fundamentally different structures. An electrolyzer is built up of cells, coupled to form a stack, and then connected to build an electrolyzer module; if necessary, they are clustered for large capacities. Therefore, a part of each electrolyzer has a modular design. Methanation, which is based on the principle of classical plant engineering, behaves differently.

The modular design of electrolyzers can be divided into two levels. On the micro level, a large number of identical cells are stacked one on top of the other to build the electrolyzer cell stack (see Figure 3-12).

Figure 3-12: PEM electrolyzer stack [23]

On the macro level, a number of identical electrolyzer stacks are connected to an electrolyzer system to increase the rated output. As mentioned, the STORE&GO project "Innovative large-scale energy

storage technologies and PtG concepts after optimization" deals with large-scale PtG concepts. Covering global PtG demand in 2050 would require the installation of about 6,500 to 14,200 GW electrolysis power capacities (see estimation on PtG demand in Deliverable D7.5). Not only a large number of electrolyzers are necessary, but they must also have a correspondingly high rated power. Even the manufacturers of electrolyzers have recognized the need for plants with a high nominal output and are offering even already today, systems up to the three-digit MW range. So far, however, no plants of this size have been realized. The largest electrolyzers are used in such projects as H2Future (with 6 MW) and REFHYNE (with 10 MW). Due to the technical limitations (the nominal power of a single stack is limited due to design features such as the sealing of the cells), these high rated outputs can be achieved only with a modular design. Figure 3-13 shows examples of a modular electrolyzer design on a macro level.

To achieve high rated output (> 10 MW), several stacks/electrolysis modules must be interconnected (see Figure 3-13), since a stack, as well as the resulting electrolysis module, is limited in size (nominal power). Currently, a single electrolyzer stack has a nominal power of about 2 MW (cf. [24], [25], [26]). Therefore, a modular design is mandatory. However, the number and size of electrolysis modules/stacks are not selectable or changeable but are determined by the manufacturer. Module control and operation are ideally optimized. This also includes the steady state and transient behavior. For small electrolyzers, with a capacity < 2 MW, it is possible to choose between an electrolyzer consisting of a single stack or one consisting of several smaller stacks (i.e., modular design).

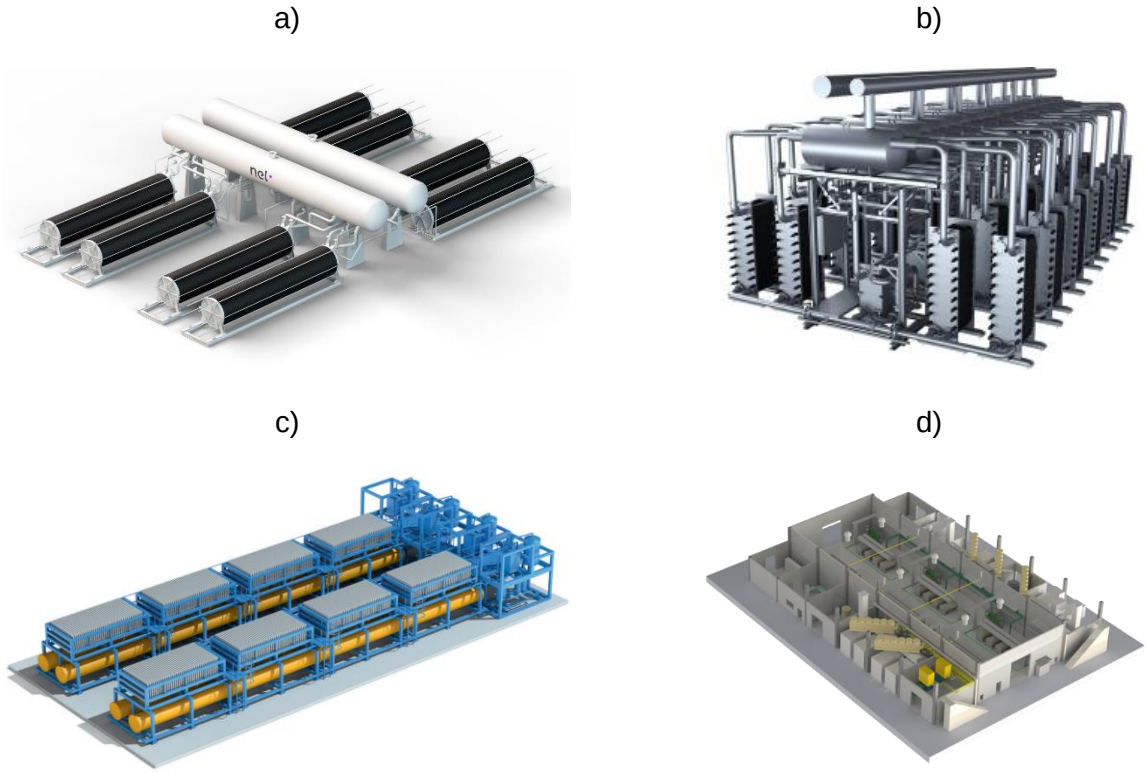

Figure 3-13: Examples of modular electrolyzer design (a-[24], b-[26], c-[27], d-[25])

Due to the wide range of possible applications, the PtG system has different modes of operation, such as continuous or intermittent. The different input load profiles of the use case (powered by a wind farm, photovoltaic power plant, or public grid) determine the operating hours, efficiency, hydrogen production, and number of start-stop cycles of the PtG plant. These characteristic features have a direct impact on the economic profitability of the plant (discussed in detail in chapter 8).

A modular design can have advantages in applications with intermittent load profiles by merging individual modules to a network managed by an intelligent controller:

- *Operation in the optimum efficiency range*
  Up to a certain share of the nominal power of the plant, the individual electrolysis modules can be operated in the optimum efficiency range.
- *Minimization of start/stop cycles, which increases the service life of the individual modules*
  In order to provide a certain power, not all modules must be in operation and thus switched on. This reduces the number of start/stop cycles, which can have a positive effect on service life.
- *Possibility of individual module maintenance*
  Not all modules need to be in operation. Maintenance work can be carried out on the shut-down modules.
- *Adaptation to input; extension or reduction easily possible*
  If the power from the power supply changes (e.g., the wind farm is extended) or more gas have to be produced, the power of the electrolyzer can be easily extended by adding modules.

The most important thing about the modular design of electrolyzers is the intelligent control of the individual modules. This must be adapted to the application (wind, PV, power supply, energy input) and optimized according to the corresponding target parameter (efficiency, service life, maintenance).

Regarding the modular design of methanation plants, these systems are built on the concept of classic plant engineering, as mentioned. The advantages and disadvantages of the modular design trend are discussed in COPIRIDE [28] and F3-Factory [29]. A modular plant design can make a chemical plant more flexible and efficient, but at the cost of a loss of EoS. [30] analyzed the fixed capital investment of modular plants and concludes as follows:

> *Based on the results derived with the developed model, we expect that positive effects resulting from modular design on engineering and construction costs can nearly compensate the loss of economy of scale considering the complete modular production plant. Concluding, investment costs are not expected to be tremendously higher for modularly built plants so that other influences attributed to the modular concept can take effect like early production start with small production capacities followed by sequential capacity increase, efficiency increases and further advantages* […]. *This would mean an economic improvement and a reduction of investment risk in view of the modular plant's life cycle.* [30]

The reduction of economic risk (especially for new technologies) due to modular design is also mentioned in [31] and [32]. Regardless of whether it is a single large methanation plant or a plant constructed from individual modules, the intelligent control system has enormous implications for optimal plant operation.

4 Technology characteristics – State of the art and future prospects

This chapter identifies the state-of-the-art characteristics of electrolysis and methanation technologies, as well as the expectations for their development. A reasonable set of key performance indicators (KPIs) is defined for electrolysis and methanation and are evaluated for the appropriate sub-technologies.

4.1 Electrolysis

The three electrolysis technologies under investigation differ in their individual characteristics, like energy input (electricity and eventually heat), operating temperature, pressure, and start-up times, especially when comparing low- and high-temperature electrolysis or different use cases. Hence, no definition of uniform KPIs throughout the whole category of electrolysis, or a determination of distinct and comparable values for each underlying technology, is possible. The following KPIs have been identified and defined as a subset of the characteristics that are relevant for hydrogen production from renewable electricity for energy storage and grid balancing as a major use case of PtG, particularly in relation to STORE&GO.

Key Performance Indicators:

1. Operational characteristics
   - Cell temperature
   - Operating pressure
   - Current density
2. Capacity
   - H_2 production per stack
   - Max. nominal capacity per system
   - Cell area
3. Efficiency
   - Nominal electrical system/stack efficiency
4. Durability
   - Stack/System lifetime
   - Efficiency degradation
5. Flexibility
   - Load flexibility
   - Cold/Warm start-up time
6. Economic characteristics
   - CAPEX
   - OPEX

4.1.1 SoA and recent development

Renewable hydrogen has gained increasing attention due to its potential fields of application in a carbon-free energy system (e.g., mobility, energy storage), and electrolysis technology has significantly evolved over recent years. Table 4-1 illustrates these technological developments as described in comprehensive studies that compare the current state of the art to expected improvements.

Table 4-1: Electrolysis – State-of-the-art and recent development

Parameter	AEC			PEMEC			SOEC[1]
	2011[2]		2017[3]	2011[2]		2017[3]	2017[3]
	SoA	prospect (5-10 yrs)	SoA	SoA	prospect (5-10 yrs)	SoA	SoA
Operation							
Cell temperature (°C)	60-80	60-80	60-90	50-80	60-90	50-80	700-900
Cell pressure (bar)	< 30	60	10-30	< 30	60	20-50	1-15
Current density (A/cm²)	0.2-0.4	<0.6	0.25-0.45	0.6-2.0	1.0-2.5	1.0-2.0	0.3-1.0
Capacity							
H_2 production per stack (Nm³/h)	< 760	< 1,000	1,400	< 10	< 30	400	< 10
Max. nominal stack capacity (MW_{el})	3.2-4.5	4.2-5.5	6	< 0.1	< 0.15	2	< 0.01
Max. cell area (m²)	4	4	3.6	0.03	0.13	0.13	0.06
Efficiency							
Nominal stack efficiency ($\%_{LHV}$)	51-71%	55-71%	63-71%	54-71%	60-73%	60-68%	100%[4]
Nominal system efficiency ($\%_{LHV}$)	43-67%	50-68%	51-60%	40-67%	55-70%	46-60%	76-81%
Durability							
Stack lifetime (kh)	< 90	< 90	55-120	< 20	< 50	60-100	8-20
Degradation (µV/h)	< 3	< 3	1-2	<14	< 9	4-8	< 7.3
Flexibility							
Min. part load (%)	20-40	10-20	> 20	< 10	< 5	> 0	-100

[1] due to pre-commercial status of SOEC, reliable data from earlier states is not available in a comparable extent
[2] values acc. to [33], if not mentioned differently
[3] values acc. to [34], if not mentioned differently
[4] operation at thermo-neutral voltage

Table 4-1 shows a positive development of water electrolysis over the last eight to 10 years. For several characteristics, like stack and system capacity and stack lifetime and degradation, the development so far outperforms the values proposed in 2011. Systems have significantly improved, especially in terms of PEM electrolysis. For example, the maximum available system and stack production capacities are currently far beyond the values proposed only a few years ago. The same is true for stack lifetime and degradation rates, as well as flexibility properties. This highlights the efforts that have been put into the technology and shows its relevance for future energy systems.

While the pre-commercial status and intense development of high-temperature electrolysis makes a detailed analysis of individual parameter evolution difficult, the values given in Table 4-1 for the current state of the art show that the technology is about to progress along with concurrent low-temperature systems. However, no verification of performance in large-scale applications has been made.

4.1.2 Expected future development

A comprehensive overview of the future development of the KPIs is given in Table 4-2, which is based on the state of the art and future targets for hydrogen production from renewable electricity for energy storage and grid balancing prepared by FCH 2 JU in their Multi-Annual Work Plan [35].

Table 4-2: State-of-the-art and future targets for hydrogen production from electrolysis for energy storage and grid balancing

No.	Parameter	Unit	AEL			PEMEL			SOEL		
			SoA	FCH 2 JU target		SoA	FCH 2 JU target		SoA	FCH 2 JU target	
			2017	2020	2030	2017	2020	2030	2017	2020	2030
Generic System											
1	Electricity consumption @ rated capacity	kWh/kg	51	50	48	58	55	50	41	40	37
2	CAPEX @ rated capacity (system incl. commissioning)	€/(kg/d)	1600	1250	800	2900	2000	1000	12000	4500	1500
		€/kW	753	600	400	1200	873	480	7024	2700	973
3	OPEX incl. stack replacement	€/(kg/d)/yr	32	26	16	58	41	21	600	225	75
		€/(kW yr)	15	12	8	24	18	10	351	135	49
		$\%_{CAPEX}$/yr	2	2,08	2	2	2,05	2,1	5	5	5
Specific System											
4	Hot idle ramp time	sec	-	-	-	10	2	1	-	-	-
5	Cold start ramp time	sec	-	-	-	120	30	10	-	-	-
Stack											
6	Degradation[1)]	%/1000h	0,1	0,1	0,1	0,3	0,2	0,1	2,8	1,9	0,5
7	Current density	A/cm²	0,5	0,7	0,8	2,0	2,2	2,5	-	-	-
8	Use of critical raw material as catalysts	mg/W Co	7,3	3,4	0,7	-	-	-	-	-	-
		mg/W PGM	-	-	-	5,0	2,7	0,4	-	-	-
		mg/W Pt	-	-	-	1,0	0,7	0,1	-	-	-

KPIs and values based on [35]

[1)] Degradation is defined differently for high and low temperature electrolysis:
AEC/PEMEC: percentage efficiency loss when run at nominal capacity;
SOEC: percent loss of production rate at thermo-neutral conditions and constant efficiency

4.1.2.1 Operational characteristics

The three technologies under investigation—AEC, PEMEC, and SOEC—differ significantly in their operational characteristics only in terms of their principles of operation. AEC and PEMEC represent low-temperature electrolysis, both supplied with liquid water and conventionally operated at temperatures of 80 to 90 °C. Operation at higher temperatures would be preferable by means of electric energy consumption, which is driven by reversible cell voltage. In the conventional case, alkaline cells are limited to between 100 and 120 °C using commercial diaphragms [36,37], while the Nafion® membranes used in PEM cells are known to loose water, and thus ionic conductivity, at temperatures above 100 °C [38]. Though laboratory applications are tested at elevated temperatures of 200 °C and beyond using alternative materials and solvents (cf. [36] and [38]), significant research efforts have to be made in material science to find a way to outperform commercial cells, including in economic terms. Therefore, an increase in operational temperatures for alkaline and PEM beyond 100 °C is not expected in the foreseeable future [33–35,37].

For solid oxide electrolysis, operating temperatures are typically in ranges of 650 to 1,000 °C [39]. On the lower side, this range is limited to about 600 °C, which allows a sufficiently quick start-up from standby in transient operation [33]. Generally, electric energy demand decreases as cell temperature increases, while the share of reaction enthalpy that can be covered by thermal energy increases. Hence, high-temperature electrolysis is more beneficial whenever an external heat supply is accessible.

Regarding storage densities, the compression of gaseous hydrogen is an energy-demanding task that significantly decreases overall system efficiencies. The elevation of operating pressure for electrolysis is a potential way to provide high storage densities. However, pressurized operation depends largely on the manufacturer's design choice and system philosophy. Systems with output pressures of up to 80 bar are reasonable in the near future, depending on the demand, thus eliminating the first stage of external compression and allowing direct feed into distribution gas grids [12,40]. Though pressurized systems of 100 bar and above for the direct usage at hydrogen fuel stations have been investigated by several manufacturers and research projects, no widespread rollout is expected within the next few years [41].

Concerning current electrolysis cell densities, the state of the art has not significantly changed in recent years (cf. Table 4-1). Most of the literature foresees only marginal increases in the intermediate term, reaching values of 0.8 to 1.0 A/cm² (AEC), 2.5 to 3.0 A/cm² (PEMEC), and about 1.0 A/cm² (SOEC), respectively (cf. [12,33,40]). Significant increases are expected over the long-term. This is particularly interesting in the case of alkaline cells, with values of up to 2.0 A/cm² [40], as this could result in a decreasing CAPEX, which would be a competitive advantage for this already mature technology. Moreover, PEMEC and SOEC are expected to increase their densities up to a factor of 2 until 2050 (PEMEC: ~3.5 A/cm², SOEC: < 2.0 A/cm²; according to [40]).

4.1.2.2 Capacity

The hydrogen production rate per stack, or, rather, nominal stack capacity, is rapidly rising for all three electrolysis technologies and is already outperforming expectations, as shown in Table 4-1. Hence, estimations of the future development of stack and system sizes based on the literature are difficult. The comprehensive study of E4tech done in 2014 [12] proposed stack capacities of up to 7.8 MW_{el} for alkaline and up to 10 MW_{el} for PEM cells for the intermediate term (2030), which is, at least for AEC, not that far beyond actual values. Total system capacities are somewhat different; the estimations for alkaline electrolysis are close to the maximum stack values (tending single stack systems), while PEM-based processes are expected to use multiple stacks with total capacities of up to 90 MW_{el} by 2030 [12].

Regarding the active cell area, which partly correlates with the maximum stack capacity, the value is expected to increase as the technology develops, especially for PEM and solid oxide cells. Future cell areas may be in the range of

- less than 10 m² for alkaline electrolysis,
- less than 1 m² for PEM and
- less than 0.1 m² for solid oxide electrolysis,

resulting in a difference of one magnitude between each technology [40].

4.1.2.3 Efficiency

At the current state of the art, the electric efficiency of PEM electrolysis is slightly below that of alkaline technology [34]. This gap may grow in the near future but will narrow over the long term. According to recent studies, values above 70%$_{el,LHV}$ (related to LHV) on the system level will be reached [39,40]. The electric efficiency of high-temperature electrolysis is already exceeding 76%$_{el,LHV}$ on the system level [34], and only marginal improvements are expected [40]. Due to the possibility of heat being supplied from external sources (e.g., industrial waste heat, solar or geothermal energy), the technology already provides electric efficiencies of 100 %$_{el,LHV}$ and above (for endothermal operation) on the stack level and is primarily a matter of thermal management and the availability of external heat.

4.1.2.4 Durability

As mentioned, improvements in the durability of electrolysis stacks and systems have been significant and have even outperformed the proposed targets in recent years (cf. Table 4-1). An additional increase in stack lifetimes is expected for all available technologies, reaching values of 125.000 h and above for low-temperature electrolysis cell stacks (AEC, PEMEC) and up to 100.000 h for SOEC stacks [40].

On the system level, lifetimes are already at quite competitive levels of 20 to 30 years for alkaline and PEM technology. SOEC technology is expected to reach a similar lifetime, of about 20 years, as soon as it is available on the required scale, though little improvement is expected in the longer term. AEC and PEMEC systems may be able to improve their lifetimes slightly, with alkaline reaching up to 40 years for large-scale applications [40].

Degradation rates, and therefore stack lifetimes, are highly dependent on operational parameters, such as operating temperature and pressure. Transient operation also has a significant effect. As the impacts of start–stop cycles are not yet well-quantified, systematic studies are necessary to understand these degradation mechanisms [34].

4.1.2.5 Flexibility

As illustrated in Table 4-1, the part load behavior of state-of-the-art electrolyzers is already quite close to technical limitations. For alkaline electrolysis, the minimum load is limited by the diffusion of hydrogen across the diaphragm to the oxygen side, which results in flammable mixtures at low production rates [34]. Nevertheless, further improvements in AEC technology are expected to reduce minimum load values to 10% [40].

Limitations in the part load behavior of water electrolysis on the stack level are becoming less important, as weaknesses in this area can be overcome by using a modular construction for electrolysis systems, including multiple stacks. In this way, load ranges can be expanded through the adapted operation of individual units [40].

Start-up times from standby and cold state are also important aspects of operational flexibility. While it is expected that start-up times from standby will reach similar levels for all three technologies in the long run at levels below 1 minute, start-up from cold state is far more dependent on the technology. Whereas PEMEC systems are already showing reaction times in the range of single seconds, little improvement is expected for alkaline cells. Major improvements are proposed for high-temperature electrolysis, which is showing long warm-up times of multiple hours. This value may reach the level of alkaline cells, or even below, in the long run (by 2050), given proper heat management [34,40].

4.1.2.6 Economic characteristics

Capital costs for electrolysis are expected to significantly decrease, as it gains substantial market uptake due to learning curve effects and scaling of production, as discussed in STORE&GO Deliverable D7.5 [2]. Additional reductions expected from system scaling are discussed in section 3.1; these are mainly dependent on future system sizes.

Average operating expenditures are similar for PEMEC and AEC at 2% of CAPEX per year and at 5% of CAPEX per year for solid oxide cells. These values are not expected to change significantly in the intermediate future, as shown by the data given by FCH 2 JU [35] presented in Table 4-2. Furthermore, these costs are very sensitive to location and size [12]. Therefore, they have to be estimated in relation to the individual application.

4.2 Methanation

In this Deliverable, the methanation process covers the production of SNG (synthetic natural gas) from hydrogen gas, produced in an upstream electrolysis process, and carbon dioxide. This definition covers very different kinds of process chains, with a primary distinction between biological and chemical (catalytic) methanation. The KPIs used to evaluate these processes are defined below and generalize the characteristics of methanation. These KPIs are meant to be used to monitor and assess the development of the methanation process as part of the PtG concept and provide comparability among the different technologies.

KPIs:

1. Operational characteristics
   - Process temperature
   - Operating pressure
   - GHSV
2. Capacity
3. Conversion efficiency
4. Durability
   - Catalyst lifetime
   - Availability
5. Flexibility
   - Response characteristics
   - Cold start-up time
6. Economic characteristics
   - CAPEX
   - OPEX

4.2.1 SoA and medium-term prospects

Unlike for water electrolysis, few comprehensive reviews have evaluated recent developments in the underlying processes and applications of methanation technology, likely due to the lack of focus on that conversion step. In the PtG (or, rather, power-to-methane) process chain, methanation is primarily used to be able to integrate the produced gas into the existing infrastructure, such as for feeding into regional gas grids. In this context, the additional methanation step is taken into account in order to facilitate the acceptance of PtG and ensure rapid implementation. On the other hand, the underlying processes are already quite mature. Chemical CO and CO_2 methanation processes have been investigated for more than 100 years since being discovered by Sabatier and Senderens [42], while biological methanation is principally comparable to the processes used in biogas plants and can even be integrated into the same reactor (i.e., in-situ process) [43]. Therefore, most recent developments have tackled the optimization of reactor technologies, upsizing, and cost reductions [15,17,42,43].

Table 4-3 gives an overview of the technology characteristics of chemical and biological methanation.

Table 4-3: Technology characteristics for state-of-the-art methanation processes

Parameter	Chemical (catalytic) methanation		Biological methanation	
Operation				
Process temperature (°C)	200-700	[15,19,42]	15[1)]-98[2)]	[15,43]
Delivery pressure (bar)	< 80	[15]	> 1	[15,17]
GHSV (h^{-1})	3.000-6.000	[15]	< 110	[17]
Capacity				
Max. nominal production capacity (MW_{SNG})	< 500	[15]	< 15	[15]
Efficiency				
Conversion efficiency (%)	70-85	[15,44]	95-100	[15]
Durability				
Catalyst lifetime (kh)	24.000	[15]	-	[15]
Availability (%)	85	[15]	90	
Tolerance to trace elements (e.g. H_2S)	low	[17]	high	[17]
Flexibility				
Response characteristic (min)[3)]	< 5	[15]	seconds	[15]
Cold start-up time	hours	[15]	minutes	[15]

[1)] mesophilic methanogens
[2)] thermophilic methanogens
[3)] deployment time from standby

Table 4-3 illustrates the major differences between chemical and biological methanation. The elevated process temperature, resulting from the chemical process, allows the reuse of the reaction heat to, for example, supply an upstream high-temperature electrolysis application. By contrast, low-temperature heat, which has to be maintained for anaerobic digestion in biological methanation reactors, is hardly utilizable. Additionally, due to the low GHSV of the biological methanation, it requires

significantly higher reactor volumes to produce a given amount of SNG than are required by its catalytic counterpart. Meanwhile, the biological methanation route outperforms the catalytic one in terms of flexibility, conversion efficiency, and tolerance to impurities (like H_2S) in the input gas stream.

4.2.1.1 Operational characteristics

Recent research has investigated the thermal coupling of high-temperature electrolysis, operating at temperatures of up to 1000 °C and catalytic methanation (cf. [45,46]). Thermal coupling would allow the electrolysis to operate at its highest electrical efficiency by providing the necessary heat, such as for water pre-treatment (vaporization), from the exothermal methanation process. However, temperatures above 500 °C have to be avoided (depending on the catalyst), as sintering of the active catalyst leads to a loss of active surface area, resulting in reduced activity [47]. Catalysts for methanation processes at temperatures up to 700 °C are already available on the market [42,48]. Additionally, elevated temperatures in the methanation process do not thermodynamically favor the synthesis towards products [44]. Nevertheless, the integration with solid-oxide electrolysis is expected to foster further research and the utilization of high-temperature catalytic methanation.

The maintenance of methanogen-compatible temperature levels is critical for biological methanation. This results in a relatively low temperature level of 20 to 40 °C for the mesophilic case [15]. To achieve elevated temperature levels utilizable as heat supply (waste heat recovery), using thermophilic processes with optimal temperatures of up to 98 °C (*Methanopyrus* of the order of *Methanopyrales*; cf. [43]) is preferred, which also shows increased methane production rates [49].

As methanation represents an exothermal reaction with a negative change in molecules, the synthesis is thermodynamically favored at increased pressures. This is true for both chemical and biological methanation (cf. [19,42–44]). Since elevated pressure levels in the process are also preferable for storage density and transport (including injection to gas grids), an increase of this parameter is expected in future applications. This also allows an integration with pressurized electrolysis as a future field of application (cf. section 4.1).

4.2.1.2 Capacity

A limiting factor for the performance capacity of single methanation reactors is the gas hourly space velocity (GHSV) used in the reactor (the term “methane production rate” is also used for biological methanation, but it is not directly comparable). For biological methanation, this parameter is highly dependent on the methanogens (bacteria/archaea) used in the process. Therefore, a significant increase of maximum production capacity for that technology is not expected in the intermediate future. Catalytic methanation is already commercially available in multi-MW sizes (< 500 MW_{SNG} according to [15]; single plants for CO methanation from coal are also reaching capacities of up to 7 GW_{SNG} output [42]) but lacks electrolyzers in comparable sizes, which are required for PtG applications.

4.2.1.3 Conversion efficiency

Conversion efficiency heavily depends on operating conditions (temperature, pressure, dwell time) and usually has to be optimized to specific boundary conditions and integrated processes (e.g., HT-electrolysis, biogas plant). Furthermore, in many applications, the dedicated use-case defines the mandatory conversion rate and is therefore a determinant of what is necessary for recirculation and subsequent gas conditioning. If the product gas is to be fed-in to existing gas grids, the related requirements concerning gas quality, especially H_2 and CO_2 contents, have to be met. Hence, certain synthetic gas applications do not need the highest conversion rates in the methanation process.

4.2.1.4 Durability

Sensitivity to sulfur compounds in the feed gas is a main cause of catalyst poisoning in chemical methanation. Therefore, extensive knowledge of gas composition, particularly of CO_2 streams from industrial or biogenic processes, as well as of impurities is mandatory to ensure appropriate catalyst lifetimes. To achieve lifetimes above several hundred hours, state-of-the-art nickel catalysts require sulfur contents in the range of several parts per billion [42].

As mentioned, temperatures above 500 °C lead to the thermal degradation of conventional catalyst materials. Therefore, the application of high-temperature methanation will require the implementation of alternative catalysts. Appropriate materials are already available on the market but are not yet widely used [42].

4.2.1.5 Flexibility

While biological methanation reactors are not appropriate for applications with the highest production capacities, they provide significant advantages in terms of cold start-up time and response characteristic. Therefore, applications of the technology are expected to be used to balance power for fluctuating renewable energies in future energy systems.

In catalytic systems, transient operation often leads to vapor-solid reactions, thermal degradation, or the crushing of the catalyst [42]. Thus, chemical methanation faces problems that need to be solved if it is to reach the high flexibility levels attained by its biological counterpart.

4.2.1.6 Economic characteristics

The future development of investment costs for methanation plants have been discussed in this Deliverable (cf. section 3.2) and STORE&GO Deliverable D7.5 (cf. [2]).

Operational and maintenance costs are expected to be around 10% of CAPEX per year for both technologies. These include costs for catalyst replacement in the catalytic case and for heating demand and miscellaneous in the biological case [15]. In general, these costs are difficult to estimate using the literature, as they heavily depend on individual system boundaries and other aspects. However, the values are expected to be in the upper region and are expected to decrease as deployment increases. Other studies also anticipate such values (cf. [17,50]).

5 New developments, technologies, and materials

Much research has been performed on the implementation of PtG systems as energy storage for future energy systems. Gruber et al. recently stated that current PtG efficiencies could reach 76%, and increase to 80% in the future [51]. This section reviews the promising new developments and findings concerning electrolysis, methanation, and CO_2 capturing/separation, the three key technologies of PtG systems.

5.1 Electrolysis

Research on electrolysis is not focused only on enhancing existing systems (e.g., PEMEC, AEC, and SOEC); it is also focused on developing new types of electrolyzers. The key factors for improving electrolysis in the research are efficiency and costs. Research on both factors seeks to enable high-capacity implementation with comparably low levelized costs of energy.

Ogawa et al. show that research on water electrolysis has been increasing since 1980. Their yearly publication analysis has shown that the category “Anode and acid stable cathode for AEC and PEMEC” has the highest publication rate, followed by research on microbial electrolyzer cells (MEC), SOEC, AEC, and PEMEC. The first two categories of research have increased particularly rapidly [52]. Gruber et al. state that electrolyzer efficiencies can already reach conversion rates exceeding 90% and efficiency of around 80% [51].

5.1.1 Conventional technologies

Research on established technologies focuses on enhancing the technology by improving individual parameters. Since higher temperatures would have a positive effect on the reaction kinetics of the redox reaction as well as on water and heat management, improved thermal stability could increase the efficiencies of electrolyzers. The main problem with high temperatures in PEMEC is the degradation of the catalyst (e.g., due to carbon corrosion from the usage of a carbon matrix to stabilize Pt). Specifically, carbon corrosion could cause the Pt catalyst to detach, leading to a severe loss of platinum surface area [53].

To solve this problem, Pt nanoparticles are produced and stabilized with a siloxane matrix. Pyrolysis experiments have shown a homogeneous distribution at a temperature of 500°C. Experiments using a pyrolysis temperature of 600°C have led to Pt agglomeration. The siloxane matrix has shown slightly higher catalytic activity in the electrolysis process than the carbon-based matrix has. Thus, siloxane may be a good option for use as a Pt catalyst stabilizer for PEMECs and could increase efficiency through higher operation temperatures [53].

Tymoczko et al. found that selective Cu positioning could optimize the platinum electrodes used in PEMEC. Research has shown that monolayer copper has a positive effect on electrolyzer performance. The submonolayer of Cu atoms in the second atomic layer of the Pt(111) has shown the most active electrocatalytic behavior for the hydrogen evolution reaction in acidic media ever reported under comparable conditions [54].

Since most systems need a fresh water supply, operation in regions without sufficient resources would not be possible. Research is being conducted on the possibility of building electrolyzer systems that can be operated with seawater. The main problem is that conventional anodes would emit toxic chlorine and are not sufficiently resistant against degradation [55,56]. One of the most promising ways is to use molybdenum as electrode material. Fujimura described the possibility of using Mn-Mo oxide electrodes prepared by anodic deposition on IrO_2-coated substrate [56]. It has been

shown that such an electrode has a high oxygen evolution throughout a long period. It has also been found that Mn-Mo oxides have to be anodically deposited at 90°C to avoid the dissolution of the oxide. The long-term oxygen evolution efficiency could reach 99.6% with this technology [57]. It has further been shown that NiFe-layered double hydroxide and Pt nanoparticles are good catalysts for the electrodes. Dresp et al. used such electrodes for a system that was run only during daytime, since it used the electricity generated from photovoltaics. SEM investigations have shown a membrane-induced stability loss. During daytime, however, recovering effects have been found. Consequently, such a day–night cycle could be a way to use seawater with conventional electrolysis, by employing excess electricity drawn from photovoltaic electricity production [55]. Another way of avoiding the need for a fresh water supply is using high-temperature SOEC. Lim et al. have shown that contaminants such as sea salt are not found in the steam produced from seawater. Electrolysis has shown almost the same performance with seawater as was shown with fresh water, as well as similar degradation levels. The influence on performance of direct electrode contamination with sea salt was not investigated [58].

Besides the optimization of working temperature and fresh water supply, much of the research focused on cost reduction has sought new materials for existing electrodes, because current technologies use expensive noble metals of the Pt group. Reducing or eliminating noble metal content could reduce costs and make it easier to establish large-scale industrial electrolyzers.

Gabler et al. performed experiments with ultrashort pulse laser-structured nickel electrodes for AEC. It was found that this technique reduces overpotential by increasing the specific surface area of the Ni electrode. This method can be improved by activating the Ni electrode with a cyclic voltammetric reduction-oxidation pretreatment [59]. Hinnemann et al. showed another possibility for new electrode materials, wherein MoS_2 nanoparticles supported on graphite were used as a new type of electrode. This was shown to be a good alternative to Pt-group metals. Furthermore, Hinnemann et al. claimed that searching for new electrode materials with a quantum chemical method would be another option [60]. The catalytic activity of MoS_x on hydrogen electrolysis has also been shown by Zeng, et al. [61].

Liu et al. prepared nanohybrids consisting of carbon nanotubes with CoP nanocrystals through the low phosphidation of Co_3O_4 nanocrystals. These nanohybrids were shown to be a good electrocatalyst for the hydrogen evolution reaction. Therefore, it might be a good option for use as anode material, especially since it is inexpensive, acid stable, and highly active [62]. According to Jin et al., cobalt-cobalt oxide/N-doped carbon sheets hybrids increase the catalytic effect on the hydrogen and oxygen evolution reaction, and also has high stability as an electrode [63].

Another promising material is nickel-cobalt-iron layered double hydroxide, which has shown excellent electrochemical properties. It is an active electrode material, employed as a positive electrode with activated carbon employed as a negative one; it is also a good catalyst for the oxygen evolution reaction. In addition, it has shown good specific power and cycle life. Its positive properties can be attributed to the synergistic effects among the metal species, as well as to the mesoporous structure of the layered double hydroxide [64].

Mangan cluster research has shown that graphitic carbon-based electrodes coated with MnO_x have a catalytic effect on the oxygen evolution reaction when used as anodes. It has been found that they show good stability against corrosion, in contrast to electrodes based on buckypaper and carbon [65].

The CELL3DITOR project has conducted research seeking an additive manufacturing method for producing SOEC stacks. It has been reported that it is possible to sinter 8YSZ (yttria-stabilized zirconia) particles at temperatures of around 1300°C to reach a relative product density of up to 96%. This could allow the 3D printing of SOEC stacks in the near future [66,67].

5.1.2 Alternative technologies

Currently, AEC and PEMEC are the main low-temperature electrolyzers for pilot and industrial applications. Both use a membrane or diaphragm to separate the O_2 and H_2, and serve as transport medium for ions between the electrodes (see Figure 5-1 A and B). Esposito describes membraneless electrolyzers as a low-cost alternative to hydrogen production [68]. In this membraneless case, the separation of O_2 and H_2 is performed using fluid flow and/or buoyancy forces. Flow-by electrolyzers (see Figure 5-1 C) use the laminar flow of the electrolyte, which is parallel to the electrodes, while flow-through/buoyancy electrolyzers use a pressurized environment to force the electrolyte through the electrodes into different chambers (see Figure 5-1 D). In both cases, the products are separated. With this technology, a product purity of up to 99.8% H_2 can be achieved [68].

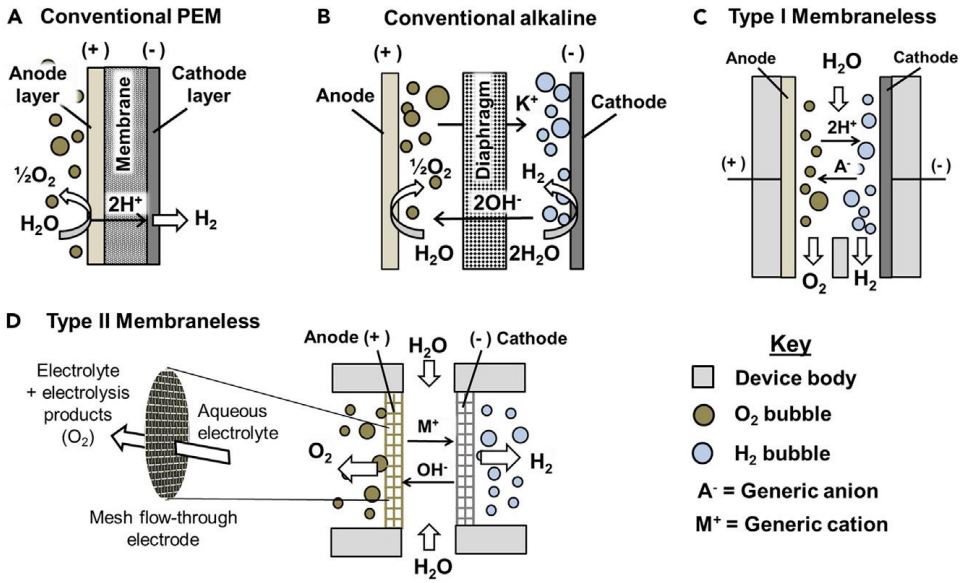

Figure 5-1: Schematic of classic (A & B) and alternative membraneless (C & D) electrolyser cells [68]

The design of membraneless electrolyzers is very simple compared to that of conventional ones, leading to a long service life, high tolerance to impurities, and operability in extreme conditions. Further, it works without an expensive membrane. Both lead to lower CAPEX and allow easier manufacturing. Additive manufacturing such as 3D printing could lead to lower investment costs. However, the high ohmic resistance of the electrolytic solution and the low voltage efficiency at high operating current densities are the main disadvantages of this technology. Lower purity compared to PEMEC is also a problem, which may make downstream purification necessary. Future challenges could be the scaling-up and material-related issues [68].

Experiments with plasma electrolysis have been performed on a small scale. This is a combination of electrolysis and pyrolysis. The redox reaction occurs without contact between the electrodes and the water. Electrolysis is performed at temperatures of 3,700°C. In plasma electrolysis, the power efficiency reaches 30% of the input voltage. This could provide a rapid and cost-effective option in the near future. Future research will focus on large-scale options for this kind of electrolyzer technology [69,70].

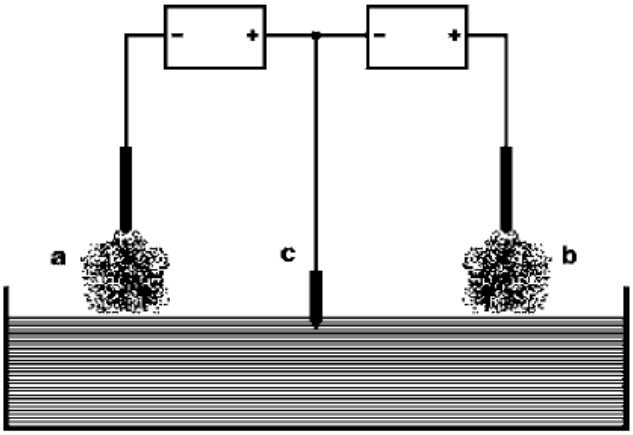

Figure 5-2: Schematic of a plasma electrolyzer [70]

5.2 Methanation

As mentioned, two different types of methanation can be used for PtG applications: catalytic and biological methanation. This section discusses new developments regarding both types.

Most of the research on catalytic methanation focuses on improving the cost and efficiency of the catalysts. Since the methanation reaction prefers low temperatures (<400°C) due to its exothermic character, catalysts have to be found that fulfill the necessary catalytic activity, even for low temperatures [71,72]. This is required to reach high-quality SNG, since natural gas networks are covered by strict regulations regarding it. For example, the requirement that must be met for the SNG to be fed into the natural gas grid is a CH_4 content of 96 vol.% or higher [73]. The second largest research area focuses on gas cleaning (specifically H_2 and CO_2 separation).

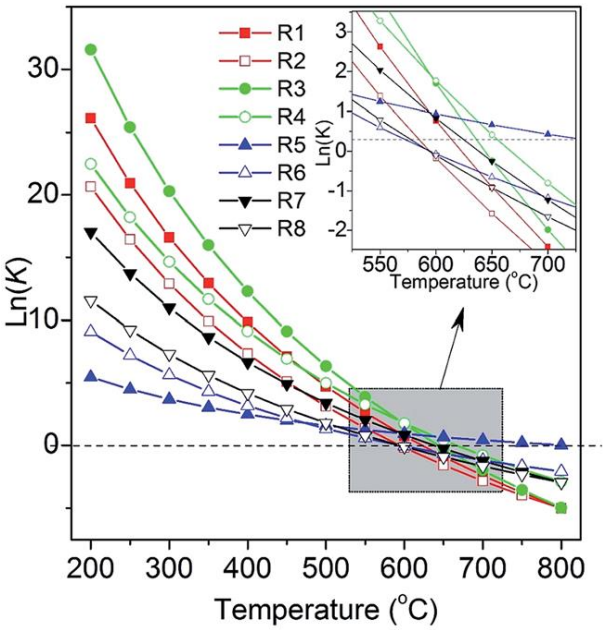

Figure 5-3: Equilibrium for different reactions that occur during methanation. R1 ($\boldsymbol{CO + 3H_2 \leftrightarrow H_2O + CH_4}$), R2 ($\boldsymbol{CO_2 + 4H_2 \leftrightarrow 2H_2O + CH_4}$) and R4 ($\boldsymbol{2CO \leftrightarrow C + CO_2}$) are the most important ones during methanation [71]

Studies have shown that the order of catalytic active materials for methanation is Ru > Fe > Ni > Co > Rh > Pd > Pt > Ir (see Figure 5-4). However, Ru and Co are very expensive compared to Ni. Therefore, Ni is the most frequently used catalyst. The problem with Ni is that it can form $Ni(CO)_4$, which has to be avoided since it is highly poisonous at low temperatures. The metals

are usually dispersed on supports as nanoparticles to achieve a high specific surface area for the catalyst. Al_2O_3 is one of the most common supports, but SiO_2,CeO_2, TiO_2, ZrO_2, and other oxides are also used [71]. Liu et al. analyzed Al_2O_3, CeO_2, and ZrO_2 as support materials and found that Al_2O_3 had the highest conversion rate. The second fastest reaction rate was with ZrO_2, and the third was with CeO_2. This effect can be seen in Figure 5-5 [74].

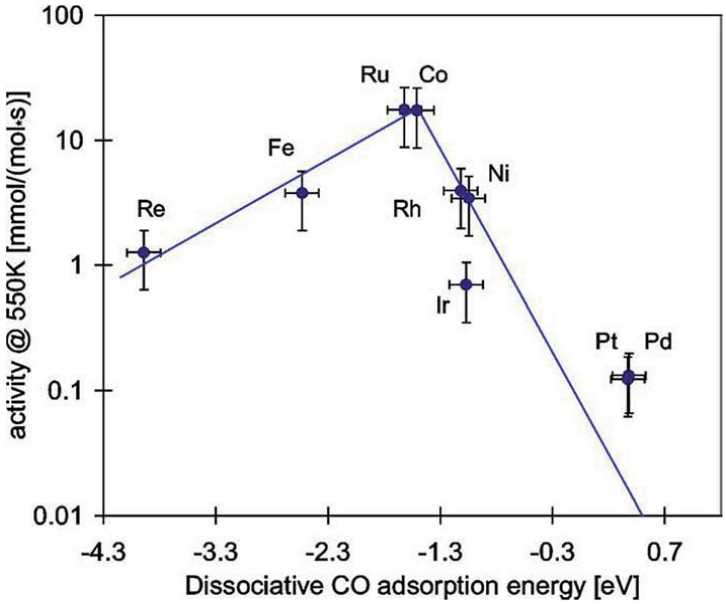

Figure 5-4: Activity of different catalysts for the methanation process [71]

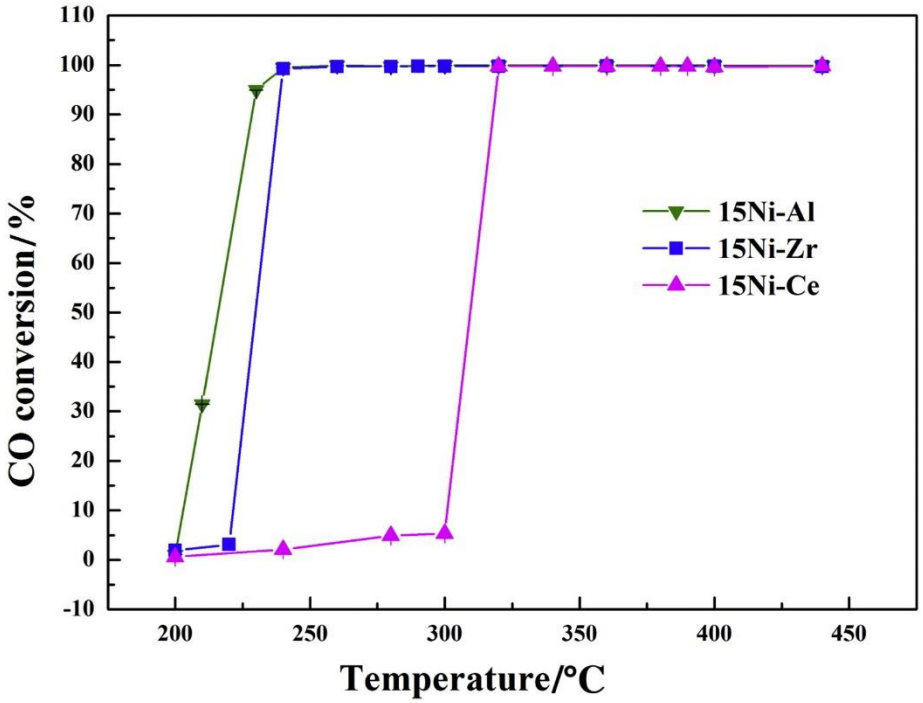

Figure 5-5: CO conversion rate on different support materials [74]

Biegger et al. developed an innovative methanation system that uses a washcoated honeycomb catalyst combined with a polyimide membrane for gas upgrading. The cordierite monoliths of the honeycomb catalyst are coated with γ-Al_2O_3 and nickel. Lab tests conducted with varying conditions have shown the production of high-quality SNG, with a CH_4 content of up to 68 vol.%. The membrane technology improved gas quality by raising the CH_4 content above 96 vol.% [73].

According to Gruber et al., it is possible to reach 77.5 % efficiency with a Ni-catalyzed fixed bed methanation reactor with an Al_2O_3-based support [51].

Besides improving the methanation process itself, it is also possible to improve the overall efficiency of PtG systems by enhancing the implementation of the methanation process in the overall process route. Kirchbacher et al. investigated one such possibility in 2018 by studying the direct integration of raw biogas into a methanation- and membrane-based PtG application. In this study, the PtG application was coupled with two-stage fermentation [75].

As shown in Figure 5-6, gas upgrading works well, and the requirements for the Austrian gas grid have been reached [75].

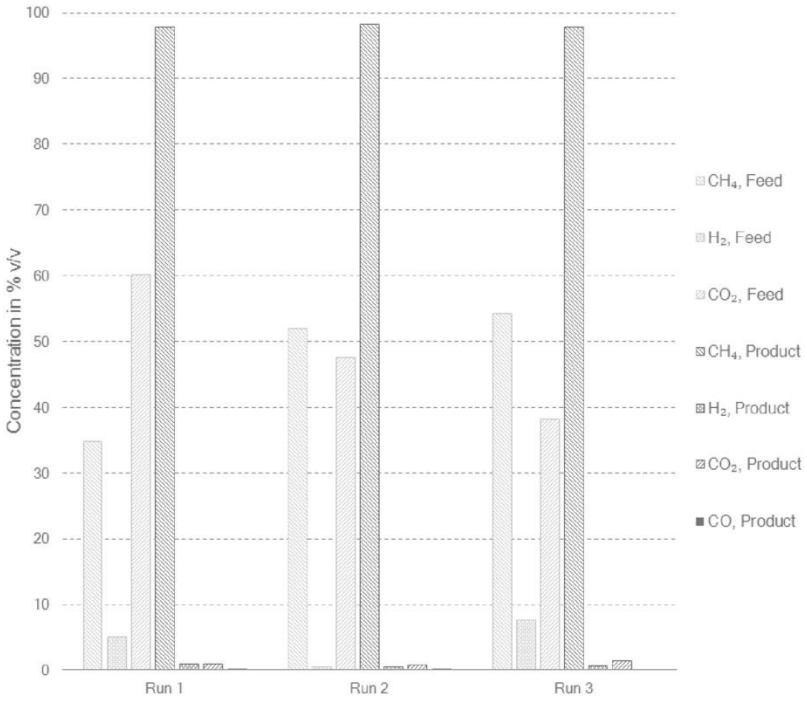

Figure 5-6: Results of the gas upgrading system of Kirchbacher et al. for different biogas compositions [75]

5.3 CO_2 separation

Absorption is currently the dominant CO_2 separation method in industrial scale. However, membrane technology is considered as a promising technology, but is still under development. The biggest problem with membrane technology in the industrial scale is its insufficient long-term stability and wetting under real operating conditions. Real gases consist of minor SO_x, NO_x, CO, and water content, which have a negative effect on the lifetime of polymeric membranes. Therefore, testing under real conditions is essential to make such technologies feasible for industrial scale. The catalyst of the methanation reactor has been based on Ni with Al_2O_3 as support (Meth 134® by C&CS). Thus, the reactor temperature of the setup has always been above 250 °C. The membrane material has been polyimide [76].

To commercialize the technology, the following factors have to be improved [76]:

- Plasticization resistance
- Thermal and chemical resistance
- Long-term stability
- Cost effectiveness

Norahim et al. has given a short overview of current polymers in a review on membrane separation technologies. It was found that polyimides perform better than the other polymeric membranes that were tested. This can be seen in Table 5-1 [76].

Table 5-1: Overview of currently developed membrane separation technologies [76]

Material	**Testing conditions**			**Performance**	
Polymer	T [°C]	p [bar]	CO_2:N_2	p_{CO2} [Barrer]	Selectivity CO_2/N_2
Polysulfone	RT	4	Single gas	0.71	1.61
Polysulfone	25	N/A	Single gas	6	38
Matrimid® 9725	25	10	Single gas	6.2	27.5
Matrimid® 9725	35	9	50:50	4	23
Matrimid® 5218	30	2	10:90	8	27
Matrimid® 5218 (HF)	35	4	55:45	16	28
Matrimid® 5218/PES, 80/20 (HF)	35	4	55:45	30	36
6FDA-TMPDA	35	60	10:90	400	17
Pebax® MH-1657	25	5	Single gas	55.8	40.2
Pebax® MH-1657	25	2	10:90	480	48
Pebax® MH-1657	30	2	Single gas	60	57
Pebax® MH-1657	30	0.6	Single gas	73	45
Pebax® MH-1657/PEG	30	0.6	Single gas	151	47
Pebax-1074	25	3	Single gas	111	50
Polytherimide	25	1	Single gas	1943	2.3
Cellulose acetate	N/A	3	Single gas	401	32.92

Table 5-1 also shows that, between Matrimid® and hexafluoro-substituted aromatic polyimides (6-FDA), the latter perform better due to the greater free volume following from the bulky $–C(CF_3)_2$ group in it [76].

6 Potential future fields of application

PtG is being promoted as a promising technology for providing chemical energy produced from renewable electric power in future low-carbon energy systems. The technology is known to provide significant advantages in storage density and, in combination with methanation, even acts as a carbon sink by supporting the long-term fixation of CO_2. Nevertheless, the process has conversion efficiency issues; this energy efficiency question constitutes a major disadvantage compared to the direct usage of renewable electric energy. Nevertheless, PtG is expected to be used in future renewable energy systems in certain applications. These future fields of PtG application are discussed below, as we provide an overview of the most promising research activities and proposed solutions.

6.1 Energy storage and transportation

Even though state-of-the-art PtG applications display significant conversion losses due to efficiency issues, they still have major advantages in achievable storage densities compared to other technologies, like the direct storage of electric energy in batteries (cf. Figure 6-1). PtG applications use significantly less space for larger storage capacities, keeping the sealing of land areas to a minimum, which is a desirable economic aspect. PtG also allows the long-term storage of excess energy in widely applicable energy forms, while the discharge times of competing technologies are far more limited, as shown in Figure 6-1. Additionally, the costs for storage and the transportation infrastructure required to handle increasing amounts of renewable power will be marginal, as the existing gas infrastructure can be used as long as the produced gas meets the appropriate requirements.

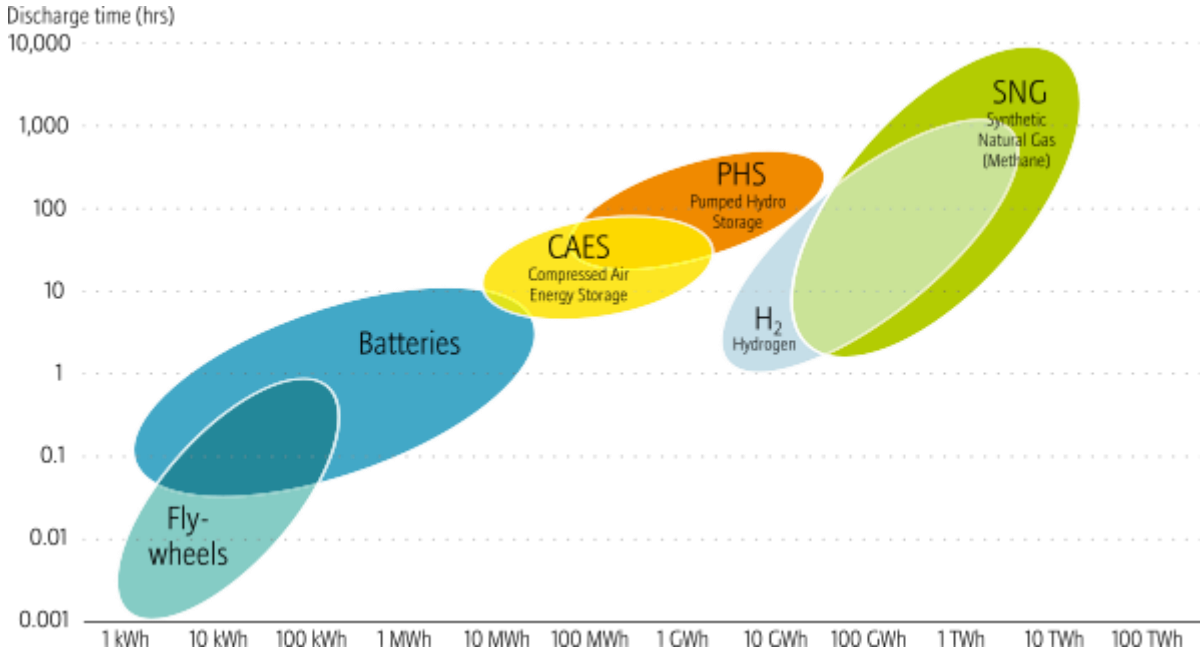

Figure 6-1: Storage capacity of different energy storage applications
Source: Renewables global futures report [77], Fraunhofer Institute, Germany, 2014; edited by author

The injection of hydrogen, or rather hydrogen-enriched methane, into existing regional (and supra-regional) gas grids and infrastructure has been intensively discussed in recent PtG considerations. This issue is critical, as the national requirements for gas quality and composition differ between gas-transiting countries. However, recent studies show that an increase of hydrogen content in the existing infrastructure is not necessarily a problem for subsequent utilization [78].

To allow centralized production and reduce efforts for transportation of energy TenneT plans to build an artificial island in the middle of the Dogger Bank in the North Sea, which has an average depth of 25 m and is therefore a promising location for offshore wind farms. This artificial island, dubbed the “North Sea Wind Power Hub,” is planned to connect wind farms with power of up to 100 GW by mid-century and provide the advantage of shorter power cables and reduced transport and maintenance costs. It will later be connected to grids in the Netherlands, United Kingdom, Belgium, Germany, Norway and Denmark [79,80]. A PtG plant could be used for storage of excess electricity production in the North Sea Wind Power Hub.

The question of disused natural gas fields is important in discussions about reusing existing gas infrastructure. Recent research [81,82] has shown that natural underground storage such as pore-space storage can easily be used for hydrogen injection to enable long-term storage without significant losses. As a positive side effect, investigations have shown that the presence of microbes in these underground storage spaces causes the transformation of hydrogen gas to methane when CO_2 is injected. This would avoid the need for subsequent methanation steps as part of the PtG plant. It is currently being investigated as part of Austria’s *Underground Sun Conversion* [83] research project. If the results are promising in terms of efficiencies, conversion rates, efforts for injection, and the removal of product gases (gas purity), this approach may be able to significantly reduce infrastructure costs for future PtG applications.

A similar approach was discussed by Jensen et al., who proposed the application of highly efficient PtG plants in combination with the underground storage of CO_2 and CH_4. The research claims that this would incur storage costs comparable to those for pumped hydro and much lower than those for previously proposed technologies [84]. Besides the integration of existing natural storages, this approach benefits from the thermal coupling of high-temperature electrolysis and methanation to achieve high round-trip efficiencies for electricity storage of 70% and beyond. The system is planned to use electrical surpluses for water electrolysis based on reversible solid oxide cell technology. This renewable hydrogen gas will then be chemically converted to SNG, while highly integrated thermal management between endothermal electrolysis and exothermal methanation will be used to increase overall electrical efficiency. The process can also be reverted by oxidizing the previously stored SNG in a reversible solid oxide cell, producing electrical energy if required. CO_2 from the oxidation process is again stored in underground storage. A schematic of the process is shown in Figure 6-2. [84]

This kind of application illustrates PtG’s potential as an energy-balancing method for handling excess and peak loads in future energy systems, which are dominated by fluctuating renewable energy sources like wind and solar power. By using high-temperature electrolysis in combination with integrated exothermal processes (e.g., methanation) or by being supplied with renewable waste heat from external sources, electrical conversion efficiencies above 85% are expected (cf. goals of the HELMETH project [46]), which are almost competitive with the direct storage of electric power (e.g., in batteries), especially when discharge times are considered (cf. Figure 6-1). A similar objective is being pursued by the Austrian HydroMetha research project [45]. In addition to the integrated thermal coupling of electrolysis and methanation, the process includes a chemical reduction of CO_2 to CO in the electrolysis step. This so-called “co-electrolysis” leads to further performance gains: first, the methanation of CO, instead of CO_2, is higher exothermal, providing additional heat, which can be recoupled to the solid oxide electrolysis cell; second, the chemical conversion of CO_2 within the electrolysis cell at elevated temperatures (e.g., 800°C instead of 250°C) allows for higher efficiency due to the reduced Gibbs Free Energy in the reaction [85]. Hence, overall conversion efficiency can be increased.

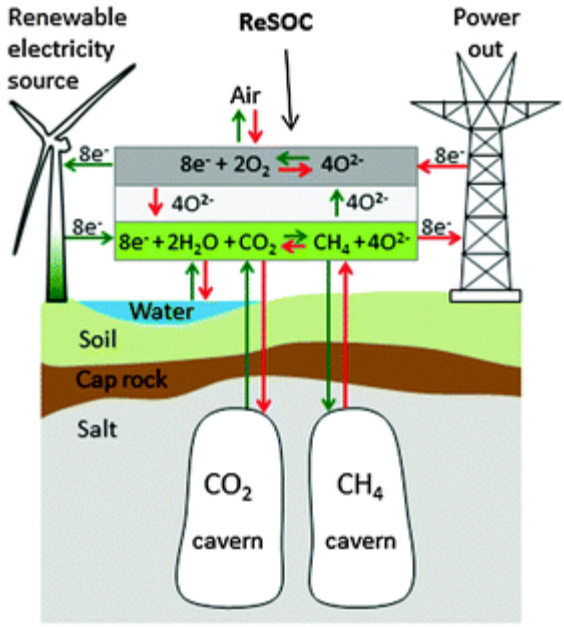

Figure 6-2: Schematic diagram of the rSOC electricity storage system [84]

6.2 Industrial processes

Due to its significant losses in energy conversion, PtG is often considered questionable as an energy source for carbon-demanding processes that could be electrified in the intermediate future. Hence, the electrification of individual processes for the direct usage of renewable electrical energy is the best method, providing the highest primary energy efficiencies and decarbonization in future energy systems dominated by renewables. However, PtG is still expected to play a valuable role in sectors where a complete electrification of incorporated processes is not expected in the near future but where the usage of fossil fuels and resources must be mitigated. In this context, PtG can serve as an interim technology on the path from highly established to stepwise, adaptable industrial processes, such as in steel production and chemical industries, where high amounts of fossil natural gas are processed.

Besides this prolonged sustainable usage of sophisticated production and conversion processes, highly efficient alternatives for almost non-electrifiable value chains have to be developed. In the steel industry, the direct reduction of iron by using renewable hydrogen from water electrolysis has been discussed in recent years. Various projects, such as H2Future [86], GrInHy [87], and HYBRIT [88], are seeking to identify the process chains that could meet today's standards.

The most common reduction agent in steelmaking is based on coal and therefore fossil resources. Hence, this must be replaced by renewable alternatives. The projects mentioned above aim to use product gases from a PtG application as a reduction agent. An example of a process scheme related to the HYBRIT approach with its specific energy carrier flow is shown in Figure 6-3 [89].

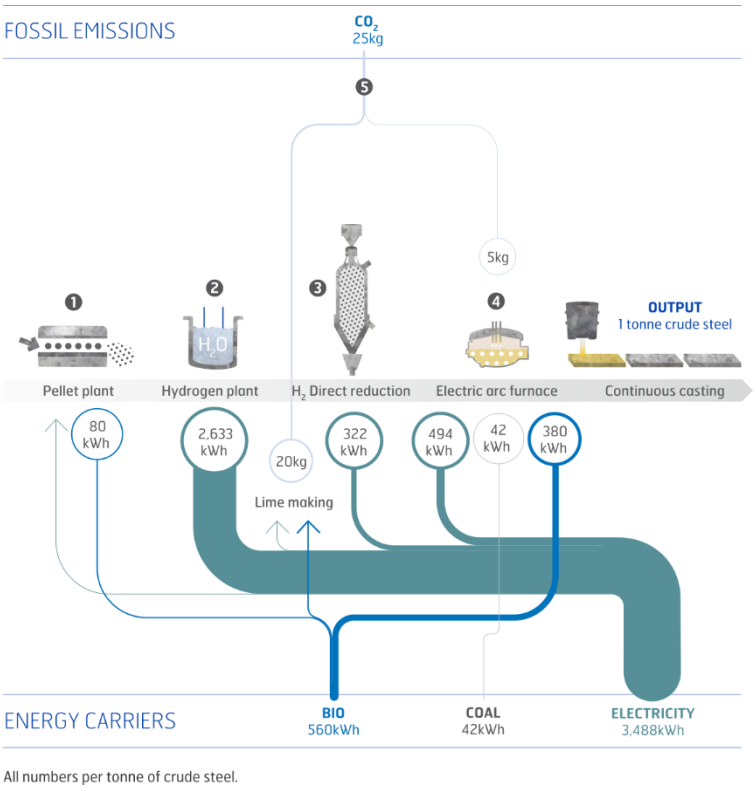

Figure 6-3: Scheme of the HYBRIT process flow and its energy balance [89]

In addition to the direct utilization of gases produced by PtG applications, particularly hydrogen and SNG, there are many ways that these could be further processed to generate renewable hydrogen- or carbon-based end-products. This process is commonly generalized under the term “Power-to-X” (PtX). PtX can provide sustainable solutions for decarbonization and CCU. Besides the long-term fixation of CO_2 (e.g., in renewable polymers), renewable hydrogen will be important in chemical industry. The fertilizer industry, for example, is a major emitter of CO_2 related to ammonia production, mainly based on hydrogen production from natural gas [90]. Alternatives are currently being investigated (cf., e.g. [91]).

6.3 Mobility

Another application of PtG, or rather PtX, is the generation of synthetic fuels, such as methane, methanol, and ethanol [92], as substitutes for fossils in conventional internal combustion engines, or using hydrogen directly in fuel cell electric vehicles (FCEV) [93]. Even though today’s focus is more on battery electric vehicles (BEVs), the competiveness in terms of cruising range is only partly given. Renewable gaseous and liquid fuels still outperform batteries in terms of energy density, as shown in Figure 6-1. This is especially true for light and heavy-duty commercial vehicles like trucks and buses, but also applies to shipping, which is highly dependent on fossil fuels.

Using hydrogen and carbon dioxide as base materials allows for the generation of a wide range of potential fuels. Using SNG in the form of liquefied natural gas (LNG) could be useful, especially in shipping [94]. An overview of potential synthetic fuel production routes is shown in Figure 6-4. Many public transport buses are already powered by natural gas rather than diesel. Hence, switching to SNG from renewable sources would not require additional adaptations or investments for vehicles.

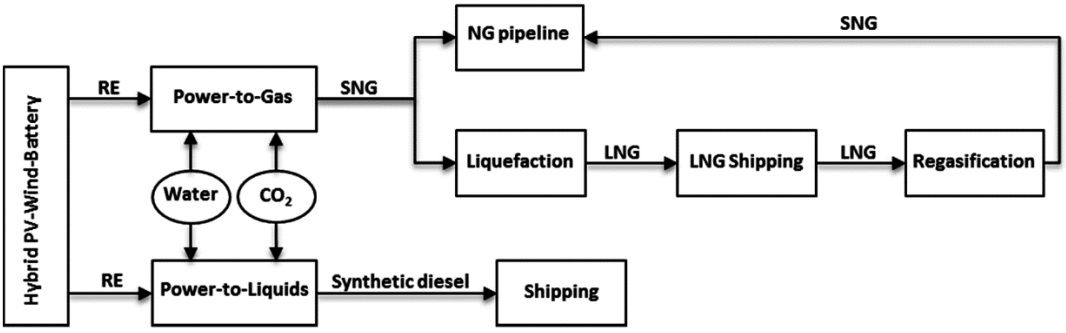

Figure 6-4: Overview of possible synthetic fuel production process routes [94]

For the direct usage of hydrogen in the mobility sector, energy conversion is performed in fuel cells rather than in combustion engines. This avoids the conversion losses of methanation (or any other fuel generation process), increasing overall energy efficiency.

Fuel cell-based drive systems are already available in many vehicles (cf. Figure 6-5). As mentioned, utility vehicles (for transporting both humans and goods) are benefiting from the range and weight advantages produced by the elevated energy densities (relative to batteries). Appropriate implementation for busses (cf. [95]) and trucks (cf. [96]) have been investigated and tested in various independent studies and pilot projects for fleets of up to medium size. Hence, hydrogen is a promising renewable mobility and fuel option for long-range fleets (e.g., in the transport sector), with short dwell times. [97]

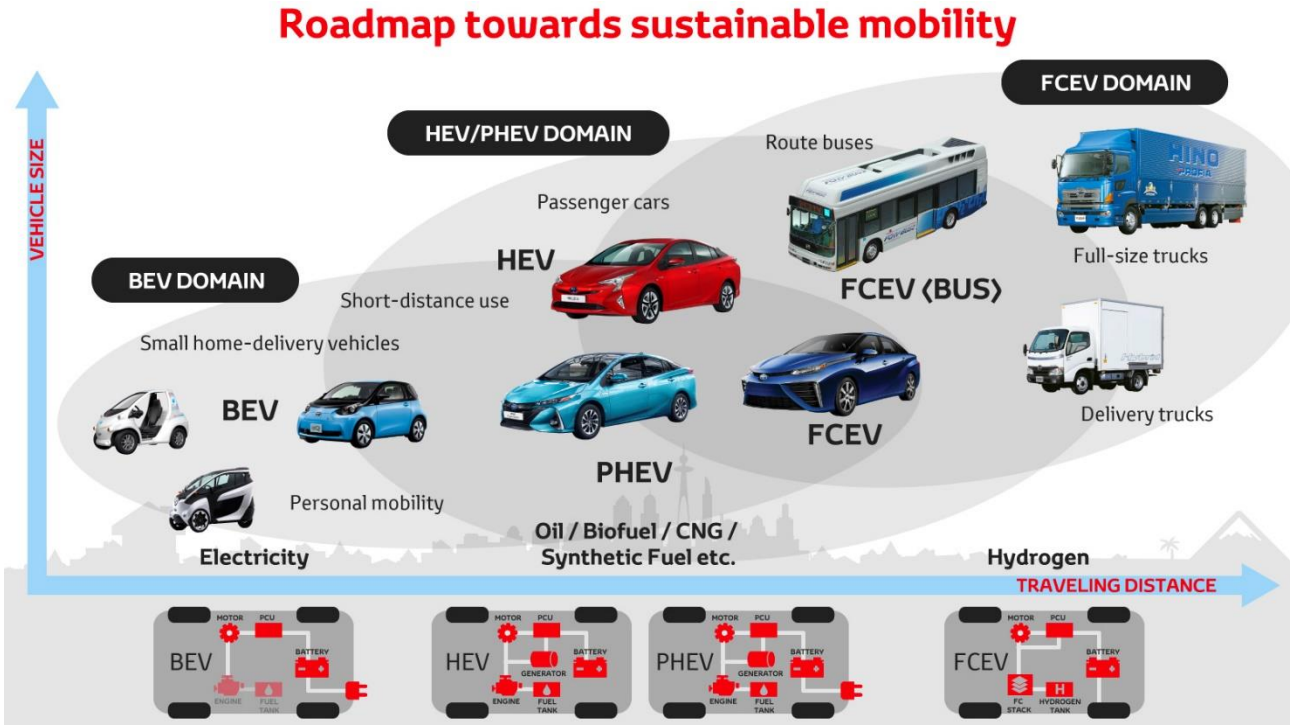

Figure 6-5: Overview of BEV and FCEV application fields [97]
(HEV…hybrid electric vehicle, PHEV…plug-in hybrid electric vehicle)

7 Economic evaluation

The many potential applications of PtG in the energy system may lead to various functions and benefits, from which numerous fields of application can be derived. The economic evaluation and analysis of the optimal plant configuration below is based on the specific production costs for SNG. The following fields of application are investigated:

1. PtG plant powered by a photovoltaic power plant (PtG-PV)
2. PtG plant powered by a wind farm (PtG-Wind)
3. PtG plant powered by the public grid (PtG-Grid)

The calculations and analyzes of SNG production costs are carried out using PResTiGE (Power-to-Gas Assessment Tool) developed at the *Energieinstitut an der JKU Linz* (see Figure 7-1). PResTiGE is a toolbox for current and prospective techno-economic and environmental benchmarking of PtG systems. The EXCEL tool comprises data from demo sites and benchmark systems as options for electricity storage or applications of the gaseous products H_2 or CH_4 in the transportation sector at different scales, in forms that are regionally adaptable over all process steps of the PtG system and product application. The assessment results reveal the optimal PtG system configuration and implementation (i.e., with minimal cost and maximal system benefits). Sensitivities can be systematically analyzed to explore the robustness of the results.

Figure 7-1: Overview of the tool PResTiGE

The quantitative economic assessment via PResTiGE is based on the specific production costs of hydrogen or SNG, which are calculated from the total annual costs in relation to the amount of annually produced energy. The total annual costs are calculated using the so-called “annuity method” following VDI 2067.

In calculating SNG production costs, an interest rate of 4% and a period of 20 years are assumed. No price change factor is taken into account. The total annual costs include capital- , demand- , operating-related, and other costs. The capital-related costs are investment and replacement costs. Annual demand-related costs include energy costs and costs for auxiliary energy. Operating-related

costs include annual costs for the maintenance, operation, and cleaning of the plant. Other cost items include insurance, levies, and administration costs. The calculated SNG production costs do not include taxes and charges or any electricity and gas network tariffs, as these depend on the country in which the PtG plant is being built.

The following chapters describe the most important input parameters for calculating SNG production costs, such as electricity costs and quantities, investment costs, efficiency of the PtG plant, lifetime of the electrolyzer, costs for CO_2, revenue from the utilization of waste heat and oxygen, and hot standby power consumption. The SNG production costs for different technologies and time horizons are also calculated, and a sensitivity analysis is carried out.

7.1 Electricity costs and quantities

The electricity costs and power available for the plant are crucial for both the economic assessment and plant operation. These input parameters vary depending on the field of application. Likewise, the electricity market is subject to constant change. This chapter describes the electricity procurement scenarios, including prices and quantities.

7.1.1 Electricity from photovoltaic power plant or wind farm

In the PtG-PV and PtG-Wind scenarios, the PtG plant obtains electricity directly from a photovoltaic power plant or wind farm. Two options are investigated to analyze the different operation modes:

1. Use of the total electricity generated. Here, the PtG plant is designed for the maximum output of PV/wind (PtG-PV-100% and PtG-Wind-100% scenarios)

2. Use of a part of the electricity generated. Here, a certain amount of the power produced from PV/wind is fed into the public grid. The remaining produced electricity is used to produce SNG by the PtG plant (PtG-PV-50%, PtG-PV-75%, PtG-Wind-50%, and PtG-Wind-75% scenarios)

When operating the PtG plant with electricity from a wind farm or photovoltaic power plant, only the directly generated power can be used in the electrolyzer. Figure 7-2 and Figure 7-3 show the typical electricity production characteristics of a wind farm and photovoltaic power plant. The generation profiles are based on the electricity production of a wind farm (14 MW) and PV power plant (about 3 MW_p) in Austria, which were scaled up to a maximum power of 100 MW for comparison. The analyzed operating modes differ in the share of power fed into the grid, which ranges from 0% (no feed-in) to 50% (half of the power is fed into the grid) of the nominal power of the production plant. The remaining share of the produced power is used by the PtG plant. For example, in Figure 7-2 and Figure 7-3, the maximum grid feed-in is 25% of the maximum power of the wind farm/PV power plant. The remaining power, 75% of the maximum power, is used by the PtG plant to produce SNG. In a future energy system with a high proportion of PV and wind power, this operation mode could be used to feed urgently needed electricity into the grid as a kind of base load. In addition, renewable gas could be produced with the electricity power peaks that would otherwise severely burden the grid and lead to grid expansion. The renewable gas serves as a long-term energy storage (transfer energy from the summer to the winter) or as an energy source in industry and mobility applications.

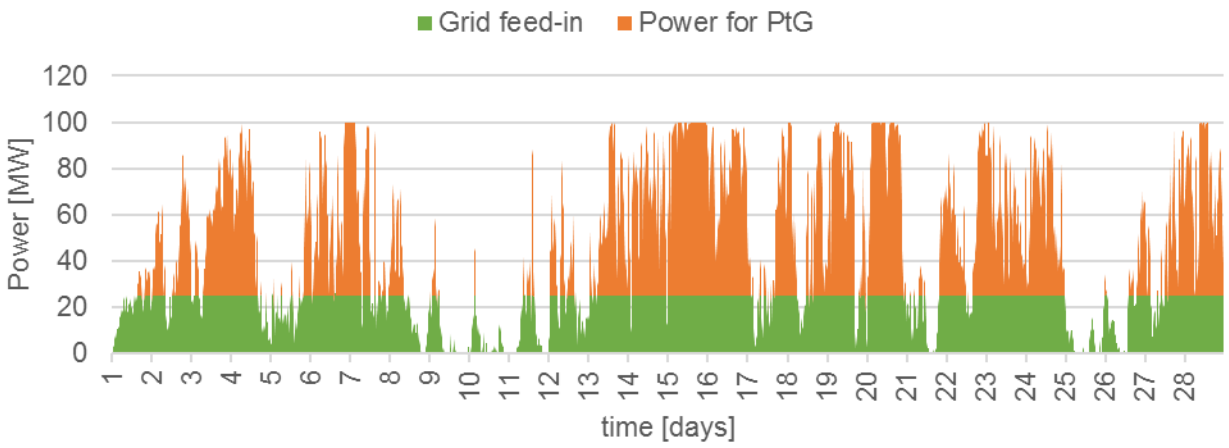

Figure 7-2: Typical electricity production characteristic of a 100 MW wind farm. The power is divided in the share of grid feed-in (green coloured) and power for the PtG-plant (orange coloured). In this example is the maximum grid feed-in 25 % of the maximum power of the wind farm (25 MW), the electrolyzer (75 MW) uses the surpluses

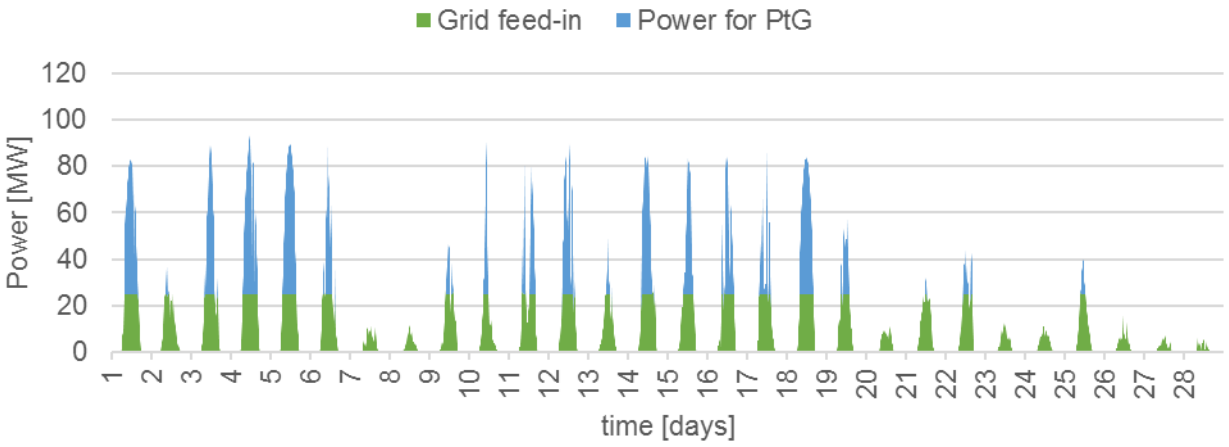

Figure 7-3: Typical electricity production characteristic of a 100 MW photovoltaic power plant (app. 123 MW_p). The power is divided in the share of grid feed-in (green colored) and power for the PtG-plant (blue colored). In this example is the maximum grid feed-in 25 % of the maximum power of the photovoltaic plant (25 MW), the electrolyzer (75 MW) uses the surpluses

The different generation characteristics of the wind farm and the PV power plant are shown in the ordered annual production curve, where the ordered power values are presented over the year, indicating the frequency of the power over the course of a year (see Figure 7-4). The area under the production curve reflects the energy produced.

The wind farm runs at a rated power for a longer time than the PV power plant does. The PV power plant generates at only about 4,300 h/a energy (no production at night), while the wind farm generates over 7,700 h/a. Thus, a 100 MW wind farm generates significantly more energy than a 100 MW PV system.

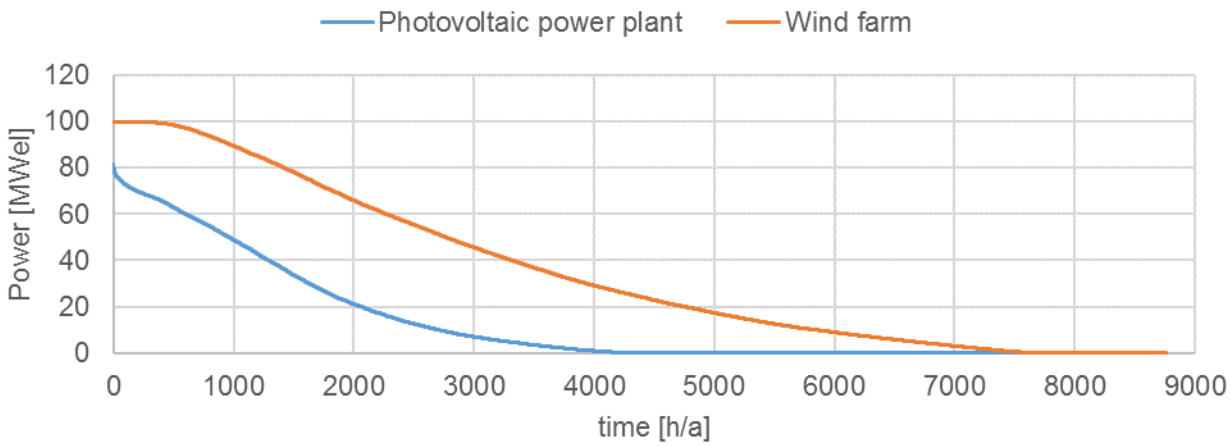

Figure 7-4: Ordered annual production curve of a 100 MW wind farm and PV power plant

The generation characteristics of the renewable energy plant strongly influence the operation and economic efficiency of the PtG plant. Key data on the wind farm and PV power plant are summarized in Table 7-1.

Table 7-1: Key data of the wind farm and PV power plant

Characteristic	Unit	Wind farm	PV power plant
Maximum power	MW	100	100
Annual energy production	MWh	310,056	139,483
Full-load hours	h/a	3,101	1,136
Time power = 0	h/a	1,018	4,473
Time power > 0	h/a	7,742	4,287

Electricity procurement costs PV

According to [98], the levelized costs for electricity (LOEC) from PV power plants were about 54 to 84 €/MWh in 2014 depending on the location. In 2050, the LOEC are estimated to be in a range of 25 to 44 €/MWh in southern Germany (at 1,190 kWh/kW_p) and 18 to 31 €/MWh in southern Spain (at 1,680 kWh/kW_p). A more recent study [99] claims that the current costs (2018) for electricity from large PV power plants in Germany are in a range of 37.1 to 67.7 €/MWh. The estimated costs for 2035 are in a range of 21.6 to 39.4 €/MWh. A more conservative estimation of electricity costs from PV in 2050, of about 55 to 84 €/MWh, is provided in the EU Reference Scenario [100]. However, this estimation seems already outdated, since the current costs are lower.

Following the literature, this Deliverable assumes electricity costs from large-scale PV power plants at locations with an average solar radiation of 40 €/MWh, 30 €/MWh, and 20 €/MWh for 2020, 2030, and 2050, respectively.

Electricity procurement costs for wind

In [101], the generation costs for onshore wind farms in Germany are estimated at about 30–60 €/MWh and 25–50 €/MWh in 2030 and 2050, respectively. In a more optimistic scenario, where a higher potential for cost reduction is taken into account, the electricity costs from wind power decline to 25–45 €/MWh and 20–35 €/MWh, respectively. The average electricity costs for projects in Germany in 2016/17 for an average-quality site was about 65 €/MWh. When compared to other parts of the world (e.g., Morocco, Peru, Mexico), the costs for electricity from onshore wind farms are even

lower, as shown in wind auctions, where the average bids were in a range of 27–34 €/MWh. The average bids at wind auctions for offshore wind farms are higher, at about 50–72 €/MWh. According to [99], the 2018 costs for electricity from onshore wind farms in Germany were in a range of 40–82 €/MWh, depending on the location. Although the offshore wind farms have higher full-load hours, the costs for electricity are higher, at about 75–138 €/MWh. In the long term, until 2035, the costs for electricity from onshore wind turbines in Germany will decline to 35–71 €/MWh, and the costs for offshore wind turbines will decline to 57–101 €/MWh. Analogous to the cost estimation for electricity from PV power plants, the costs for electricity from wind turbines in 2050 are overestimated in the EU Reference Scenario at 72–90 €/MWh [100], as the costs are lower today.

Following the literature, this Deliverable assumes average costs for electricity form wind power plants (onshore as well as offshore) of about 60 €/MWh, 50 €/MWh, and 40 €/MWh for 2020, 2030, and 2050, respectively.

7.1.2 Electricity from the spot market

Based on 2017 spot market prices for electricity with a time resolution of 15 minutes in Austria, forecasts for 2020, 2030, and 2050 are prepared. The forecasts depend on the development of the average spot market price and price volatility.

For the grid-connected 100 MW_{el} PtG plant, it is assumed that an ideal power grid provides the power. This means that the required power is available at any given time. The investigated operating modes differ in terms of the full-load hours (from 1,000–8,000 h/a) of the plant.

Average spot market prices

The average spot market price in 2017 was about 34.5 €/MWh and fluctuated between a minimum price of -102 €/MWh and a maximum of 170 €/MWh (see Figure 7-5) [102].

The EU Reference Scenario 2016 forecast average electricity prices before taxes for households, services, and industry until 2050. The price consists of annual capital costs, fixed costs, variable costs, fuel costs, taxes on fuels and ETS payments, and grid costs. For the industry sector, the price remains quite stable, ranging from 90 to 100 $€_{2013}$/MWh from 2010 to 2050. It is expected to reach about 97 $€_{2013}$/MWh by 2030 and about 99 $€_{2013}$/MWh by 2050 [100].

The 2014 study in [103] forecasts the development of wholesale electricity prices until 2050. The analysis assumes that prices will decline until 2020, mainly due to the priority feed-in of renewable energy. The subsequent increase in prices is explained as being caused by rising costs for CO_2 emissions and fuel prices, as well as the effects of the nuclear phase-out. The demand for new capacity to secure peak load coverage also increases. The estimated wholesale electricity prices in Germany are 67 $€_{2011}$/MWh and 87 $€_{2011}$/MWh for 2030 and 2050, respectively.

The Sustainable River Management study [104] examines the possible long-term development of spot market electricity prices in Austria on the basis of two independent electricity price models (*ewi Energy Research & Scenarios GmbH* and *enervis energy advisor GmbH*) for 2025, 2035, and 2050. According to the enervis model, the electricity prices are 56.0 $€_{2016}$/MWh, 75.7 $€_{2016}$/MWh, and 75.4 $€_{2016}$/MWh for 2025, 2035 and 2050, respectively. The prices calculated with the ewi model are similar, at 56.9 $€_{2016}$/MWh, 75.8 $€_{2016}$/MWh, and 78.6 $€_{2016}$/MWh for 2025, 2035, and 2050, respectively.

The EU Energy Outlook 2050 report examines long-term trends in the European energy system, including developments in electricity prices. The development of average, unweighted electricity prices until 2040 heavily depends on the primary energy and CO_2 prices. From 2040, electricity

prices will stagnate despite increasing gas and CO_2 prices due to high wind and photovoltaic feed-ins, which are increasingly leading to low (and often negative) electricity prices. Future developments depend on the expansion of renewable energies and will therefore vary across countries. In 2030, the electricity price is expected to be about 70 €/MWh; in 2050, the price will rise to about 80 €/MWh (in a range from 70–120 €/MWh depending on the amount of RES installed) [105].

In a Greenpeace scenario regarding an energy concept for Germany, electricity prices (base spot market price) are estimated to be much lower, at about 45 €/MWh in 2030 and 22 €/MWh in 2050, than in other studies on the development of electricity prices. This is justified by the fact, that starting from 2030, power plants with small marginal costs are price-determining. These include increasingly renewable energy plants with marginal costs close to zero and the remaining coal-fired power plants. As renewable energy use expands, the use of conventional power plants will become increasingly rare, which will bring the electricity costs closer to those of renewable energies [106].

[107] analyzes how implementing 65% of renewable energy until 2030 and a gradual phase-out of coal power generation in Germany will affect electricity prices, CO_2 emissions, and the electricity market. In three different scenarios, stock market electricity prices of 53–61 €/MWh are estimated for 2030. The development of the electricity prices is mainly dependent on the assumption of increasing CO_2 emissions and fuel prices. The accelerated phase-out of coal power generation would lead to an increase from 57 €/MWh to 61 €/MWh. With a simultaneously accelerated expansion of renewables to 65% in 2030, the costs would decrease to 53 €/MWh.

The study of [108] on the climate-protection contribution of the power sector until 2040 also forecast wholesale electricity prices. In this study, electricity prices also rise due to the assumed increase in coal and gas costs. It is estimated that prices will rise until about 2028 and then stabilize in a range of 60–65 €/MWh.

Table 7-2 summarizes the electricity prices forecasted for 2030 and 2030 in the analyzed sources.

Table 7-2: Forecast for electricity prices in 2030 and 2050

2030 €/MWh	**2050 €/MWh**	**Source**
97	99	[100]
67	87	[103]
56.0/75.7* 56.9/75.8*	75.4 78.6	[104]
70	80 (70–120)	[105]
45	22	[106]
53–61	-	[107]
60-65	-	[108]
66	**74**	**Mean value**
66	**79**	**Median value**

* … values for the year 2025/2035

For the further calculations in this report, the median value (where outliers have less priority) in the examined studies was assumed to be approximately 65 €/MWh for 2030 and 80 €/MWh for 2050. For 2020, the average spot market prices observed in 2017 were assumed (around 35 €/MWh).

For the estimation of future spot market prices, the price volatility for 2030 and 2050 will also be changed, in addition to the average prices. Both volumes and prices will likely be more volatile due to the expanding renewable power generation. Based on the literature review, a mean spot market price of 65 €/MWh for 2030 and 80 €/MWh for 2050 is assumed (see Table 7-2). The rising volatility is taken into account by multiplying the deviation from the mean value occurring in one hour by a volatility factor. This factor is set to 1.5 (+50%) for 2030 and 2 (+100%) in 2050. The resulting trends in spot market prices over the year are shown in Figure 7-5. The figure shows higher spot market prices in 2030 and 2050 and higher volatility in the form of significantly larger fluctuations in spot market prices compared to the 2017 reference data.

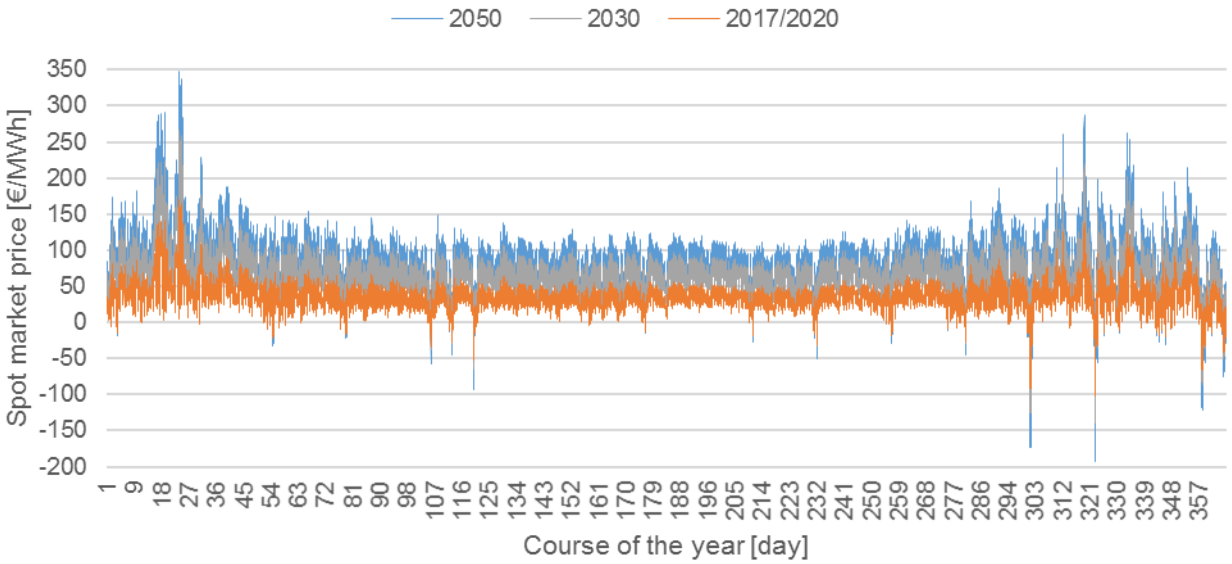

Figure 7-5: Spot market prices for 2017 and forecasts for 2020, 2030 and 2050

Fluctuations in spot market prices are taken into account in the economic evaluation of the operating modes of the PtG plant. Depending on the specific production costs, the cost-optimal full-load hours are determined for the respective application. The amounts of electricity, and thus the capacity utilization of the PtG plant, are dependent on the electricity procurement costs.

It is assumed that the PtG system is always operated at times with the cheapest electricity prices. This means that, when operating the system with certain full-load hours, electricity may be purchased only up to a certain price. This situation results in a separate average electricity price for each full-load hour (see Table 7-3).

If, for example, a PtG plant in 2050 is operated only when the spot market prices are below 69 €/MWh, the plant will reach 3,000 full-load hours, and the average electricity purchase price will be around 16.2 €/MWh. This value is below the average spot market price of 80 €/MWh in 2050, since only the cheapest hours of the year are used. When operating the PtG plant with higher full-load hours (e.g., 8,000 h/a), the mean electricity purchase price (66.7 €/MWh) converges with the average spot market price in 2050 (80 €/MWh), as almost all hours, even those with higher prices, have to be used to achieve the required operating time.

Table 7-3: Mean prices for electricity from the spot market for certain full load hours in 2020, 2030 and 2050

Full-load hours [h/a]		1,000	2,000	3,000	4,000	5,000	6,000	7,000	8,000
2020	Price limit [€/MWh]	17.6	25.2	29.5	33.0	36.7	40.6	45.2	54.6
	Mean price [€/MWh]	0.7	3.2	6.4	9.9	13.9	18.3	23.2	28.8
2030	Price limit [€/MWh]	38.8	50.4	56.8	62.0	67.5	73.3	80.3	94.3
	Mean price [€/MWh]	2.5	7.7	13.9	20.6	28.0	36.0	44.8	54.6
2050	Price limit [€/MWh]	45.1	60.5	69.0	76.0	83.3	91.1	100.4	119.1
	Mean price [€/MWh]	2.6	8.7	16.2	24.5	33.6	43.5	54.4	66.7

7.2 Other key parameters

Besides the electricity costs and quantities, other PtG plant parameters are crucial for the economic assessment and plant operation.

7.2.1 Investment costs

The specific investment costs for the different nominal power levels of the electrolyzer and methanation units are based on the calculations done in Deliverable D7.5 “Report on experience curve and economies of scale” [2] and in chapter 4 “Economies of Scale” in this Deliverable. Besides the electrolyzer and the methanation unit, the analysis considers a H_2 storage tank used to buffer the hydrogen. The specific investment costs are estimated considering about 100 €/m³ for a maximum pressure of 50 bar [109]. In addition, it is assumed that the electrolyzer already produces the hydrogen at the pressure required for methanation, so no compressor is required. The CO_2 is also already available in compressed form.

The investment cost of the whole PtG plant consists of the investment costs of the electrolyzer, methanation unit and the H_2 storage tank, plus the sum of these multiplied by various factors (Lang factor, cf. [110]) representing additional costs. In general, the factors are rather low compared to common cost estimations in chemical plant engineering because the electrolyzer and methanation units are already delivered as complete systems and do not come with additional costs. The following additional costs are covered: engineering, materials and services for civil engineering (foundations, earthworks for laying cables and pipes, surface mounting), assembly of the main components, process control technology (material and assembly), electrical engineering (material and assembly), approval, site equipment, construction and assembly monitoring, safety testing, quality control, commissioning, and other costs. A detailed list of the individual factors can be found in the appendix (see Table A 6).

Taking into account the abovementioned costs (costs of the main parts plus additional costs), the investment costs for a 100 MW_{el} PtG plant (PEM electrolyzer, H_2 storage tank, and catalytic methanation) total around 223 m.€, 107 m.€, and 54 m.€ in 2020, 2030, and 2050 respectively. A detailed list of the investment costs for PtG plants of different sizes and of other technologies (AEC, PEMEC, and SOEC combined with catalytic or biological methanation) is provided in the appendix (see Table A 7).

7.2.2 Efficiency of electrolyzer

The efficiency of the electrolyzer system is based on the efficiency curve of a PEM electrolyzer in the *Energiepark Mainz* [111]. It is assumed that efficiency increases by 10% until 2050 (see Figure 7-6). The average electrolyzer efficiency used for the economic calculation is determined from the different electricity input profiles resulting from the use cases.

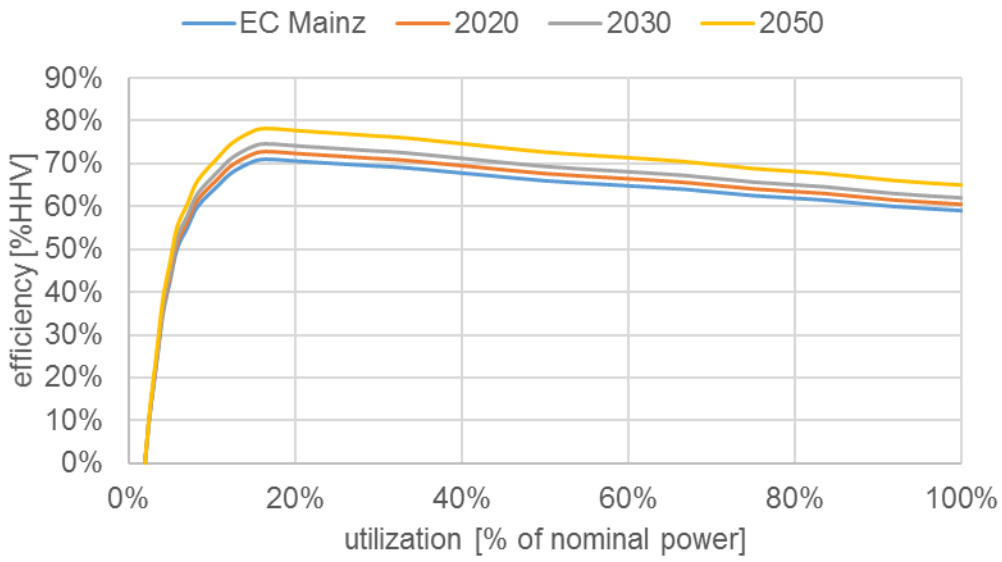

Figure 7-6: Efficiency of the electrolyzer for 2020, 2030 and 2050 based on efficiency curve of electrolyzer in the Energiepark Mainz [111]

7.2.3 Lifetime of electrolyzer

The lifetime of the electrolyzer stack is calculated by considering a maximum operating time of about 40,000 h, 60,000 h, and 140,000 h in 2020, 2030, and 2050 respectively (cf. [40], [39]), divided by the operating time (time power EC > 0). However, the lifetime of the electrolyzer stack is limited by the maximum lifetime of the whole electrolyzer system of 15, 20, and 30 years in 2020, 2030, and 2050 respectively [40]. The influence of the amount of start/stop cycles on the lifetime of the electrolyzer stack cannot be taken into account because there are no reliable data on the maximum amount of start/stop cycles an electrolyzer stack can sustain [40]. In general, the effects of transient operation, which occur by coupling with a wind farm or PV power plant, on the lifetimes of electrolyzer stacks and systems are insufficiently investigated. [34]

7.2.4 Costs for CO_2

The costs for CO_2 capture vary widely, from about 5 to 350 €/t depending on the CO_2 source and technology. In general, with the exception of direct air capture, the costs for CO_2 capture are roughly 50 €/t CO_2. However, for biomass/wastewater and bioethanol the costs can be significantly lower, at about 5 €/t CO_2. The costs for CO_2 capture from the chemical industry can also be lower due to the already high purity of CO_2 in the gas stream. By contrast, the costs for CO_2 from direct air capture are comparatively high, varying widely from 150 to 360 €/t CO_2 [109], [2]. The CO_2 required for methanation is assumed to be 50 €/t.

7.2.5 Sale of oxygen and heat

As a by-product of hydrogen production via water electrolysis ($2\ H_2O \rightarrow 2\ H_2 + O_2$), about 8 kg of oxygen is produced per kg of hydrogen. By selling oxygen, the production costs of SNG can be reduced. This is particularly advantageous when oxygen is needed at the site of the PtG plant (e.g., in wastewater treatment plants). The oxygen price is about 50 €/t (cf. [112]) for large quantities (e.g., industrial use). Higher costs are incurred for small amounts in bottles (e.g., medical oxygen) of around 5 €/kg (cf. [112]) on average. Our economic analyses assume that the oxygen produced by an electrolyzer can be sold at a price of 50 €/t.

The overall efficiency of PtG plants can be significantly increased by using the waste heat. However, the integration of waste heat is highly dependent on the existing framework conditions at the plant

site and the technology used. Alkaline and PEM electrolyzers have a waste heat temperature in a range of 60 to 80°C and a waste heat output (depending on efficiency) in a range of about 30% of the electrical power. High-temperature electrolyzers (SOEC) supply the waste heat at a significantly higher temperature, in a range of around 650 to 1,000°C, with a waste heat output (depending on efficiency) of about 15% of the electrical power. If the produced hydrogen is converted into SNG together with CO_2 in the case of catalytic methanation, further waste heat potential with a temperature in a range of about 200 to 350°C and a capacity of about 15% of the plant output is available. In biological methanation, the temperature level of the waste heat is significantly lower, at about 60°C, and a similar waste heat output is achievable. Depending on the waste heat source, the heat can be used for heating in buildings, integration into the district heating grid, steam generation, natural gas preheating, or CO_2 separation. To increase the resource and overall efficiency, waste heat recovery should be attempted wherever possible. Our economic analyses assume that waste heat can be sold at a price of about 55 €/MWh (cf. [113], European District Heating Price Series from 1980–2013)

7.2.6 Hot standby power consumption of the electrolyzer

To enable rapid reaction the electrical power input, the electrolyzer is partially operated in a hot standby mode. It is assumed that, if no power from a renewable energy source is available, the electrolyzer will remain in a hot standby mode for one hour. After this time, the electrolyzer switches to cold standby mode. The hydrogen production costs consider the energy consumption and costs of hot standby. The additional energy consumption or energy costs for the hot standby mode are taken into account in the calculation of the hydrogen production costs.

A brief literature review examines the power consumption of the electrolyzer in the hot standby mode (see Table 7-4). In [40], the power consumption for maintaining hot standby is estimated at about 1–5% of the nominal electrical power of the electrolyzer. In the future, at least for PEMEC and SOEC, falling values are expected. To model and simulate a PtG process, [114] has assumed a hot standby power of 15% of rated power for an AEC. In [115], for a 5 MW alkaline electrolyzer, the power for the necessary energy input in the hot standby operating mode is given as 2% of the nominal power of the electrolyzer. This is a little more than that for a 5 MW PEMEC, which has a power consumption in hot standby of about 1.6 % of the nominal power of the electrolyzer. In the performance of a 24 kW pressurized AEC operated in a hydrogen filling station, the standby power consumption is less than 1 kW. This result is about 4.2% of the nominal power of the electrolyzer. [116]

Table 7-4: Hot standby power consumption [% of nominal power] of different electrolyzer technologies

AEC	PEMEC	SOEC	Source
	1–5%		[40]
15%	-	-	[114]
2%	1.6%	-	[115]
4.2%	-	-	[116]

Based on this brief literature review, the hot standby power consumption of AEC is set as 4% of the nominal electrical power and 2% for PEMEC and SOEC.

7.3 Quantification of SNG production costs

The economic evaluation of the different modes of operation is based on the specific production costs for SNG for the three framework conditions (the PtG plant is powered by wind, PV, or public electricity grid). The total specific SNG production costs are calculated for the different cost share

conditions (i.e., investment costs, operating costs, electricity costs, water, and CO_2). Revenues for the sale of oxygen and heat are also reported.

The analysis of the SNG production cost in this chapter is based on a PtG plant (PEM electrolyzer with catalytic methanation) with a nominal power of 100 MW_{el} in 2050. For comparison, the production costs for SNG in 2020 and 2030 are also calculated. Detailed results can be found in the appendix.

7.3.1 PtG powered by wind or PV

In the case of direct electricity procurement from a wind farm or photovoltaic power plant, the operating mode of the PtG plant (e.g., full load hours, operating hours, efficiency, start/stop cycles) is conditioned by the electricity generation profile of the wind farm or photovoltaic power plant (see chapter 7.1.1). In addition, the different use cases (nominal power of the PtG plant) are conditioned by the share of power fed into the grid. Table 7-5 presents the key characteristic data (energy for the electrolyzer, full-load hours, start/stop cycles, and operating hours) for the PtG plants (50–100 MW) if powered by a 100 MW wind farm or PV power plant in 2050 (data for 2020 and 2030 can be found in the appendix). Additionally, based on the operational conditions of the PtG plant, resulting from the energy source, also the characteristics of the electrolyzer (e.g., efficiency, lifetime) are influenced. Furthermore, considering the investment costs of the electrolyzer and methanation system, which are different due to EoS, is also crucial in calculating economic efficiency.

For example, if 25% of the electricity of a 100 MW wind farm is fed into the grid, power peaks exceeding 25 MW are available for the PtG plant to produce SNG. To utilize all these surpluses, an electrolyzer with a nominal power of 75 MW is necessary. In this case, the electrolyzer is operated with about 2,242 full-load hours, 1,054 start/stop cycles, and an operating time of 4,328 hours per year. In comparison, coupling the PtG plant to a PV power plant with a maximum power of 100 MW where 25% of the generated electricity is fed into the grid would result in very different operating conditions. Due to the generation characteristic of the PV system, the electrolyzer shows fewer full-load hours (918 h/a), fewer start/stop cycles (545 cycles/a), and less operating time (2,038 h/a).

Table 7-5: Characteristic data for different use cases – PtG-plant (50–100 MW) is powered by a wind farm or PV power plant in 2050

General Parameters	**Unit**			
Share grid feed-in	%	50	25	0
Share PtG	%	50	75	100
Nominal power EC	MW	50	75	100
Specific investment costs EC	€/kW_{el}	190	179	172
PtG - wind farm		PtG-Wind-50%	PtG-Wind-75%	PtG-Wind-100%
Energy for EC	MWh	80.971	168.169	310.056
Full load hours	h/a	1.619	2.242	3.101
Start/stop cycles	cycles/a	1.015	1.054	553
Time power = 0	h/a	5.997	4.432	1.018
Time power > 0	h/a	2.763	4.328	7.742
Average efficiency EC	%	68,3	68,9	69,4
Lifetime EC stack	a	30	30	30
Nominal methanation	MW_{SNG}	27,3	41,3	55,5
Specific investment costs methanation	€/kW_{SNG}	163	143	130
PtG - PV power plant		PtG-PV-50%	PtG-PV-75%	PtG-PV-100%
Energy for EC	MWh	28.283	68.882	139.483
Full load hours	h/a	566	918	1395
Start/stop cycles	cycles/a	542	545	373
Time power = 0	h/a	7.493	6.722	4.473
Time power > 0	h/a	1.267	2.038	4.287
Average efficiency EC	%	71,2	70,6	70,3
Lifetime EC stack	a	30	30	30
Nominal methanation	MW_{SNG}	28,5	42,4	56,2
Specific investment costs methanation	€/kW_{SNG}	161	142	130

The specific production costs of SNG from this PtG plant, which is directly coupled with a photovoltaic power plant, are in a range of 9.6–22.0 Cent/kWh (see Figure 7-7). The differences can be attributed to the full-load hours achieved (e.g., scenario PtG-PV-50% 566 h/a vs. PtG-PV-100% 1,395 h/a). Due to the lower full-load hours in the PtG-50% scenario, the investments have a higher share. This is also the case with the SNG production costs (10.1–14.1 Cent/kWh) if the PtG plant is coupled with a wind farm (PtG-Wind-50% 1,619 full-load hours vs. PtG-Wind-100% 3,101 full-load hours). On the other hand, for the wind-coupled PtG plant, the share of the investment costs are lower than that for the PV coupled plant due to the higher full-load hours. Meanwhile, the share of electricity costs in the PtG-Wind case are higher, as wind power costs about 40 €/MWh and PV about 20 €/MWh in 2050.

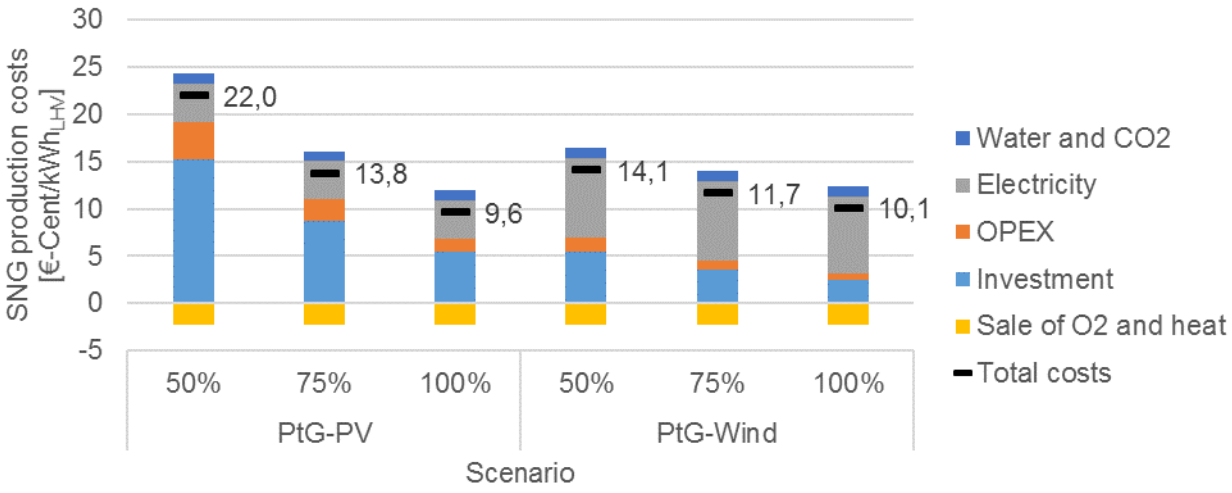

Figure 7-7: Specific SNG production costs for the scenarios PtG-PV and PtG-Wind in 2050 for different usage shares of the generated electricity

To show the near-future development of SNG production costs, the costs for 2020 and 2030 were calculated (see Figure 7-8; a detailed breakdown of the SNG production costs, as in Figure 7-7 for 2050, can be found in the appendix). In the PtG-PV-100% scenario, SNG costs of about 43 Cent/kWh in 2020 are calculated. By 2030, the costs are halved, to about 21 Cent/kWh. In the distant future (2050), there will be a further halving of costs, to about 10 Cent/kWh. In the PtG-Wind-100% scenario, SNG production costs in 2020 of about 29 Cent/kWh are reached and are significantly lower than in the PtG-PV-100% scenario. However, the costs fall to about 17 Cent/kWh in 2030. By 2050, the costs will drop to around 10 Cent/kWh, which is the same as in the PtG-PV-100% scenario.

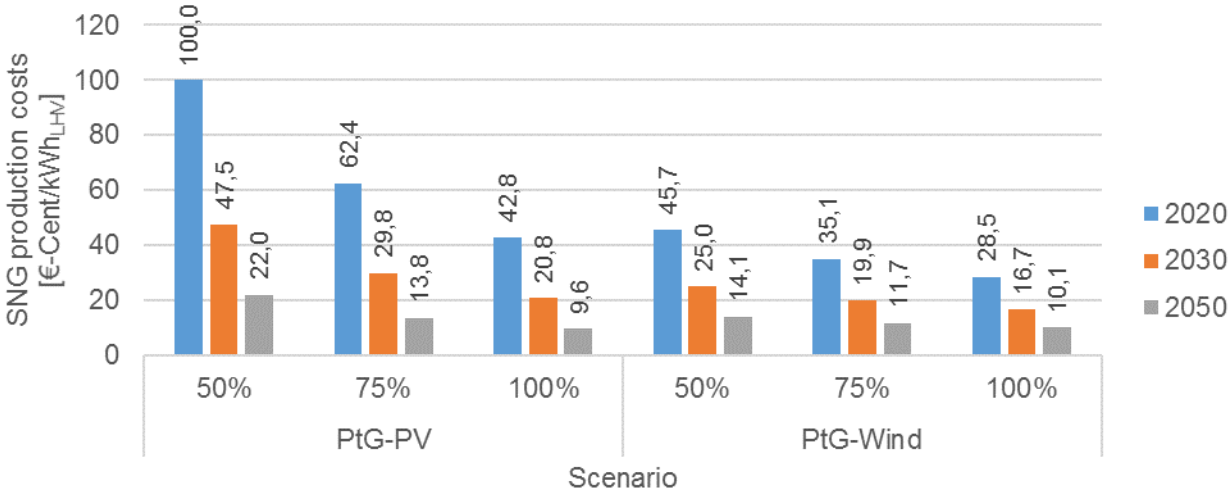

Figure 7-8: Specific SNG production costs in 2020, 2030 and 2050

In the early applications (e.g., 2020, 2030), the use of surplus electricity from PV or wind (PtG-PV-50%, PtG-PV-75%, PtG-Wind-50%, PtG-Wind 75% scenarios) is not feasible for reaching acceptable SNG production costs (see Figure 7-8). Depending on market conditions, it may make sense in 2050 to feed up to 25% of the electricity into the grid and produce SNG with the remaining 75%, since the SNG production costs (especially in the PtG-Wind-75% scenario) will not increase significantly relative to the PtG-Wind-100% scenario.

7.3.2 PtG grid

In the operating mode PtG grid, it is assumed that the PtG plant is connected to the public electricity grid and operated at times with the cheapest electricity prices on the spot market (for a detailed description of electricity costs, see chapter 7.1.2).

The specific production costs for SNG in 2050 with a 100 MW_{el} PtG plant (PEMEC/catalytic methanation) that receives power from the public grid are shown given operation with different full-load hours in Figure 7-9.

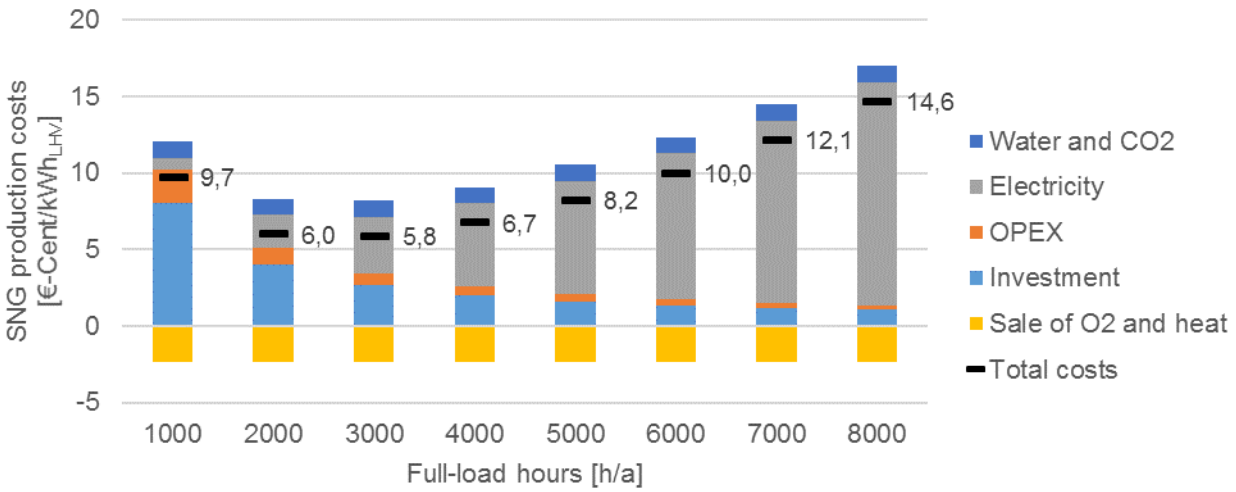

Figure 7-9: Specific SNG production costs for the scenario PtG-Grid in 2050 for different full-load hours

The specific SNG production costs range from 5.8 to 14.6 Cent/kWh, whereby the lowest costs are achieved by operating with about 3,000 full-load hours, and the highest costs arise at 8,000 full-load hours.

At low full-load hours (< 3,000), the SNG production costs are dominated by the share of the investment costs. The higher the full-load hours of the PtG plant, the lower is the share of investment costs; the share of electricity costs is dominant. For example, at 7,000 full-load hours, the investment costs are about 1.2 Cent/kWh, whereas electricity costs are about 11.9 Cent/kWh. The high share of electricity costs occurs because the higher operating time requires that the PtG plant be operated when electricity prices are relatively high. This increases the average electricity price (see Table 7-3). Moreover, at higher full-load hours, the investment costs are allocated to a larger amount of gas, which reduces the proportion of investment costs in the SNG production costs. The advantage of the declining share of investment costs at high full-load hours cannot be offset by the increase in the proportion of electricity costs, which leads to increased SNG production costs.

A PtG plant can be used in a variety of ways in an energy system, where one fundamental goal is the production of renewable gas. It may be reasonable (while taking the market situation for renewable gases into account, of course) to not operate the plant with 3,000 full-load hours in order to achieve the lowest SNG production costs but to increase the output of the PtG plant by increasing the full-load hours, although this would lead to higher SNG production costs. However, as mentioned, excessively high full-load hours (> 5,000) lead to significantly higher SNG costs. Incidentally, in a renewable energy-based energy system with a large proportion of fluctuating energy sources, a PtG plant should be operated in a way that does not unduly charge the power grid but helps to support it—for example, by converting the surpluses from wind and PV produced in the summer into gas and transferring them into the winter months via long-term storage and sector coupling. Since bottlenecks in power generation are likely to occur in the winter, leading to higher electricity prices, PtG plants

should not be operated at these times. Thus, the continuous operation (full-load hours > 6000) of PtG plants is not desirable. The full-load hours required for a reasonable operation of PtG plants (gas production, costs, and system suitability) are regarded to be in a range of 2,000 to 5,000, at costs of about 5.8 to 8.2 Cent/kWh.

Besides the specific SNG production costs for the PtG-Grid scenario in 2050, we also calculated the costs for 2020 and 2030 (see Figure 7-10; a detailed breakdown of the SNG production costs, as in Figure 7-9 for 2050, can be found in the appendix). The costs for 2020 and 2030 are significantly above those for 2050 when operating the PtG plant at low full-load hours. The SNG costs for operating the plant at 8,000 full-load hours are similar due to the lower electricity prices in 2020 and 2030, since the share of investment costs is already very low at high full-load hours. The hours with the lowest cost differ over time. By 2020, the lowest cost (about 13.5 Cent/kWh) will be at around 6,500 full-load hours. In 2030, the lowest SNG production costs (about 9.5 Cent/kWh) are around 3,500 hours; in 2050 (about 6 Cent/kWh), they are about 2,500 h/a.

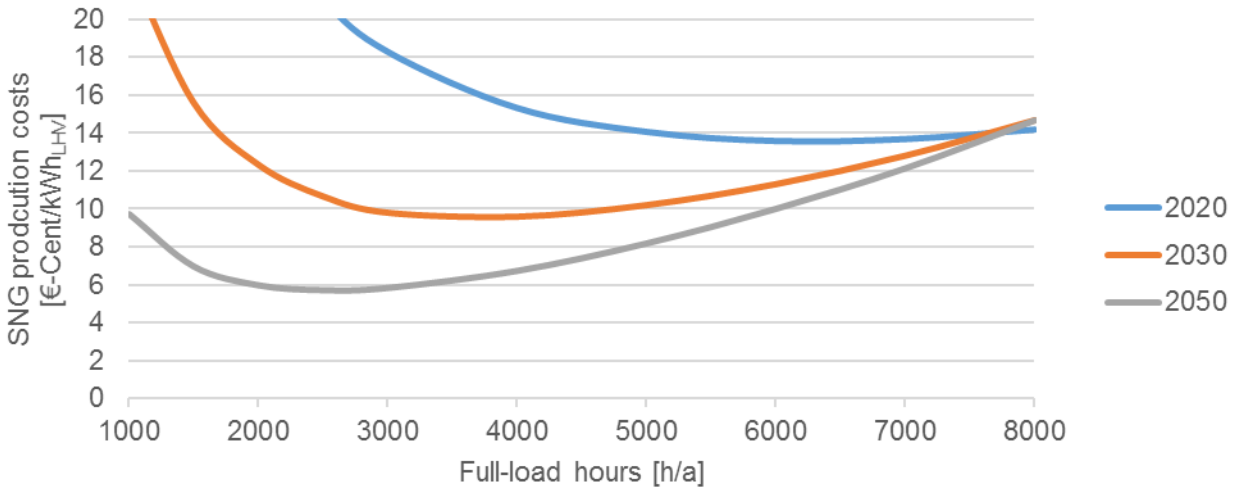

Figure 7-10: Specific SNG production costs for the scenario PtG-Grid in 2020, 2030 and 2050

In early applications, PtG plants will need to run at high full-load hours (> 5,000) to achieve low SNG production costs. Later, the lowest costs will be achieved at fewer full-load hours (2,000–4,000 h/a) when the plant is operated only at the lowest electricity prices. However, several factors, such as the requirement for green gas production, may argue for higher full-load hours, albeit with somewhat higher SNG costs.

SNG production costs at alternative electricity prices in 2050

Since the electricity market is subject to constant change and is heavily dependent on climate and energy policy conditions and decisions, forecasting electricity prices in 2050 is not easy and fraught with great uncertainties. For this reason, an additional scenario was calculated. If electricity prices remain the same as in 2017, because they develop until 2050 in a direction different from what is forecast by studies and the assumptions made in chapter 7.1.2, this will have a significant impact on SNG production costs. Figure 7-11 shows the 2050 SNG production for the PtG-Grid scenario for different full-load hours with electricity costs at their 2017 levels. The SNG production costs at current electricity prices (mean of about 35 €/MWh) are significantly lower, in a range of 3.5–9.2 Cent/kWh, than the SNG production costs at the predicted electricity prices in 2050 (mean of about 80 €/MWh). There is also a shift in the range of full-load hours (from 3,000 to 5,000) where the lowest SNG-production costs occur.

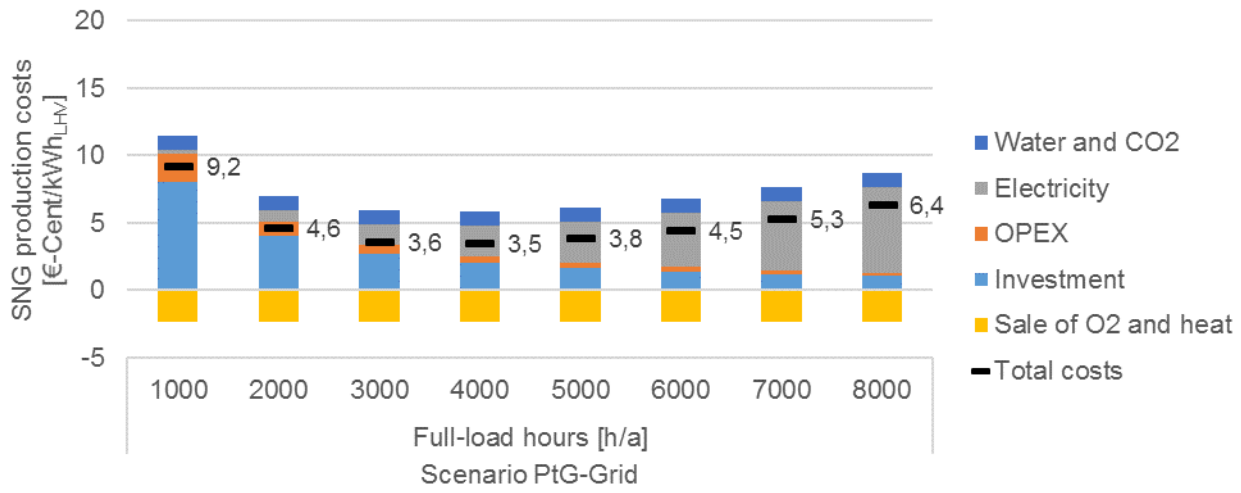

Figure 7-11: Alternative electricity costs - Specific SNG production for the scenario PtG-Grid in 2050 for different full-load hours with electricity costs from 2017

7.4 Sensitivity analysis

A sensitivity analysis is carried out to investigate the influence of different parameters on SNG production costs. The parameters enabling the greatest possible reduction in SNG production costs and measures can be derived from the results.

The sensitivity analysis is performed for the PtG-PV-100%, PtG-Wind-100%, and PtG-Grid-6000h/a scenarios in 2020. The reference values, including the SNG production costs as the target value and the individual parameters to be examined, are listed in Table 7-6.

Table 7-6: Reference values for the sensitivity analysis of the PtG-PV-100%, PtG-Wind-100% and PtG-Grid-6000h/a scenarios in 2020

		PtG-PV-100%	PtG-Wind-100%	PtG-Grid-6000h/a
SNG production costs	Cent/kWh	42.8	28.5	13.6
Parameter				
Electricity costs	€/MWh	40	60	18.3
Investment costs	Mio. €	233.4	232.9	230.7
OPEX	Mio. €/a	5.3	5.3	5.3
Efficiency PtG-plant	%	52%	52%	48%
Site-related full-load hours	h/a	1.391	3.096	-
Volatility electricity costs	%	-	-	100%
CO_2 costs	€/t	50	50	50
Sale price of oxygen	€/t	50	50	50
Sale price of heat	Cent/kWh	0,055	0,055	0,055
Lifetime EC	a	30	30	30
Lifetime methanation	a	20	20	20

The results of the sensitivity analysis, derived by varying the parameters shown in Table 7-6 by +/- 25% with respect to the reference value, are shown in Figure 7-12.

All three investigated scenarios in 2020 (PtG-PV-100%, PtG-Wind-100%, and PtG-Grid-6000h/a) behave similarly with regard to the influence of the parameters on SNG production costs. Plant effi-

ciency, investment costs, full-load hours, and electricity costs are among the parameters that influence SNG production costs most strongly when changing by +/-25%, while OPEX, CO_2 costs, lifetime, and the sale price of oxygen or heat all have a minor influence.

For example in the scenario PtG-Grid-6000h/a, reducing electricity purchase costs by 25% will lower SNG production costs by up to 10%. Likewise, a 25% increase in efficiency will reduce costs by up to 19%. The SNG costs are very sensitive to efficiency reduction (however, this case is unrealistic, as the efficiency of equipment is constantly increasing); a reduction of 25% leads to a price increase of up to 32%. Investment costs also strongly influence SNG production costs (a reduction of 25% reduces SNG costs by up to 16%). The number of full-load hours at the PtG plant depends on the location of the photovoltaic power plant and wind farm. If the PV or wind farm is placed in a better location (e.g., if 25% higher full-load hours are achieved), SNG costs will fall by up to 17%.

The sensitivity analysis for the three scenarios in 2030 and 2050 also shows similar results (see detailed results in the appendix). However, electricity costs and efficiency become increasingly dominant.

Reducing SNG costs requires purchasing low-cost electricity, maximizing plant efficiency, reducing investment costs, and in cases where the plant is connected to a PV or wind park, building the PV or wind park in good locations with high full-load hours.

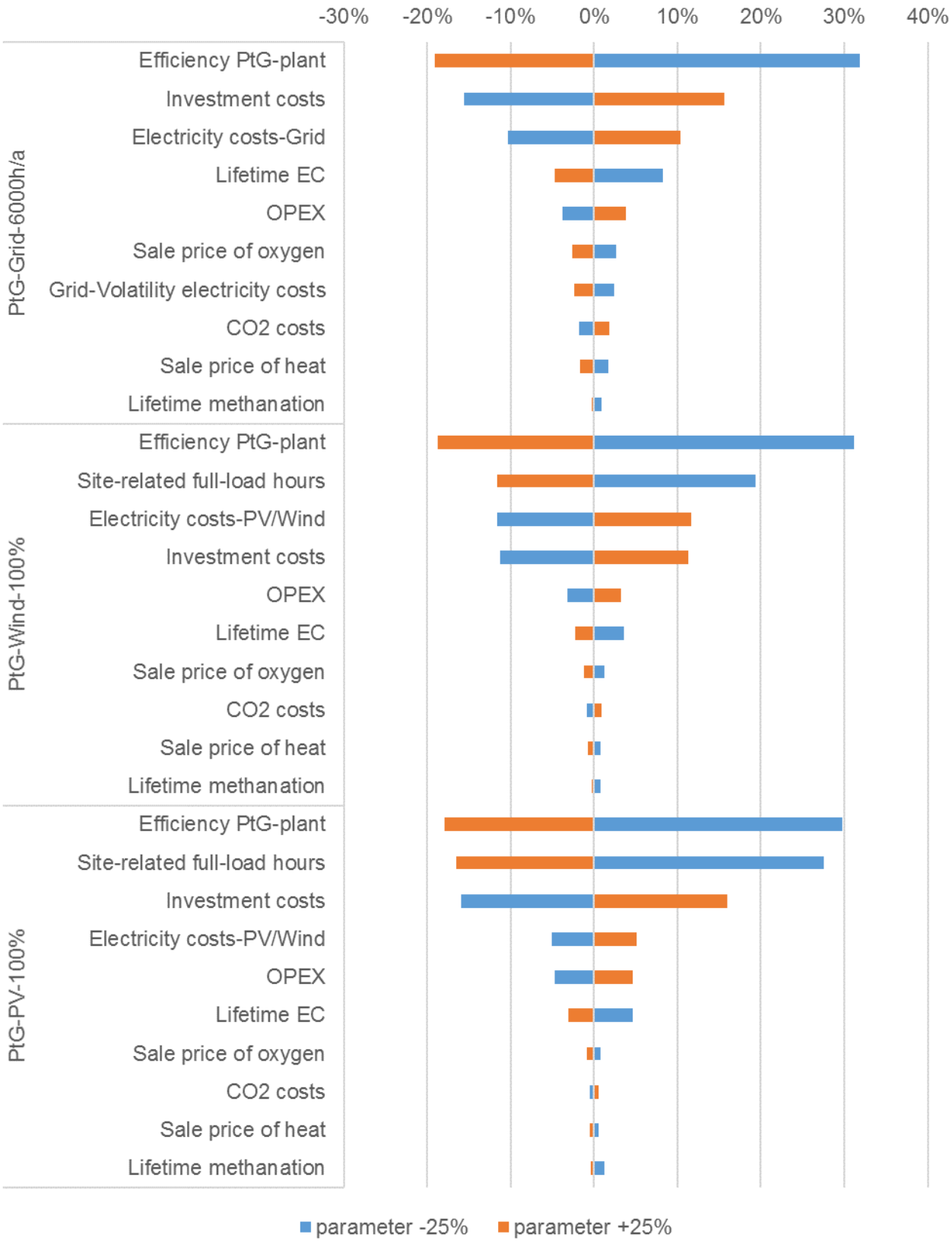

Figure 7-12: Sensitivity analyses of specific SNG production costs in 2020 for the PtG-PV-100%, PtG-Wind-100% and PtG-Grid-6000 h/a scenario

7.5 Comparison of PtG technologies

This chapter compares SNG production costs among PtG technologies. The SNG production costs are calculated in the same way as in chapter 7.3 for a 100 MW_{el} PtG plant built with a PEM electrolyzer and catalytic methanation unit (PEMEC-CAT). In addition, the following technologies are considered:

- PEMEC-BIO: PEM electrolyzer coupled with a biological methanation unit
- AEC-CAT: Alkaline electrolyzer coupled with a catalytic methanation unit
- AEC-BIO: Alkaline electrolyzer coupled with a biological methanation unit
- SOEC-CAT: Solid oxide electrolyzer coupled with a catalytic methanation unit (only this combination is analyzed, since coupling with a biological methanation is not feasible for using waste heat)

The resulting SNG production costs in 2020, 2030, and 2050 for the PtG-PV-100% and PtG-Wind-100% scenarios are shown in Figure 7-13 and Figure 7-14 respectively. Both scenarios behave similarly, but the absolute values of the costs differ. In 2020, there are virtually no differences between the technologies, with the exception of the SOEC-CAT variant. However, the SOEC-CAT case is more of a theoretical consideration, since it seems unlikely that a 100 MW SOEC will be built by 2020. In the future (2030, 2050), the variants with an alkaline electrolyzer will lead to higher SNG production costs than those with a PEM electrolyzer. There is hardly any difference in terms of the methanation technology used.

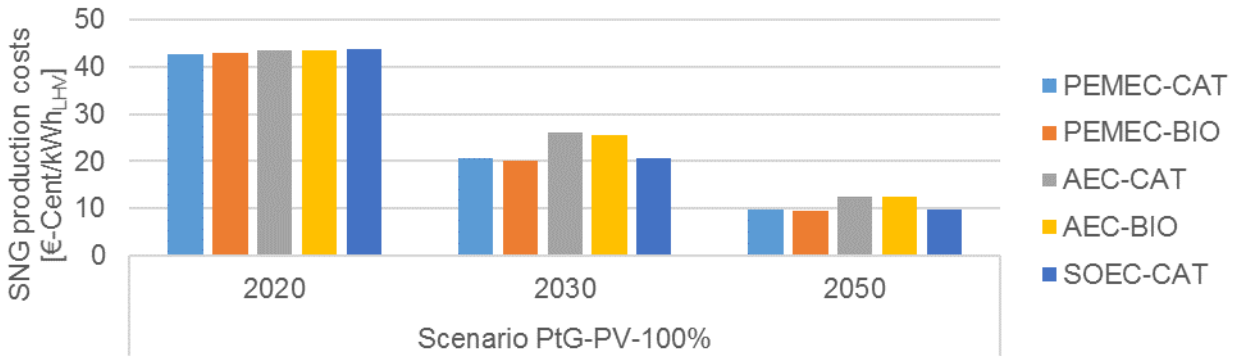

Figure 7-13: Development (from 2020–2050) of the specific SNG production costs in the scenario PtG-PV-100% for different PtG technologies

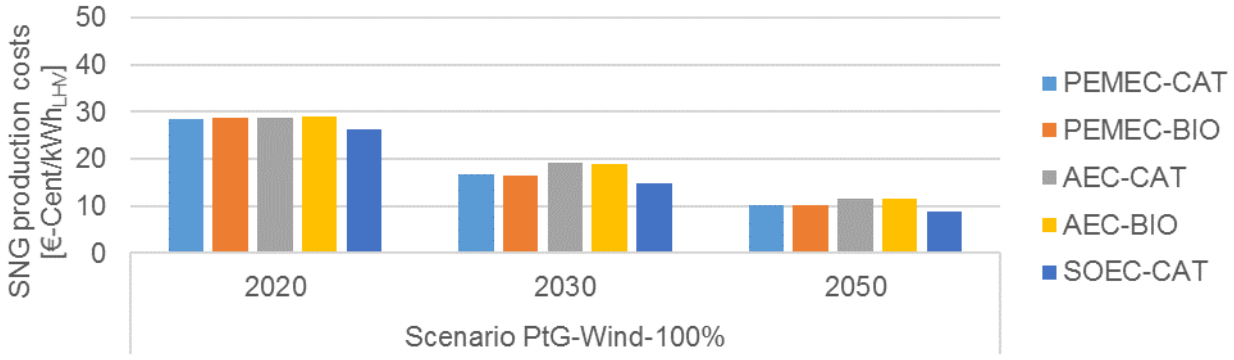

Figure 7-14: Development (from 2020–2050) of the specific SNG production costs in the scenario PtG-Wind-100% for different PtG technologies

The development of the specific SNG production costs from 2020 to 2050 for the PtG-Grid scenario for each PtG technology is shown in Figure 7-15. In general, hardly any difference in SNG production costs is observed depending on the methanation technology used. In 2020, the SNG costs are almost independent of the technology used. However, the SOEC-CAT variant is a theoretical case, as

mentioned. From about 2030, the SOEC variant leads to the lowest costs, especially when operating the PtG plant with high full-load hours. A PtG plant with a PEM electrolyzer at low full-load hours has costs similar to those of the SOEC case. By contrast, a PtG plant with an alkaline electrolyzer operated at low full-load hours has higher SNG production costs. When operating the plant at high full-load hours, the costs of the AEC variant approach those of the PEMEC variant because the investment costs (which are higher for the alkaline electrolyzer) at high full-load hours have less of an influence on the production costs.

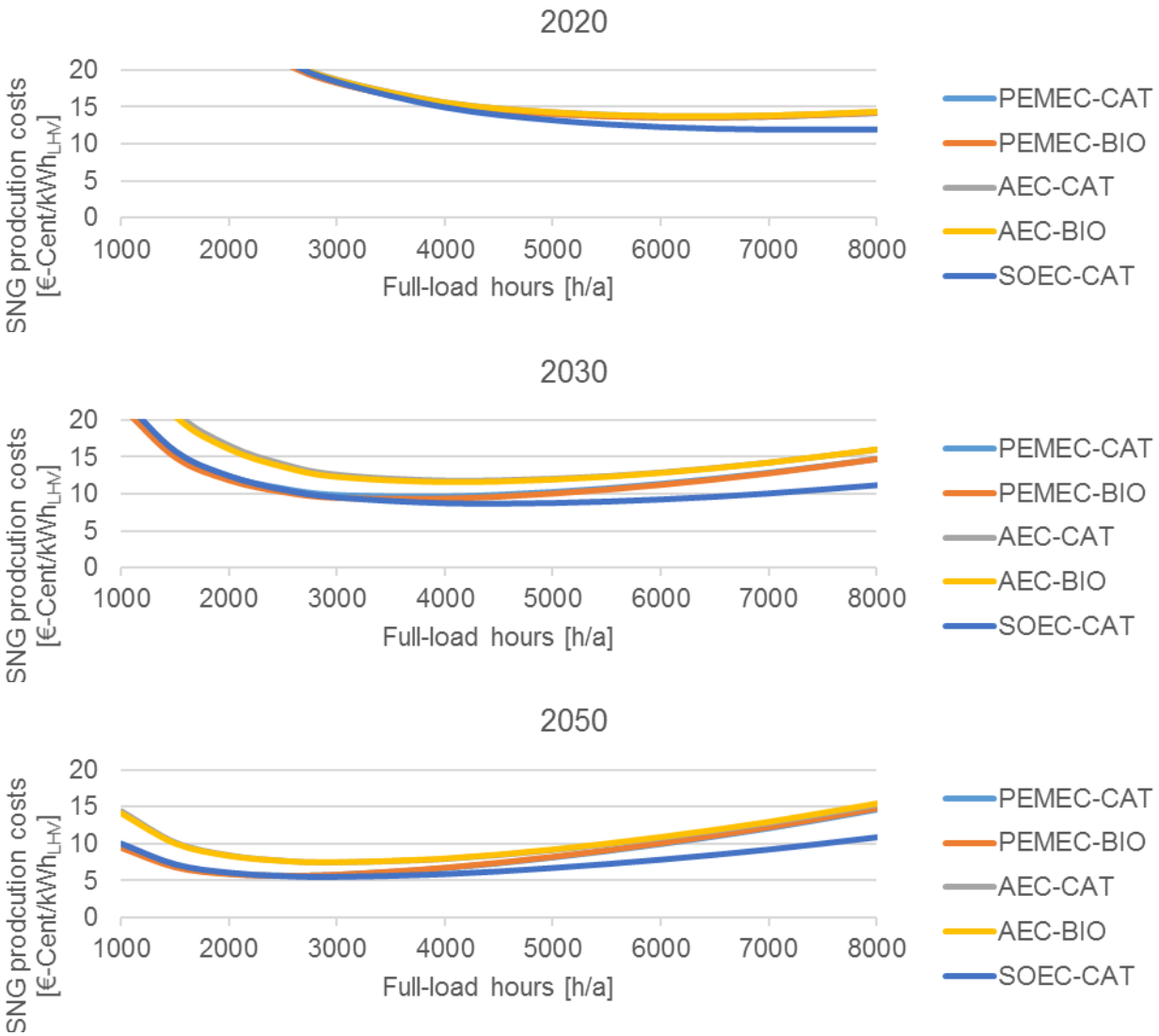

Figure 7-15: Development (from 2020–2050) of the specific SNG production costs in the PtG-Grid scenario for different PtG technologies

In general, in all scenarios (PtG-PV, PtG-Wind, and PtG-Grid), the lower SNG production costs of the PtG plant with an SOEC and catalytic methanation unit can be attributed to higher system efficiency. In this comparison, it is assumed that the waste heat can be sold in the PEMEC-CAT, PEMEC-BIO, AEC-CAT, and AEC-BIO variants. At a SOEC-CAT PtG plant, the waste heat is used internally to increase efficiency, and no waste heat is available for sale. If the waste heat cannot be sold, the SNG costs will rise. Thus, the SOEC variant would have the lowest SNG costs by far. However, to achieve these higher efficiencies, the SOEC requires an additional heat source, which is not available (in form of waste heat) at every location.

8 Summary

The scaling effects for each system must be evaluated in order to be able to determine the investment costs for PtG plants of different scales. These effects have been analyzed according to the year of installation to assess the learning curve effects generated by the increasing production of the respective systems.

Unless otherwise mentioned, cost predictions for the PtG technology in this Deliverable are stated as **real costs** (reference year 2017, €$_{2017}$). This means that the inflationary effects that are anticipated and will lead to rising nominal costs have not been considered. Additionally, **no significant changes in technology**, such as an implementation of additional functions, control elements and safety devices or efficiency improvements, have been taken into account for calculating the future investment costs.

The results show that the scaling effects for alkaline and PEM electrolysis systems are on a similar low level. These effects slightly increase in later installation years, as modules with limited scaling potential, particularly cell stacks, take decreasing shares in total system costs due to technological learning. Economies of scale show higher potential for cost reductions for solid oxide cell electrolysis, due to the differently weighted cost shares, with higher shares for properly scaled components in the "Power Electronics" and "BoP" modules. Also, methanation systems show promising cost reduction at constant levels throughout the investigated period.

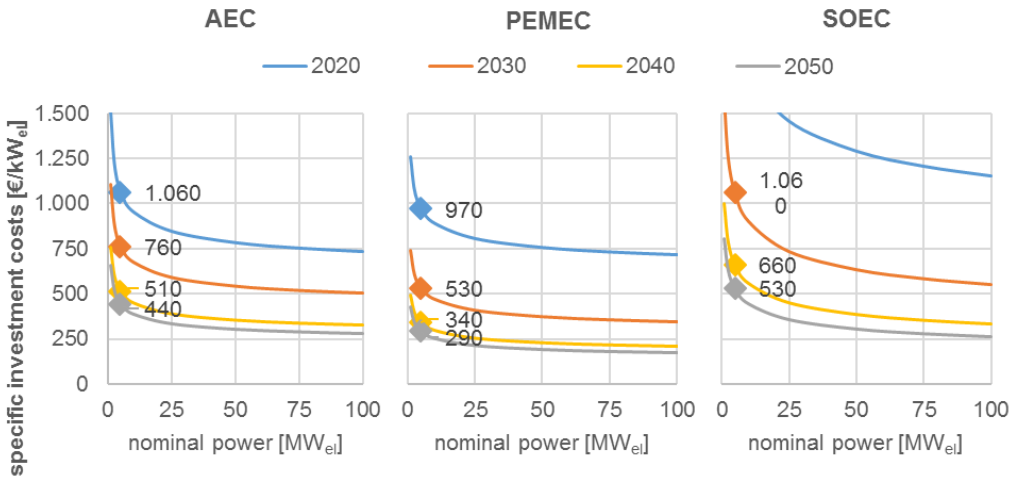

Figure 8-1: Cost development of electrolysis systems related to scaling effects and technological learning

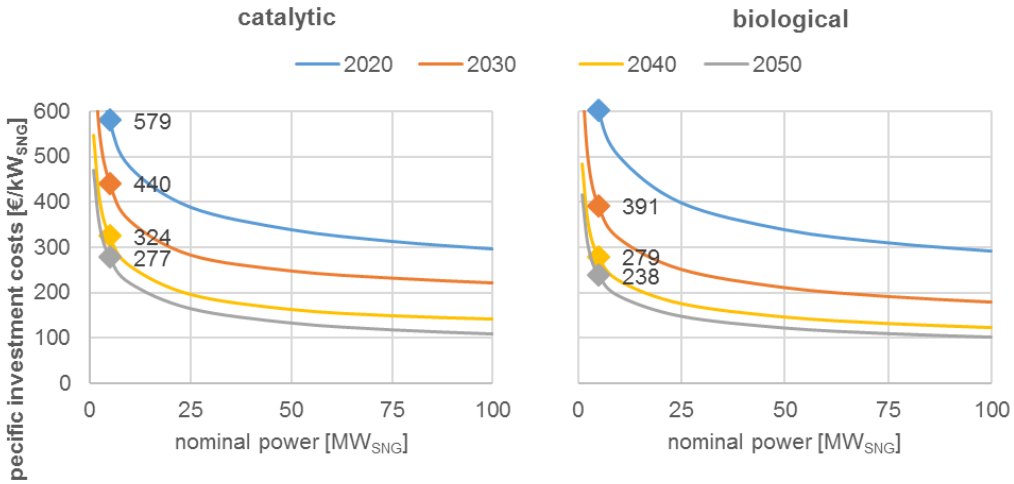

Figure 8-2: Cost development of methanation systems related to scaling effects and technological learning

The analysis of the scaling effects on electrolysis and methanation systems showed that upscaling strategies could provide significant potential for cost reduction in PtG plants; this is especially true for methanation. However, these cost reductions partly depend on additional effects gained from technological learning and on the year of installation (or, rather, the cumulative number of systems produced in the future). The modularized approach of the analysis enabled it to show that both effects influence the development of the systems' cost structures differently. Therefore, investment decisions for PtG plants will require a critical view of both effects so that the systems are properly dimensioned.

The Power-to-Gas subsystems – based on different electrolysis and methanation systems – investigated in this study can be further classified according to underlying technologies and processes. Hence, different characteristics in the system design depending on the specific requirements, framework conditions or operating purposes (e.g. gas qualities and conditions, reactor concepts and stages, heat management) have to be met. This results in an unmanageable number of individual variants, which also differ in investment costs, accordingly.

Since an analysis of all possible variants is not feasible within and neither the intention of this study, the calculations done on investment costs for electrolysis and methanation systems are to be considered as a cost estimation guideline for future projects. In any case, actual investment costs for a specific implementation, under consideration and definition of respective framework conditions in the plant design, have to be analyzed in detail by the manufacturers according to the actual state of the art and therefore may differ from the estimations made herein.

Evaluating the future techno-economic developments in PtG technologies requires well-grounded knowledge of the current state of the art. Therefore, this Deliverable includes an analysis of KPIs for the electrolysis and methanation technologies. This brief technological review also shows that rapid development in ongoing in PtG technologies. The nominal capacities available for state-of-the-art alkaline and PEM electrolysis systems are already in a range of multiple MW_{el}, where EoS are already a valuable factor for investment decisions, justifying the investigations performed on that topic. SOEC technology is expected to catch up with this development in the intermediate future, in combination with increased electrical efficiencies via the integration of external waste heat or thermal coupling to exothermal processes like chemical methanation. By contrast, no great leaps in methanation processes are expected in the near future, as is emphasized by the brief review of research on advances in materials and technologies.

Alongside with existing technologies, the investigations have shown that further research on the material side could result in significant reductions in hydrogen production costs due to increased efficiency, decreased CAPEX, and reduced sensitivity to impurities in feed water. Furthermore, new water electrolysis concepts, like membraneless cells and plasma electrolysis, will provide low-cost alternatives.

The economic evaluation performed to evaluate future generation costs for renewable SNG is based on the calculation of the specific production costs for SNG in 2020, 2030, and 2050 for a 100 MWel PtG plant for three different fields of application—a PtG plant powered by a photovoltaic power plant (PtG-PV), a PtG plant powered by a wind farm (PtG-Wind), and a PtG plant powered by the public grid (PtG-Grid). Additionally, the SNG production costs are calculated for several PtG technologies: combinations of a PEMEC, AEC, and SOEC with a catalytic or biological methanation unit. The most important parameters for the calculation of the SNG costs are the electricity procurement costs, the investment costs, the full-load hours, and the technical features of the PtG plant.

Figure 8-3 summarizes the results of all the calculations performed, providing a range of costs for each scenario. The variety among the costs is due to the different technologies used for SNG production. In general, there is little difference according to the methanation technology used. Further, there is no significant difference in 2020 between the technologies, with the exception of the SOEC-CAT case, which is more of a theoretical consideration, since a 100 MWel SOEC is unlikely to be built by 2020. In the future, the PtG plants with an alkaline electrolyzer will have slightly higher SNG production costs than those with a PEM electrolyzer. A PtG plant built with an SOEC and catalytic methanation will tend to have slightly lower SNG production costs in the future. In all scenarios (PtG-PV, PtG-Wind, and PtG-Grid), the lower SNG production costs of the PtG-plant with an SOEC and catalytic methanation unit can be attributed to higher system efficiency. However, to achieve these very high efficiencies, the SOEC requires an additional waste heat source, which is not available at every location. By contrast, it is assumed that waste heat can be sold in the PEMEC-CAT, PEMEC-BIO, AEC-CAT, and AEC-BIO variants. If waste heat cannot be sold, then the SNG costs would rise in these variants. Thus, the SOEC variant would have the lowest SNG costs by far.

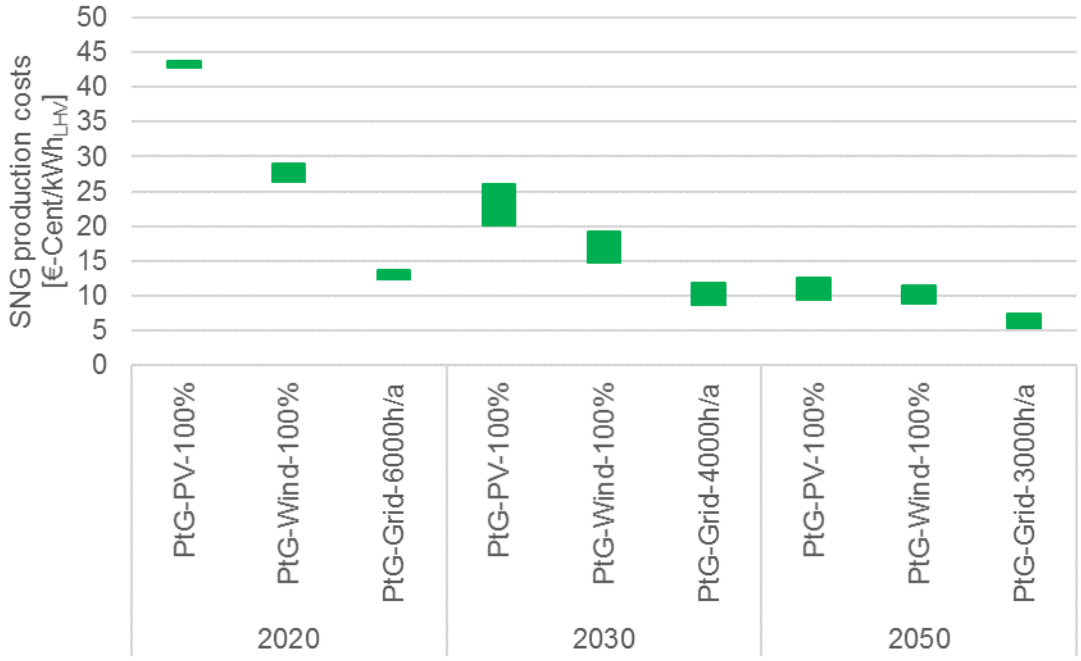

Figure 8-3: Range of SNG production costs of a 100 MW plant in 2020, 2030 and 2050 for different scenarios

The sensitivity analysis indicates that reducing SNG costs requires purchasing low-cost electricity, maximizing plant efficiency, reducing investment costs, and in cases where the plant is connected to a PV or wind park, building the PV or wind park in good locations with high full-load hours.

However, the development of PtG technology is subject to fundamental energy and climate policy decisions, and assumptions made about the future can change significantly. This has a major impact on the future SNG production costs calculated in this report.

9 References

[1] Peters MS, Timmerhaus KD. Plant design and economics for chemical engineers. 4th ed. New York: McGraw-Hill; 1991.

[2] Böhm H, Zauner A, Goers S, Tichler R, Kroon P. STORE&GO - Deliverable D7.5 - Report on experience curves and economies of scale; 2018.

[3] Steinmüller H, Reiter G, Tichler R, Friedl C, Furtlehner M, Lindorfer J et al. Power to Gas - eine Systemanalyse: Markt- und Technologiescouting und -analyse; 2014.

[4] de Bucy J. The potential of power-to-gas: Technology review and economic potential assessment; 2016.

[5] Felgenhauer M, Hamacher T. State-of-the-art of commercial electrolyzers and on-site hydrogen generation for logistic vehicles in South Carolina. International Journal of Hydrogen Energy 2015(40):2084–90.

[6] Energieinstitut an der JKU Linz. Cost data based on requests for different projects; 2017.

[7] Nel. Nel Hydrogen Electrolyser - The world's most efficient and reliable electrolyser. [October 25, 2018]; Available from: https://nelhydrogen.com/assets/uploads/2017/01/Nel_Electrolyser_brochure.pdf.

[8] Walker SB, van Lanen D, Fowler M, Mukherjee U. Economic analysis with respect to Power-to-Gas energy storage with consideration of various market mechanisms. International Journal of Hydrogen Energy 2016;41(19):7754–65.

[9] Smolinka T, Wiebe N, Thomassen M. Cost Break Down and Cost Reduction Strategies for PEM Water Electrolysis Systems. Luzern; 2017.

[10] Parra D, Patel MK. Techno-economic implications of the electrolyser technology and size for power-to-gas systems. International Journal of Hydrogen Energy 2016;41(6):3748–61.

[11] Morgan ER, Manwell JF, McGowan JG. Opportunities for economies of scale with alkaline electrolyzers. International Journal of Hydrogen Energy 2013;38(36):15903–9.

[12] Bertuccioli L, Chan A, Hart D, Lehner F, Madden B, Standen E. Development of Water Electrolysis in the European Union. Final Report; 2014.

[13] Perry RH, Green DW, Maloney JO. Perry's chemical engineers' handbook. 7th ed. New York, NY: McGraw-Hill; 1999.

[14] Matches. Matches' 275 Equipment Cost Estimates. [November 21, 2018]; Available from: http://matche.com/equipcost/Default.html.

[15] Grond L, Schulze P, Holstein J. Systems Analyses Power to Gas - Deliverable 1: Technology Review - Final Report; 2013.

[16] Electrochaea. Final Report - Power-to-Gas via Biological Catalysis (P2G-Biocat); 2017.

[17] Graf F, Krajete A, Schmack U. Techno-ökonomische Studie zur biologischen Methanisierung bei Power-to-Gas-Konzepten; 2014.

[18] Graf F, Götz M, Henel M, Schaaf T, Tichler R. Technoökonomische Studie von Power-to-Gas-Konzepten. Bonn; 2014.

[19] Götz M, Lefebvre J, Mörs F, McDaniel Koch A, Graf F, Bajohr S et al. Renewable Power-to-Gas: A technological and economic review. Renewable Energy 2016;85:1371–90.

[20] Merrow EW. An Analysis of Cost Improvement in Chemical Process Technologies. RAND; 1989.

[21] Daugaard T, Mutti LA, Wright MM, Brown RC, Componation P. Learning rates and their impacts on the optimal capacities and production costs of biorefineries. Biofuels, Bioprod. Bioref. 2015;9(1):82–94.

[22] Wolfgang Lemb. MODULARE BAUWEISE: ERFOLGSFAKTOR FÜR DEN MASCHINEN UND ANLAGENBAU? Frankfurt/Main; 2016.

[23] GINERELX. Electrolyzer Stacks. [October 19, 2018]; Available from: https://www.ginerelx.com/electrolyzer-stacks.

[24] Nel ASA. Nel Hydrogen Electrolysers Brochure. [October 15, 2018]; Available from: https://nelhydrogen.com/assets/uploads/2016/05/Nel-Electrolysers-Brochure-2018-PD-0600-0125-Web.pdf.
[25] McPhy. Augmented McLyzer. [October 15, 2018]; Available from: https://mcphy.com/en/our-products-and-solutions/electrolyzers/augmented-mclyzer/.
[26] Siemens AG. SYLIZER 300. [October 15, 2018]; Available from: https://www.siemens.com/content/dam/webassetpool/mam/tag-siemens-com/smdb/corporate-core/sustainable_energy/hydrogensolutions/brosch%C3%BCren/ct-ree-18-047-db-silyzer-300-db-de-en-rz.pdf.
[27] thyssenkrupp Uhde Chlorine Engineers. Industrial Solutions - Hydrogen from large-scale electrolysis; Available from: file:///C:/Users/AK192105/Downloads/thyssenkrupp_electrolytic_hydrogen_brochure.pdf.
[28] Fraunhofer ICT-IMM. COPIRIDE Report Summary. [December 17, 2018]; Available from: https://cordis.europa.eu/result/rcn/163487_en.html.
[29] BAYER TECHNOLOGY SERVICES GMBH. F3 FACTORY. [December 17, 2018]; Available from: https://cordis.europa.eu/result/rcn/149331_en.html.
[30] Sievers S, Seifert T, Franzen M, Schembecker G, Bramsiepe C. Fixed capital investment estimation for modular production plants. Chemical Engineering Science 2017;158:395–410.
[31] Sánchez A, Martín M. Scale up and scale down issues of renewable ammonia plants: Towards modular design. Sustainable Production and Consumption 2018;16:176–92.
[32] Heitmann M, Huhn T, Sievers S, Schembecker G, Bramsiepe C. Framework to decide for an expansion strategy of a small scale continuously operated modular multi-product plant. Chemical Engineering and Processing: Process Intensification 2017;113:74–85.
[33] Smolinka T, Günther M, Garche J. NOW-Studie: Stand und Entwicklungspotenzial der Wasserelektrolyse zur Herstellung von Wasserstoff aus regenerativen Energien. Kurzfassung des Abschlussberichts; 2011.
[34] Buttler A, Spliethoff H. Current status of water electrolysis for energy storage, grid balancing and sector coupling via power-to-gas and power-to-liquids: A review. Renewable and Sustainable Energy Reviews 2018;82:2440–54.
[35] Fuel Cells and Hydrogen 2 Joint Undertaking. Multi - Annual Work Plan 2014 - 2020; 2018.
[36] Allebrod F, Mogensen MB, Hjelm J, Ebbesen SD. High Temperature and Pressure Electrolysis: Technical University of Denmark; 2013.
[37] Allebrod F, Chatzichristodoulou C, Mogensen MB. Alkaline electrolysis cell at high temperature and pressure of 250 °C and 42 bar. Journal of Power Sources 2013;229:22–31.
[38] Carmo M, Fritz DL, Mergel J, Stolten D. A comprehensive review on PEM water electrolysis. International Journal of Hydrogen Energy 2013;38(12):4901–34.
[39] Schmidt O, Gambhir A, Staffell I, Hawkes A, Nelson J, Few S. Future cost and performance of water electrolysis: An expert elicitation study. International Journal of Hydrogen Energy 2017;42(52):30470–92.
[40] Smolinka T, Wiebe N, Sterchele P, Palzer A, Lehner F, Jansen M et al. Studie IndWEDe: Industrialisierung der Wasser-elektrolyse in -Deutschland: -Chancen und -Herausforderungen für nachhaltigen Wasserstoff für Verkehr, Strom und -Wärme. Berlin; 2018.
[41] Sartory M, Wallnöfer-Ogris E, Salman P, Fellinger T, Justl M, Trattner A et al. Theoretical and experimental analysis of an asymmetric high pressure PEM water electrolyser up to 155 bar. International Journal of Hydrogen Energy 2017;42(52):30493–508.
[42] Rönsch S, Schneider J, Matthischke S, Schlüter M, Götz M, Lefebvre J et al. Review on methanation – From fundamentals to current projects. Fuel 2016;166:276–96.
[43] Lecker B, Illi L, Lemmer A, Oechsner H. Biological hydrogen methanation - A review. Bioresour Technol 2017;245(Pt A):1220–8.
[44] Ghaib K, Ben-Fares F-Z. Power-to-Methane: A state-of-the-art review. Renewable and Sustainable Energy Reviews 2018;81:433–46.

[45] FFG - Österreichische Forschungsförderungsgesellschaft mbH. FFG Projektdatenbank - HydroMetha. [December 13, 2018]; Available from: https://projekte.ffg.at/projekt/2903976.
[46] Karlsruher Institute of Technologie. HELMETH project: Integrated High-Temperature ELectrolysis and METHanation for Effective Power to Gas Conversion. [December 17, 2018]; Available from: http://www.helmeth.eu/.
[47] Zhang G, Sun T, Peng J, Wang S, Wang S. A comparison of Ni/SiC and Ni/Al2O3 catalyzed total methanation for production of synthetic natural gas. Applied Catalysis A: General 2013;462-463:75–81.
[48] Rostrup-Nielsen JR, Pedersen K, Sehested J. High temperature methanationSintering and structure sensitivity. Applied Catalysis A: General 2007;330:134–8.
[49] Nishimura N, Kitaura S, Mimura A, Takahara Y. Cultivation of thermophilic methanogen KN-15 on H2-CO2 under pressurized conditions. Journal of Fermentation and Bioengineering 1992;73(6):477–80.
[50] Giglio E, Lanzini A, Santarelli M, Leone P. Synthetic natural gas via integrated high-temperature electrolysis and methanation: Part II—Economic analysis. Journal of Energy Storage 2015;2:64–79.
[51] Gruber M, Weinbrecht P, Biffar L, Harth S, Trimis D, Brabandt J et al. Power-to-Gas through thermal integration of high-temperature steam electrolysis and carbon dioxide methanation - Experimental results. Fuel Processing Technology 2018;181:61–74.
[52] Ogawa T, Takeuchi M, Kajikawa Y. Analysis of Trends and Emerging Technologies in Water Electrolysis Research Based on a Computational Method: A Comparison with Fuel Cell Research. Sustainability 2018;10(2):478.
[53] Harms C, Adam M, Soliman KA, Wilhelm M, Kibler LA, Jacob T et al. New Electrocatalysts with Pyrolyzed Siloxane Matrix. Electrocatalysis-Us 2014;5(3):301–9.
[54] Tymoczko J, Calle-Vallejo F, Schuhmann W, Bandarenka AS. Making the hydrogen evolution reaction in polymer electrolyte membrane electrolysers even faster. Nat Commun 2016;7:10990.
[55] Dresp S, Dionigi F, Loos S, Araujo JF de, Spori C, Gliech M et al. Direct Electrolytic Splitting of Seawater: Activity, Selectivity, Degradation, and Recovery Studied from the Molecular Catalyst Structure to the Electrolyzer Cell Level. Adv Energy Mater 2018;8(22):1800338.
[56] Fujimura K, Matsui T, Izumiya K, Kumagai N, Akiyama E, Habazaki H et al. Oxygen evolution on manganese–molybdenum oxide anodes in seawater electrolysis. Materials Science and Engineering: A 1999;267(2):254–9.
[57] Fujimura K, Matsui T, Habazaki H, Kawashima A, Kumagai N, Hashimoto K. The durability of manganese–molybdenum oxide anodes for oxygen evolution in seawater electrolysis. Electrochimica Acta 2000;45(14):2297–303.
[58] Lim CK, Liu Q, Zhou J, Sun Q, Chan SH. High-temperature electrolysis of synthetic seawater using solid oxide electrolyzer cells. J Power Sources 2017;342:79–87.
[59] Gabler A, Muller CI, Rauscher T, Kohring M, Kieback B, Rontzsch L et al. Ultrashort pulse laser-structured nickel surfaces as hydrogen evolution electrodes for alkaline water electrolysis. Int J Hydrogen Energ 2017;42(16):10826–33.
[60] Hinnemann B, Moses PG, Bonde J, Jorgensen KP, Nielsen JH, Horch S et al. Biomimetic hydrogen evolution: MoS2 nanoparticles as catalyst for hydrogen evolution. J Am Chem Soc 2005;127(15):5308–9.
[61] Zeng F, Broicher C, Palkovits S, Simeonov K, Palkovits R. Synergy between active sites and electric conductivity of molybdenum sulfide for efficient electrochemical hydrogen production. Catal Sci Technol 2018;8(1):367–75.
[62] Liu Q, Tian J, Cui W, Jiang P, Cheng N, Asiri AM et al. Carbon nanotubes decorated with CoP nanocrystals: a highly active non-noble-metal nanohybrid electrocatalyst for hydrogen evolution. Angew Chem Int Ed Engl 2014;53(26):6710–4.

[63] Jin H, Wang J, Su D, Wei Z, Pang Z, Wang Y. In situ cobalt-cobalt oxide/N-doped carbon hybrids as superior bifunctional electrocatalysts for hydrogen and oxygen evolution. J Am Chem Soc 2015;137(7):2688–94.
[64] Shabangoli Y, Rahmanifar MS, El-Kady MF, Noori A, Mousavi MF, Kaner RB. An integrated electrochemical device based on earth-abundant metals for both energy storage and conversion. Energy Storage Materials 2018;11:282–93.
[65] Melder J, Kwong WL, Shevela D, Messinger J, Kurz P. Electrocatalytic Water Oxidation by MnOx /C: In Situ Catalyst Formation, Carbon Substrate Variations, and Direct O2 /CO2 Monitoring by Membrane-Inlet Mass Spectrometry. ChemSusChem 2017;10(22):4491–502.
[66] Rosa M, Gooden PN, Butterworth S, Zielke P, Kiebach R, Xu Y et al. Zirconia nano-colloids transfer from continuous hydrothermal synthesis to inkjet printing. J Eur Ceram Soc 2019;39(1):2–8.
[67] Rosa M, Barou C, Esposito V. Zirconia UV-curable colloids for additive manufacturing via hybrid inkjet printing-stereolithography. Mater Lett 2018;215:214–7.
[68] Esposito DV. Membraneless Electrolyzers for Low-Cost Hydrogen Production in a Renewable Energy Future. Joule 2017;1(4):651–8.
[69] Mizuno T, Ohmori T, Akimoto T. Generation of Heat and Products During Plasma Electrolysis. In: 10th International Conference on Cold Fusion; 2003.
[70] Chaffin JH, Bobbio SM, Inyang HI, Kaanagbara L. Hydrogen production by plasma electrolysis. J Energ Eng-Asce 2006;132(3):104–8.
[71] Gao J, Liu Q, Gu F, Liu B, Zhong Z, Su F. Recent advances in methanation catalysts for the production of synthetic natural gas. RSC Adv. 2015;5(29):22759–76.
[72] Younas M, Loong Kong L, Bashir MJK, Nadeem H, Shehzad A, Sethupathi S. Recent Advancements, Fundamental Challenges, and Opportunities in Catalytic Methanation of CO 2. Energy Fuels 2016;30(11):8815–31.
[73] Biegger P, Kirchbacher F, Medved A, Miltner M, Lehner M, Harasek M. Development of Honeycomb Methanation Catalyst and Its Application in Power to Gas Systems. Energies 2018;11(7):1679.
[74] Liu YC, Zhu LJ, Wang XL, Yin S, Leng FR, Zhang F et al. Catalytic methanation of syngas over Ni-based catalysts with different supports. Chinese J Chem Eng 2017;25(5):602–8.
[75] Kirchbacher F, Biegger P, Miltner M, Lehner M, Harasek M. A new methanation and membrane based power-to-gas process for the direct integration of raw biogas – Feasability and comparison. Energy 2018;146:34–46.
[76] Norahim N, Yaisanga P, Faungnawakij K, Charinpanitkul T, Klaysom C. Recent Membrane Developments for CO2 Separation and Capture. Chem Eng Technol 2018;41(2):211–23.
[77] Teske S, Lins C, Hullin M, Williamson LE, Fattal A. Renewables global futures report: Great debates towards 100% renewable energy. Paris: REN21, Secretariat; 2017.
[78] Dörr H, Kröger K, Graf F, Köppel W, Burmeister F, Senner J et al. Untersuchungen zur Einspeisung von Wasserstoff in ein Erdgasnetz. DVGW energie | wasser-praxis 2016(11):50–9.
[79] Veenstra HJ. Geology of the Dogger Bank area, North Sea. Marine Geology 1965;3(4):245–62.
[80] Zoethout T. The €1.5 bn Plan to Build an Artificial Island for Offshore Wind. [December 13, 2018]; Available from: https://www.elektormagazine.com/news/the-1-5-bn-plan-to-build-an-artificial-island-for-offshore-wind.
[81] Bauer S. Underground Sun Storage - Publizierbarer Endbericht; 2017.
[82] RAG Austria AG. Underground Sun Storage. [December 13, 2018]; Available from: https://www.underground-sun-storage.at/.
[83] RAG Austria AG. Underground Sun Conversion. [December 13, 2018]; Available from: https://www.underground-sun-conversion.at/.

[84] Jensen SH, Graves C, Mogensen M, Wendel C, Braun R, Hughes G et al. Large-scale electricity storage utilizing reversible solid oxide cells combined with underground storage of CO 2 and CH 4. Energy Environ. Sci. 2015;8(8):2471–9.
[85] Trimis D, Anger S. Potenzial der thermisch integrierten Hochtemperaturelektrolyse und Methanisierung für die Energiespeicherung durch Power-to-Gas (PtG). gwf-Gas | Erdgas 2014(01/02 2014):50–9.
[86] Verbund Solutions GmbH. H2FUTURE PROJECT - Technology. [December 13, 2018]; Available from: https://www.h2future-project.eu/technology.
[87] Salzgitter AG. Projekt „GrInHy“ – Green Industrial Hydrogen. [December 13, 2018]; Available from: https://www.salzgitter-ag.com/de/medien/pressemeldungen/pressemeldung-der-salzgitter-ag/2016-09-05/projekt-grinhy-green-industrial-hydrogen.html.
[88] Åhman M, Olsson O, Vogl V, Nyqvist B, Maltais A, Nilsson LJ et al. Hydrogen steelmaking for a low-carbon economy: A joint LU-SEI working paper for the HYBRIT project; 2018.
[89] SSAB, LKAB, Vattenfall. Summary of findings from HYBRIT Pre-Feasibility Study 2016-2017; 2017.
[90] European Commission. Union Registry | Climate Action. [September 21, 2018]; Available from: https://ec.europa.eu/clima/sites/clima/files/ets/registry/docs/verified_emissions_2017_en.xlsx.
[91] Murakami T, Nishikiori T, Nohira T, Ito Y. Electrolytic synthesis of ammonia in molten salts under atmospheric pressure. J Am Chem Soc 2003;125(2):334–5.
[92] Çelebi Y, Aydın H. An overview on the light alcohol fuels in diesel engines. Fuel 2019;236:890–911.
[93] Evangelisti S, Tagliaferri C, Brett DJL, Lettieri P. Life cycle assessment of a polymer electrolyte membrane fuel cell system for passenger vehicles. Journal of Cleaner Production 2017;142:4339–55.
[94] Fasihi M, Bogdanov D, Breyer C. Long-Term Hydrocarbon Trade Options for the Maghreb Region and Europe—Renewable Energy Based Synthetic Fuels for a Net Zero Emissions World. Sustainability 2017;9(2):306.
[95] WaterstofNet, Hydrogen Europe, HYER. Fuel Cell Electric Buses. [December 18, 2018]; Available from: https://fuelcellbuses.eu/.
[96] Gnann T, Wietschel M, Kühn A, Thielmann A, Sauer A, Plötz P et al. Brennstoffzellen-Lkw: kritische Entwicklungshemmnisse, Forschungsbedarf und Marktpotential. Studie im Rahmen der wissenschaftlichen Beratung des BMVI zur Mobilitäts- und Kraftstoffstrategie der Bundesregierung. Karlsruhe; 2017.
[97] Toyota. Better Air - Over 5.5 million electrified vehicles on the road every year by 2030. [December 13, 2018]; Available from: https://www.toyota-europe.com/world-of-toyota/feel/environment/better-air/better-air.
[98] Fraunhofer ISE. Current and Future Cost of Photovoltaics: Long-term Scenarios for Market Development, System Prices and LCOE of Utility-Scale PV Systems; 2015.
[99] Kost C, Shammugam S, Jülch V, Nguyen H-T, Schlegl T. Stromgestehungskosten erneuerbare Energien. Freiburg; 2018.
[100] European Commission. EU Reference Scenario 2016: Energy, transport and GHG emissions Trends to 2050; 2016.
[101] Agora Energiewende. Future cost of onshore wind. Recent auction results, long-term outlook and implications for upcoming German auctions; 2017.
[102] Energy Exchange Austria. EXAA - Spotmarkt - Marktdaten - Historische Daten. [December 11, 2018]; Available from: https://www.exaa.at/de/marktdaten/historische-daten.
[103] Prognos AG, EWI, GWS. Entwicklung der Energiemärkte - Energiereferenzprognose; 2014.
[104] BMLFUW. SuREmMA: Sustainable river management - Energiewirtschaftliche und umweltrelevante Bewertung möglicher schwalldämpfender Massnahmen. Wien; 2017.

[105] Energy Brainpool GmbH & Co. KG. Update: Trends der Strompreisentwicklung – EU Energy Outlook 2050. [November 29, 2018]; Available from: https://blog.energybrain-pool.com/update-trends-der-strompreisentwicklung-eu-energy-outlook-2050/.
[106] Greenpeace e.V. Klimaschutz: Der Plan: Energiekonzept für Deutschland; 2015.
[107] Agora Energiewende und Aurora Energy Research. 65 Prozent Erneuerbare bis 2030 und ein schrittweiser Kohleausstieg: Auswirkungen der Vorgaben des Koalitionsvertrags auf Strompreise, CO2-Emissionen und Stromhandel; 2018.
[108] enervis energy advisors. Der Klimaschutzbeitrag des Stromsektors bis 2040.: Entwicklungs-pfade für die deutschen Kohlekraftwerke und deren wirtschaftliche Auswirkungen; 2015.
[109] van Leeuwen C, Zauner A. STORE&GO - Deliverable D8.3: Report on the costs involved with PtG technologies and their potentials across the EU; 2018.
[110] Weber KH. Engineering verfahrenstechnischer Anlagen: Praxishandbuch mit Checklisten und Beispielen. 2nd ed. Heidelberg: SpringerVieweg; 2016.
[111] Kopp M, Coleman D, Stiller C, Scheffer K, Aichinger J, Scheppat B. Energiepark Mainz: Technical and economic analysis of the worldwide largest Power-to-Gas plant with PEM elec-trolysis. International Journal of Hydrogen Energy 2017;42(19):13311–20.
[112] Hurskainen M. Industrial oxygen demand in Finland; 2017.
[113] Werner S. European District Heating Price Series: Report 2016:316.
[114] Fleischhacker A. MODELLIERUNG UND KOMBINIERTE SIMULATION EINES POWER-TO-GAS PROZESSES; 2014.
[115] Deutsches Zentrum für Luft- und Raumfahrt e.V., Ludwig-Bölkow-Systemtechnik GmbH, Fraunhofer ISE, KBB Underground Technologies GmbH. Studie über die Planung einer De-monstrationsanlage zur Wasserstoff-Kraftstoffgewinnung durch Elektrolyse mit Zwischenspei-cherung in Salzkavernen unter Druck. Stuttgart; 2015.
[116] Kiaee M, Cruden A, Chladek P, Infield D. Demonstration of the operation and performance of a pressurised alkaline electrolyser operating in the hydrogen fuelling station in Porsgrunn, Norway. Energy Conversion and Management 2015;94:40–50.
[117] Scataglini R, Wei M, Mayyas A, Chan SH, Lipman T, Santarelli M. A Direct Manufacturing Cost Model for Solid-Oxide Fuel Cell Stacks. Fuel Cells 2017;17(6):825–42.

Appendix

A1. System structures for EoS calculations

Electrolysis

Table A 1: System structure and scale factors for alkaline electrolysis system

AEC System Unit	Cost shares					SF
	2017	2020	2030	2040	2050	
Total costs	**1.100 €/kW**	**1.060 €/kW**	**760 €/kW**	**510 €/kW**	**440 €/kW**	
Stack	**50%**	**50%**	**47%**	**43%**	**43%**	**0,88**
Structural Rings (Frame)	15%	15%	20%	27%	30%	0,50
Sealings	4%	4%	5%	6%	7%	0,50
Membrane	7%	7%	7%	5%	5%	1,00
Anode	26%	26%	23%	19%	17%	1,00
Cathode	25%	25%	22%	19%	17%	1,00
Bipolar Plates (incl. Flowfield)	7%	7%	6%	4%	3%	0,95
Pressure Plates / Flanges	4%	4%	6%	8%	9%	0,95
Tie Rods	3%	3%	4%	6%	6%	0,50
Pre-electrode / Current Distributor	8%	8%	7%	6%	6%	1,00
Power Electronics	**15%**	**15%**	**13%**	**13%**	**13%**	**0,75**
Gas Conditioning	**15%**	**16%**	**21%**	**25%**	**27%**	**0,60**
Drying & Cooling Components			-			0,52
H_2 Purification						0,81
Balance of Plant	**20%**	**20%**	**20%**	**19%**	**18%**	**0,68**
Thermal & Fluidic Management						**0,72**
Gas- & Fluid Circuit						1,33
Gas-Water-Separators						0,60
Heat Exchanger						0,59
Circulation Pumps						0,67
Lye Tank & Treatment			-			0,50
Control Valves						0,60
Peripheral Components						**0,60**
Lye Reconditioning						0,60
Recooling Equipment						0,59
System Controlling						**0,60**

* Component/cost structure based on [2,40]; Scale factors (SF) based on [11,13,14]

Table A 2: System structure and scale factors for PEM electrolysis system

PEMEC System Unit	Cost shares					SF
	2017	2020	2030	2040	2050	
Total costs	**1.200 €/kW**	**970 €/kW**	**530 €/kW**	**340 €/kW**	**290 €/kW**	
Stack	**60%**	**55%**	**42%**	**36%**	**34%**	**0,89**
Membrane	5%	5%	3%	2%	2%	1,00
Catalyst Anode	6%	7%	11%	13%	15%	1,00
Catalyst Cathode	2%	2%	4%	4%	5%	1,00
Current Collector Anode (PTL)	8%	7%	6%	4%	3%	0,95
Current Collector Kathode (PTL)	9%	8%	6%	4%	4%	0,95
Bipolar Plates (incl. Flowfield)	51%	48%	35%	25%	21%	0,95

End Plates	1%	1%	2%	2%	2%	0,95
Pressure Plates	3%	4%	5%	7%	7%	0,95
Small Parts / Sealings	3%	4%	6%	9%	10%	0,50
Stack Assembling	2%	2%	4%	6%	6%	0,50
MEA Manufacturing	10%	12%	18%	22%	24%	0,50
Power Electronics	**15%**	**17%**	**21%**	**21%**	**21%**	**0,75**
Gas Conditioning	**10%**	**12%**	**22%**	**28%**	**30%**	**0,60**
Drying & Cooling Components			-			0,52
H_2 Purification						0,81
Balance of Plant	**20%**	**20%**	**0,73**	**0,73**	**0,73**	**0,73**
Thermal & Fluidic Management						**0,73**
Gas- & Fluid Circuit						1,33
Gas-Water-Separators						0,60
Heat Exchanger						0,59
Circulation Pumps						0,67
Ion Exchanger			-			0,60
Control Valves						0,60
Peripheral Components						**0,80**
Water Treatment						1,00
Recooling Equipment						0,59
System Controlling						**0,60**

* Component/cost structure based on [2,40]; Scale factors (SF) based on [11,13,14]

Table A 3: System structure and scale factors for solid oxide electrolysis system

SOEC System Unit	**Cost shares**					**SF**
	2017	**2020**	**2030**	**2040**	**2050**	
Total costs	**2.500 €/kW**	**1.989 €/kW**	**1.061 €/kW**	**663 €/kW**	**535 €/kW**	
Stack	**30%**	**24%**	**14%**	**12%**	**11%**	**0,87**
Elektrolyte	12%	11%	6%	3%	2%	1,00
Catalyst Anode	15%	13%	8%	4%	3%	1,00
Catalyst Cathode	23%	20%	12%	6%	5%	1,00
Current Collector (PTL)	8%	7%	4%	2%	2%	0,95
Interconnector (Flowfield)	12%	11%	6%	3%	2%	0,95
Sealings	15%	19%	30%	36%	37%	0,50
End Plates	2%	2%	3%	3%	3%	0,95
Pressure Plates	4%	5%	6%	7%	7%	0,95
Stack Assembling	9%	12%	25%	35%	39%	0,50
Power Electronics	**30%**	**35%**	**43%**	**45%**	**45%**	**0,75**
Gas Conditioning	**15%**	**15%**	**16%**	**15%**	**15%**	**0,73**
Drying & Cooling Components			-			0,52
H_2 Purification						0,81
Balance of Plant	**20%**	**20%**	**0,73**	**0,73**	**0,73**	**0,73**
Thermal & Fluidic Management						**0,73**
Gas- & Fluid Circuit						1,33
Gas-Water-Separators						0,60
Heat Exchanger						0,59
Circulation Pumps			-			0,67
Ion Exchanger						0,60
Control Valves						0,60
Peripheral Components						**0,80**

Water Treatment		1,00
Recooling Equipment		0,59
System Controlling		**0,60**

* Component/cost structure based on [40,117]; Scale factors (SF) based on [11,13,14]

Methanation

Table A 4: System structure and scale factors for catalytic methanation system

Catalytic Methanation Unit	**Cost shares**					**SF**
	2017	**2020**	**2030**	**2040**	**2050**	
Total costs	**600 €/kW**	**579 €/kW**	**440 €/kW**	**324 €/kW**	**277 €/kW**	
Reactor	**21%**	**21%**	**20%**	**19%**	**18%**	**0,68**
Reactor	57%	57%	54%	50%	48%	0,56
Catalyst	26%	26%	30%	35%	37%	1,00
Heat Management	17%	17%	16%	15%	14%	0,59
Electric Installation	**20%**	**20%**	**19%**	**18%**	**17%**	**0,75**
Gas Conditioning	**12%**	**12%**	**16%**	**21%**	**25%**	**0,60**
Drying & Cooling Components			-			0,52
SNG Purification						0,81
Balance of Plant	**47%**	**47%**	**45%**	**42%**	**40%**	**0,67**
Thermal & Fluidic Management						**0,68**
Gas- & Fluid Circuit						1,33
Circulation Pumps						0,41
Heat Exchanger						0,59
Fittings						0,60
CO2 Evaporator			-			0,54
Control Valves						0,60
Peripheral Components						**0,67**
SNG Compressor						0,77
Storage Tank						0,57
System Controlling						**0,60**

* Component/cost structure based on [2] & STORE&GO project data; Scale factors (SF) based on [1,13,14]

Table A 5: System structure and scale factors for biological methanation system

Catalytic Methanation Unit	**Cost shares**					**SF**
	2017	**2020**	**2030**	**2040**	**2050**	
Total costs	**650 €/kW**	**600 €/kW**	**390 €/kW**	**280 €/kW**	**240 €/kW**	
Reactor	**17%**	**16%**	**13%**	**10%**	**9%**	**0,51**
Reactor	77%	77%	77%	77%	77%	0,50
Heat Management	23%	23%	23%	23%	23%	0,56
Electric Installation	**21%**	**22%**	**24%**	**24%**	**23%**	**0,75**
Gas Conditioning	**13%**	**14%**	**21%**	**29%**	**34%**	**0,60**
Drying & Cooling Components			-			0,52
SNG Purification						0,81
Balance of Plant	**49%**	**48%**	**41%**	**36%**	**34%**	**0,67**
Thermal & Fluidic Management						**0,68**
Gas- & Fluid Circuit			-			1,33
Circulation Pumps						0,41

Heat Exchanger		0,59
Fittings		0,60
CO2 Evaporator		0,54
Control Valves		0,60
Peripheral Components		**0,67**
SNG Compressor		0,77
Storage Tank		0,57
System Controlling		**0,60**

* Component/cost structure based on [2] & STORE&GO project data; Scale factors (SF) based on [1,13,14]

A2. Economic evaluation

Lang factors

Table A 6: Lang factors (% of CAPEX) for calculating the investment costs for 2020, 2030, and 2050

	2020	2030	2050
Engineering	25%	15%	10%
Material and services for civil engineering	20%	20%	20%
Assembly of the main components	20%	15%	10%
Process control technology (material and assembly)	40%	40%	40%
Electrical engineering (material and assembly)	20%	20%	20%
Approval	1%	1%	1%
Site equipment	2%	2%	2%
Construction and assembly monitoring	1%	1%	1%
Safety test	3%	3%	3%
Quality control	2%	2%	2%
Commissioning	3%	3%	3%
Other costs	25%	15%	10%
TOTAL	162%	137%	122%

Investment costs

Table A 7: Investment costs for different PtG-plants

			Nominal electrical input power [MW]					
			1	**5**	**25**	**50**	**75**	**100**
2020	PEMEC-CAT	Mio. €	4,7	17,3	68,1	124,7	178,5	230,7
	PEMEC-BIO	Mio. €	4,8	17,5	68,3	124,9	178,6	230,6
	AEC-CAT	Mio. €	5,3	18,5	70,7	128,2	182,6	235,2
	AEC-BIO	Mio. €	5,4	18,7	70,9	128,4	182,7	235,1
	SOEC-CAT	Mio. €	9,3	32,3	116,0	203,7	284,0	360,1
2030	PEMEC-CAT	Mio. €	2,7	9,5	34,8	62,0	87,2	111,4
	PEMEC-BIO	Mio. €	2,7	9,2	33,5	59,6	83,8	107,0
	AEC-CAT	Mio. €	3,6	12,2	45,6	81,9	116,1	148,9
	AEC-BIO	Mio. €	3,5	11,9	44,3	79,5	112,6	144,5
	SOEC-CAT	Mio. €	5,1	16,9	57,8	99,0	135,9	170,5
2050	PEMEC-CAT	Mio. €	1,6	5,2	17,8	30,7	42,6	53,8
	PEMEC-BIO	Mio. €	1,5	4,9	17,1	29,8	41,4	52,4
	AEC-CAT	Mio. €	2,1	6,9	24,5	43,2	60,6	77,3
	AEC-BIO	Mio. €	2,0	6,6	23,8	42,2	59,4	75,9
	SOEC-CAT	Mio. €	2,7	8,5	27,6	46,4	63,0	78,4

PEMEC: Proton Exchange Mebrane Electrolyzer; AEC: Alkaline Elektrolyzer; SOEC: Solid Oxide Electrolyzer; CAT: catalytic methanation; BIO: biological methantion

Table A 8: Characteristic data for different use cases – PtG-plant (25–100 MW) is powered by a wind farm or PV power plant in 2020

General Parameters	**Unit**			
Share grid feed-in	%	50	25	0
Share PtG	%	50	75	100
Nominal power EC	MW	50	75	100
Specific investment costs EC	€/kW_{el}	755	730	714
PtG - wind farm		PtG-Wind-50%	PtG-Wind-75%	PtG-Wind-100%
Energy for EC	MWh	80.971	168.169	310.056
Full load hours	h/a	1.619	2.242	3.101
Start/stop cycles	cycles/a	1.015	1.054	553
Time power = 0	h/a	5.997	4.432	1.018
Time power > 0	h/a	2.763	4.328	7.742
Average efficiency EC	%	63,7	64,2	64,6
Lifetime EC stack	a	15	15	13
Nominal methanation	MW_{SNG}	25,5	38,5	51,7
Specific investment costs methanation	€/kW_{SNG}	401	362	336
PtG - PV power plant		PtG-PV-50%	PtG-PV-75%	PtG-PV-100%
Energy for EC	MWh	28.283	68.882	139.483
Full load hours	h/a	566	918	1395
Start/stop cycles	cycles/a	542	545	373
Time power = 0	h/a	7.493	6.722	4.473
Time power > 0	h/a	1.267	2.038	4.287
Average efficiency EC	%	66,4	65,8	65,5
Lifetime EC stack	a	15	15	15
Nominal methanation	MW_{SNG}	26,6	39,5	52,4
Specific investment costs methanation	€/kW_{SNG}	397	360	335

Table A 9: Characteristic data for different use cases – PtG-plant (25–100 MW) is powered by a wind farm or PV power plant in 2030

General Parameters	**Unit**			
Share grid feed-in	%	50	25	0
Share PtG	%	50	75	100
Nominal power EC	MW	50	75	100
Specific investment costs EC	€/kW_{el}	374	356	345
PtG - wind farm		PtG-Wind-50%	PtG-Wind-75%	PtG-Wind-100%
Energy for EC	MWh	80.971	168.169	310.056
Full load hours	h/a	1.619	2.242	3.101
Start/stop cycles	cycles/a	1.015	1.054	553
Time power = 0	h/a	5.997	4.432	1.018
Time power > 0	h/a	2.763	4.328	7.742
Average efficiency EC	%	65,2	65,7	66,2
Lifetime EC stack	a	20	20	19
Nominal methanation	MW_{SNG}	26,1	39,4	53,0
Specific investment costs methanation	€/kW_{SNG}	295	265	245
PtG - PV power plant		PtG-PV-50%	PtG-PV-75%	PtG-PV-100%
Energy for EC	MWh	28.283	68.882	139.483
Full load hours	h/a	566	918	1395
Start/stop cycles	cycles/a	542	545	373
Time power = 0	h/a	7.493	6.722	4.473
Time power > 0	h/a	1.267	2.038	4.287
Average efficiency EC	%	68,0	67,4	67,1
Lifetime EC stack	a	20	20	20
Nominal methanation	MW_{SNG}	27,2	40,4	53,7
Specific investment costs methanation	€/kW_{SNG}	292	263	244

SNG production costs 2020

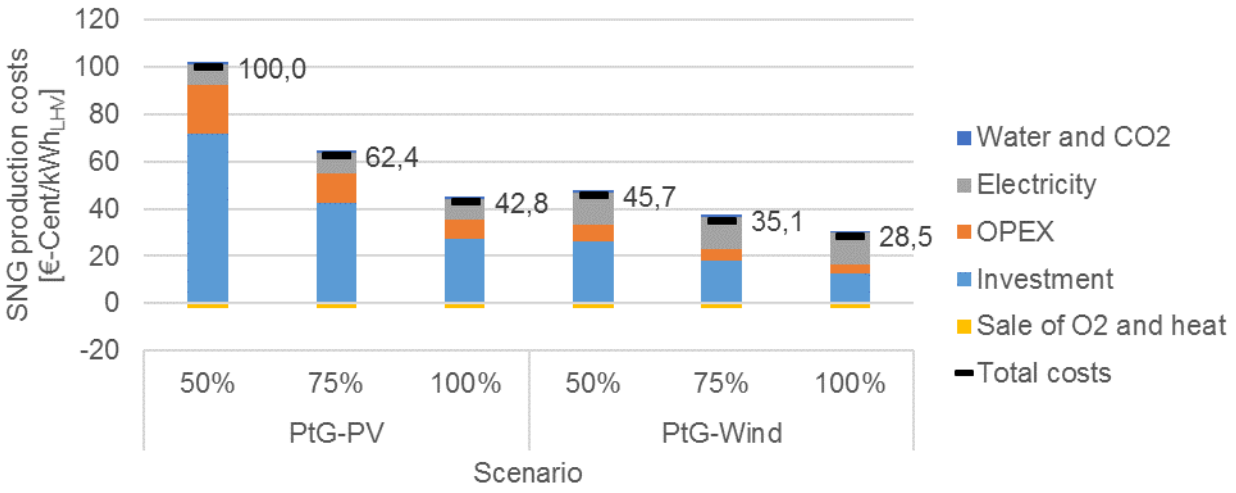

Figure A 1: Specific SNG production costs for the scenarios PtG-PV and PtG-Wind in 2020 for different usage shares of the generated electricity (50% grid/50% PtG-plant, 25% grid/75% PtG-plant, 0% grid/100% PtG-plant)

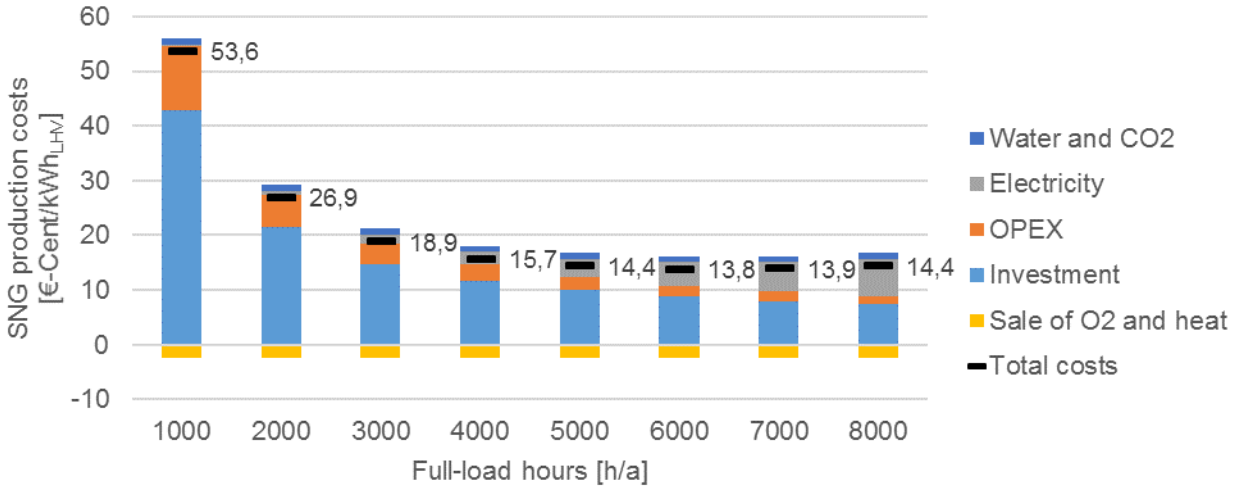

Figure A 2: Specific SNG production for the scenario PtG-Grid in 2020 for different full-load hours

SNG production costs 2030

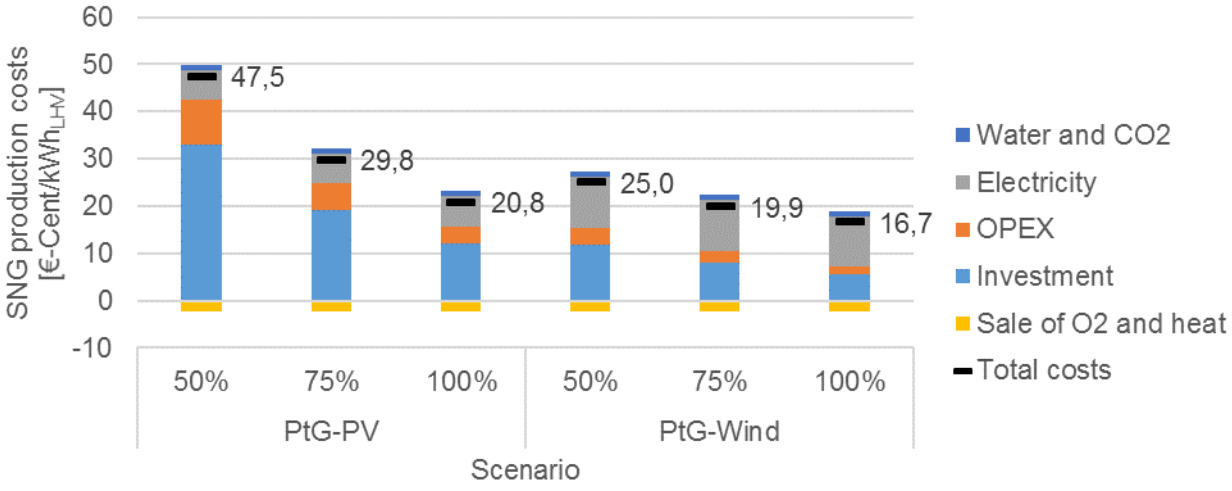

Figure A 3: Specific SNG production costs for the scenarios PtG-PV and PtG-Wind in 2030 for different usage shares of the generated electricity (50% grid/50% PtG-plant, 25% grid/75% PtG-plant, 0% grid/100% PtG-plant)

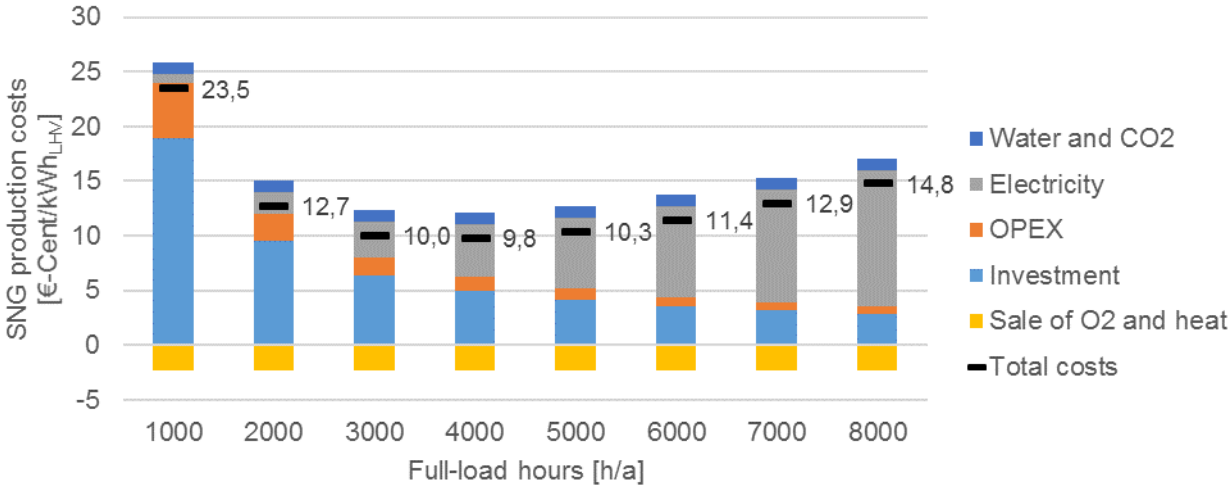

Figure A 4: Specific SNG production for the scenario PtG-Grid in 2030 for different full-load hours

Sensitivity analysis 2030

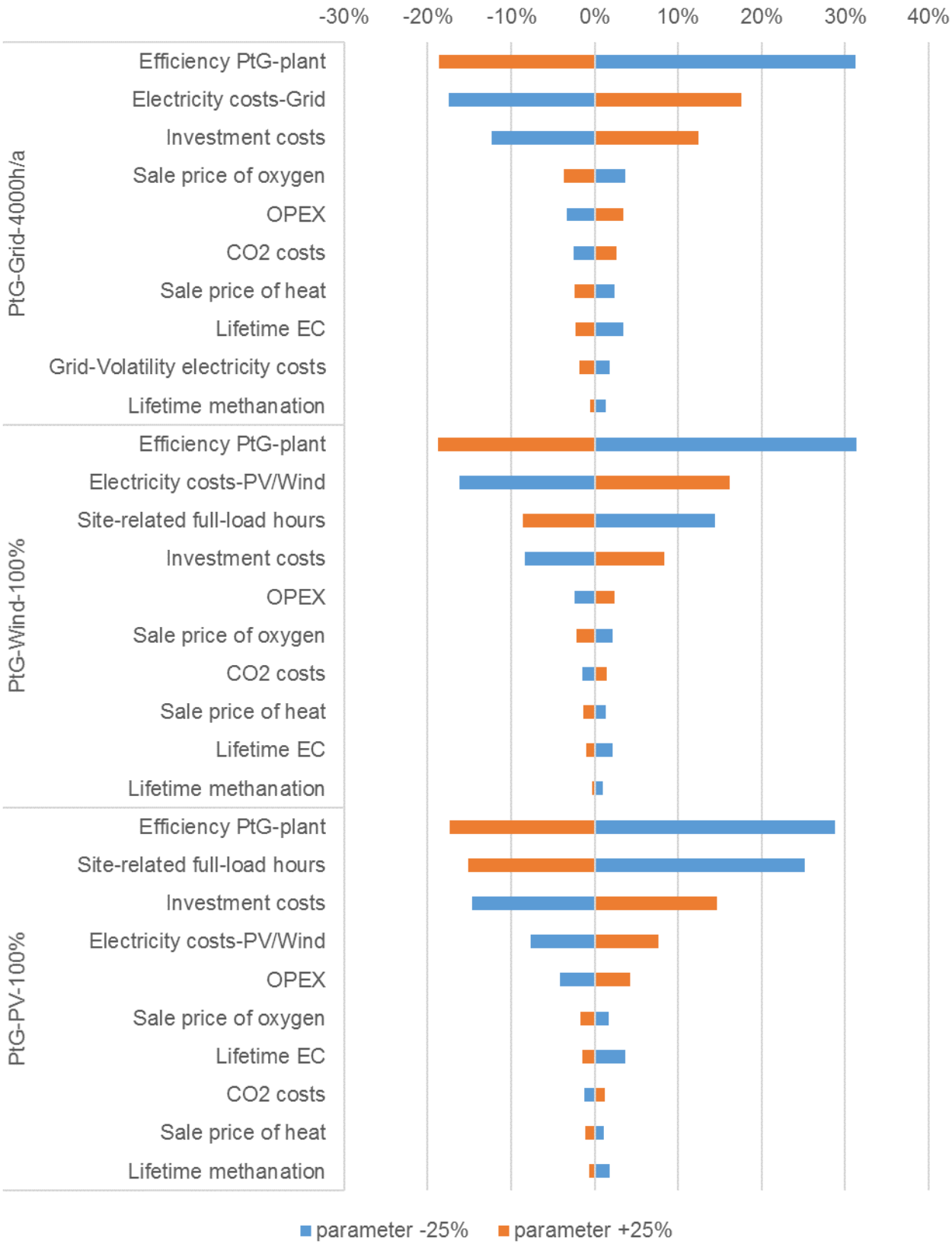

Figure A 5: Sensitivity analyses of specific SNG production costs in 2020 for the scenario PtG-PV-100%, PtG-Wind-100% and PtG-Grid-5000h/a

Sensitivity analysis 2050

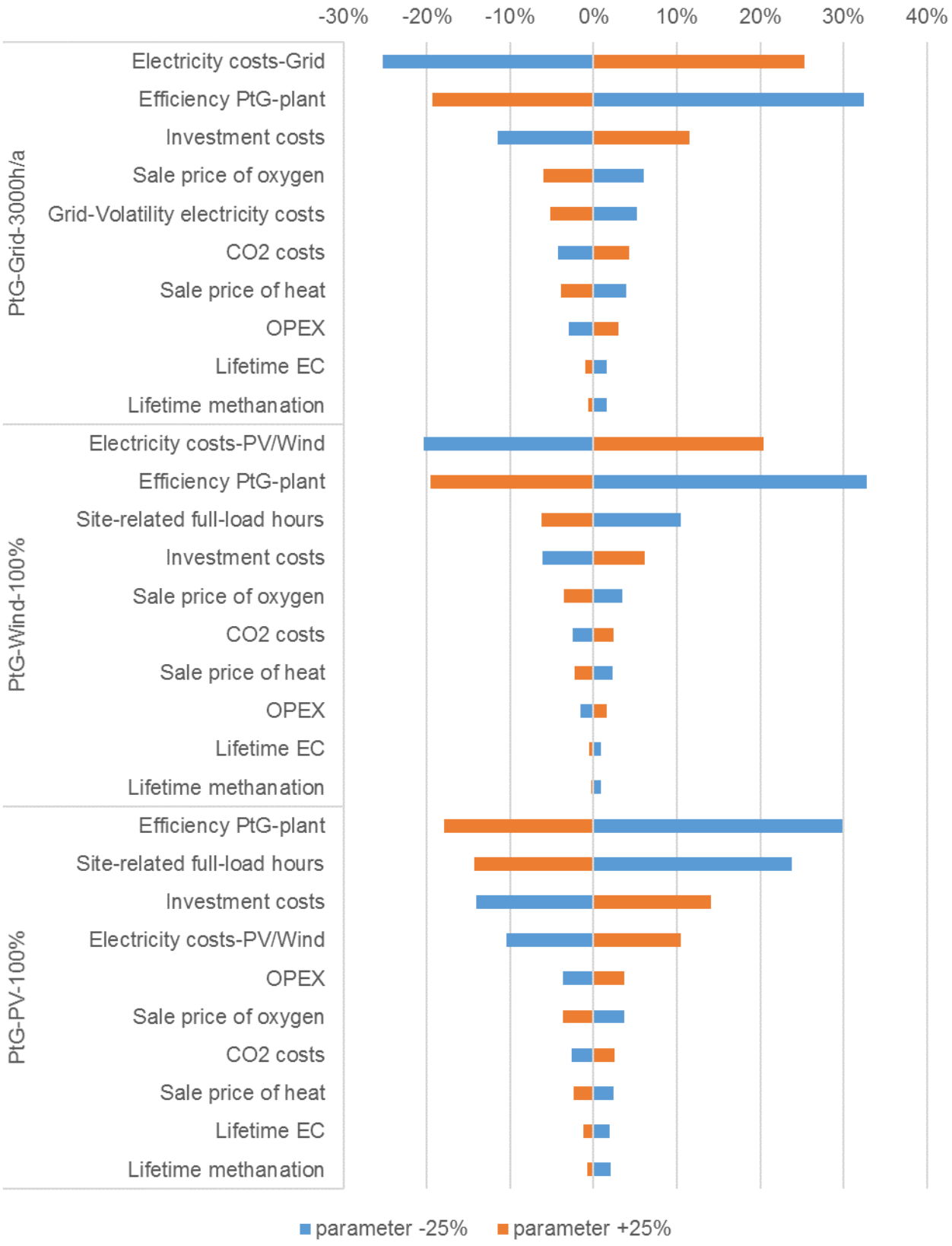

Figure A 6: Sensitivity analyses of specific SNG production costs in 2030 for the scenario PtG-PV-100%, PtG-Wind-100% and PtG-Grid-5000h/a